

ETHERIFICATION OF BIODIESEL BY-PRODUCT GLYCEROL TO PRODUCE  
FUEL OXYGENATES

A THESIS SUBMITTED TO  
THE GRADUATE SCHOOL OF NATURAL AND APPLIED SCIENCES  
OF  
MIDDLE EAST TECHNICAL UNIVERSITY

BY

BURÇİN İKİZER

IN PARTIAL FULFILLMENT OF THE REQUIREMENTS  
FOR  
THE DEGREE OF MASTER OF SCIENCE  
IN  
CHEMICAL ENGINEERING

AUGUST 2014



Approval of the thesis:

**ETHERIFICATION OF BIODIESEL BY-PRODUCT GLYCEROL TO  
PRODUCE FUEL OXYGENATES**

submitted by **BURÇİN İKİZER** in partial fulfillment of the requirements for the degree of **Master of Science in Chemical Engineering Department, Middle East Technical University** by,

Prof. Dr. Canan Özgen  
Dean, Graduate School of **Natural and Applied Sciences**

Prof. Dr. Halil Kalıpçılar  
Head of Department, **Chemical Engineering**

Prof. Dr. Timur Doğu  
Supervisor, **Chemical Engineering Dept., METU**

Assoc. Prof. Dr. Nuray Oktar  
Co-Supervisor, **Chemical Engineering Dept., Gazi Uni.**

**Examining Committee Members:**

Prof. Dr. Kırali Mürtezaoğlu  
Chemical Engineering Dept., Gazi University

Prof. Dr. Timur Doğu  
Chemical Engineering Dept., METU

Assoc. Prof. Dr. Nuray Oktar  
Chemical Engineering Dept., Gazi University

Assoc. Prof. Dr. Naime Aslı Sezgi  
Chemical Engineering Dept., METU

Asst. Prof. Dr. Erhan Bat  
Chemical Engineering Dept., METU

Asst. Prof. Dr. Levent Değirmenci  
Chemical and Process Eng. Dept., Bilecik Şeyh Edebali Uni.

**Date:** 26.08.2014

**I hereby declare that all information in this document has been obtained and presented in accordance with academic rules and ethical conduct. I also declare that, as required by these rules and conduct, I have fully cited and referenced all material and results that are not original to this work.**

Name, Last name: BURÇİN İKİZER

Signature:

## ABSTRACT

### ETHERIFICATION OF BIODIESEL BY-PRODUCT GLYCEROL TO PRODUCE FUEL OXYGENATES

İkizer, Burçin

M.S., Department of Chemical Engineering

Supervisor: Prof. Dr. Timur Doğu

Co-Supervisor: Assoc. Prof. Dr. Nuray Oktar

August 2014, 146 pages

Biodiesel, which is a renewable and environmentally friendly alternative to petroleum based diesel fuel, is produced by trans-esterification of vegetable oils and animal fats with lower molecular weight alcohols (methanol/ethanol), in the presence of a basic catalyst. Glycerol is the main side product of biodiesel production process. Economics of biodiesel production strongly depends upon the efficient utilization of its byproduct glycerol. The most attractive utilization way is its etherification for the production of fuel oxygenates. In this work etherification of glycerol with C<sub>4</sub> (i-butene) and C<sub>5</sub> [i-amylene; 2-Methyl-2-Butene (2M2B)] i-olefins were investigated for the production of transportation fuel oxygenates. Etherification of glycerol with 2M2B was firstly studied in the literature during this work. Besides mesoporous SAPO-34 like solid acid catalysts were synthesized in order to bring a new dimension to commercial solid acid catalysts and tested in etherification of glycerol with i-butene reaction.

The etherification reactions of glycerol with i-butene were carried out in an autoclave batch reactor using commercial solid acid catalyst such as Amberlyst-36, Dowex DR-2030 and Silicotungstic acid (STA) in a temperature range of 70-120°C. Glycerol etherification results obtained by using i-butene as the reactant, proved the importance of Brønsted acidity of the catalyst, as well as the pore diffusion

resistance, on the catalytic performance. Silicotungstic acid, with very high acidity, showed very good performance at  $T \leq 80^\circ\text{C}$ . However, at higher temperatures it also facilitated the oligomerization of i-butene, which caused negative effect on glycerol etherification. Both Amberlyst-36 and Dowex DR-2030 showed excellent performance in catalyzing glycerol with i-butene at 90 and  $120^\circ\text{C}$ .

Etherification of glycerol with 2-Methyl-2-Butene (2M2B) was also studied in an autoclave batch reactor using commercial solid acid catalysts such as Amberlyst-36 and Dowex DR-2030. The catalytic activities of Amberlyst-36 and Dowex DR 2030 were quite similar and a significant increase was observed in conversion values, with an increase in catalyst amount. This is due to the increased number of active sites per unit volume of the reaction mixture. Etherification of glycerol with 2M2B was investigated at 120 and  $140^\circ\text{C}$  over Amberlyst-36. Effects of reaction time and catalyst loading on glycerol conversion and product distributions were evaluated. Results proved formation of mono-, di- and tri-ethers of glycerol as a result of its etherification with 2M2B at  $120\text{-}140^\circ\text{C}$  over Amberlyst-36. At  $140^\circ\text{C}$  with 0.3 g Amberlyst-36 glycerol fractional conversion values and di-ether selectivity values approaching to 1.0 and 0.7, were highly promising.

Microporous, mesoporous and silicotungstic acid impregnated SAPO-34 catalysts were synthesized successfully in order to bring a new dimension to commercial solid acid catalyst for etherification reactions. Activity of mesoporous SAPO-34 and STA@Mesoporous SAPO-34 were tested in etherification of glycerol with i-butene. However it was seen that, these catalyst were not active in etherification of glycerol with i-butene.

Results proved that etherification of the biodiesel by-product glycerol could be successfully achieved by using 2M2B, as well as i-butene, to produce fuel oxygenates and improve the economics of biodiesel production.

**Keywords:** Glycerol,  $\text{C}_4$  and  $\text{C}_5$  olefins, etherification, biodiesel, SAPO-34, Amberlyst-36, Dowex DR-2030, Silicotungstic acid

## ÖZ

### BİYODİZEL YAN ÜRÜNÜ OLAN GLİSERİNİN ETERİFİKASYONU İLE OKSİJENLİ YAKIT KATKI MADDESİ ÜRETİMİ

İkizer, Burçin

Yüksek Lisans, Kimya Mühendisliği Bölümü

Tez Yöneticisi: Prof. Dr. Timur Doğu

Ortak Tez Yöneticisi: Doç. Dr. Nuray Oktar

Ağustos 2014, 146 sayfa

Biyodizel bitkisel ve hayvansal yağların düşük molekül ağırlıklı alkollerle (metanol/etanol) bazik bir katalizör varlığında transesterifikasyonu sonucu oluşan yenilenebilir çevre dostu petrol bazlı dizel yakıtına alternatiftir. Gliserol biyodizel üretim prosesinin önemli bir yan ürünüdür. Biyodizel üretiminin ekonomik olarak değer kazanması ancak yan ürün olan gliserolün değerlendirilmesi ile mümkün olacaktır. En dikkat çeken değerlendirme yöntemi gliserolün yakıt katkı maddesi oluşturmak için eterifikasyonudur. Bu çalışma kapsamında gliserolün C<sub>4</sub> (i-butene) ve C<sub>5</sub> [i-amilen; 2-Metil-2-Büten (2M2B)] i-olefinleri ile eterifikasyonu yakıt katkı maddesi üretmek amacıyla incelenmiştir. Ayrıca ticari katalizörlere alternatif olabilecek yeni nesil mezogözenekli SAPO-34 katalizörü sentezlenmiş ve gliserolün i-büten ile eterifikasyon reaksiyonunda aktivitesi test edilmiştir.

Gliserolün i-buten ile eterifikasyonu otoklav reaktörde ticari katı asit katalizörlerden olan, Amberlit-36, Dowex DR-2030 ve STA kullanılarak 70-120°C arasında çalışılmıştır. Reaktan olarak i-bütenin kullanıldığı gliserolün eterifikasyon reaksiyonu sonuçları, katalizörün Bronsted asiditesinin yanı sıra gözenek difüzyon direncinin katalitik aktiviteye olan etkisini ispatlamıştır. 80°C ve daha düşük

sıcaklıklarda yüksek asiditeye sahip Silikotungstik asit katalizörü en iyi performansı vermiştir. Fakat yüksek sıcaklıklarda i-bütenin oligomerleşme reaksiyonu hızlanmış ve bu durum gliserol dönüşümü üzerinde olumsuz etkiler yaratmıştır. Amberlit-36 ve Dowex DR-2030 katalizörleri 90 ve 120°C çok iyi performans göstermişlerdir.

Gliserolün 2-Metil-2-Büten (2M2B) ile eterifikasyonu da otoklav reaktörde ticari katı asit katalizörlerden olan Amberlit-36 ve Dowex DR-2030 kullanılarak çalışılmıştır. Amberlit-36 ve Dowex DR-2030 katalizörlerinin aktiviteleri oldukça benzer çıkmıştır ve katalizör miktarının artması gliserol dönüşümünü artırmıştır. Bu durum birim hacimdeki aktif sitelerin artması ile açıklanmıştır. Gliserolün 2M2B ile eterifikasyonu 120 ve 140°C’ de Amberlit-36 varlığında çalışılmıştır. Reaksiyon süresinin ve katalizör yüklemesinin gliserol dönüşümü ve ürün dağılımı üzerine etkisi incelenmiştir. 120 ve 140°C ‘de Amberlit-36 katalizörü varlığında gliserolün 2M2B ile eterifikasyonu mono-,di- ve tri- eterlerin oluştuğunu göstermiştir. 140°C’ de 0.3 g Amberlit-36 kullanıldığı durumda gliserol dönüşü ve di-eter seçiciliği sırasıyla 1.0 ve 0.7 olarak kaydedilmiştir.

Mikrogözenekli, mezogözenekli ve Silikotungstik asit emdirilmiş SAPO-34 katalizörleri ticari katalizörlere alternatif olarak başarılı bir şekilde sentezlenmiştir. Mezogözenekli SAPO-34 ve STA@Mezogözenekli SAPO-34 katalizörleri gliserolün i-büten ile eterifikasyonunda test edilmiş ve bu reaksiyon için aktif olmadıkları görülmüştür.

Sonuç olarak gliserolün eterifikasyonu i-büten ile olduğu gibi 2M2B ile de başarılı bir şekilde gerçekleştirilmiştir. Böylelikle yan ürün olan gliserol değerlendirilmiş ve biyodizel ekonomisine katkı sağlanmıştır.

**Anahtar Kelimeler:** Gliserol, C<sub>4</sub> ve C<sub>5</sub> olefinleri, eterifikasyon, biyodizel, SAPO-34, Amberlit-36, Dowex DR-2030, Silikotungstik asit

*To my family*

## ACKNOWLEDGEMENTS

I would like to express my sincerest gratitude to my supervisor Prof. Dr. Timur Dođu for the guidance he showed me in the extent of my thesis studies and for his help at the times of my frustration. His encouragement has enabled me to sustain my motivation throughout my thesis studies. Furthermore, I appreciate the contributions and welfare provided by Prof. Dr. Gölşen Dođu.

I would like to offer my sincere thanks to my co-supervisor Assoc. Prof. Dr. Nuray Oktar for her endless support and the times she shared with me all of her academic and personal life experiences during the time we spend together.

I would like to express my special thanks to Dr. Seval Gündüz and Dr. Nalan Özbay for their support for the endless sharing of their knowledge and experience with me and their grateful friendship.

I would like to express special thanks to my laboratory friends Arzu Arslan, Ayşegöl Bayat, Birce Pekmezci, Feride Akyavaşođlu, M.İlker Şener and Can Ağca who helped me in many ways.

I would like to thank my friends, Cennet Ceylan, Derya Köse, Özge Cebeci, Cemre Avşar for their valuable friendship and support through years. Furthermore, I express my special thanks to my friend and also my homemate, Tuğçe Kırbaş for her invaluable friendship and support during my studies.

I would like to thank Gazi University Chemical Engineering Department Kinetic Laboratory research group and technical staff for their positive manner and support during this study.

I would like to thank Prof. Dr. Bekir Salih, Assoc. Prof. Dr. Ömür Çelikbıçak and Burak Tavşanlı from Hacettepe University Department of Chemistry for Mass Spectrum analyses.

I would like to acknowledge every member of my family for getting me to where I am today. I thank my parents, Hasan and Hatice İkizer, for providing me every opportunity to succeed in life. My hats off to Emrah, my elder brother, for his financial support and Berrin, my elder sister, for her moral support and Baran, Berzan, Berfin, my adorable nephews, for the purest love they have bestowed all through this interval.

METU Scientific Research Coordination is acknowledged for the financial support with the research fund BAP-03-04-2013-008 and BAP-03-04-2014-002. The Scientific and Technological Research Council of Turkey (TÜBİTAK) is also acknowledged for the research fund 112M234 for their financial supports.

## TABLE OF CONTENTS

ABSTRACT .....	v
ÖZ.....	vii
ACKNOWLEDGEMENTS.....	x
TABLE OF CONTENTS .....	xii
LIST OF FIGURES .....	xvi
LIST OF TABLES.....	xix
NOMENCLATURE .....	xxi
CHAPTERS	
1. INTRODUCTION .....	1
2. BIODIESEL AS A TRANSPORTATION FUEL ALTERNATE.....	3
3. ETHERIFICATION OF GLYCEROL .....	9
3.1. ETHERIFICATION OF GLYCEROL WITH TERT-BUTYL ALCOHOL (TBA).....	9
3.2. ETHERIFICATION OF GLYCEROL WITH i-BUTENE .....	14
3.3. ETHERIFICATION OF GLYCEROL WITH 2-METHYL-2-BUTENE (2M2B) .....	18
4. POROUS MATERIALS .....	21
4.1. SILICOALUMINOPHOSPHATE-34 (SAPO-34).....	22
4.2. OBJECTIVE OF THE STUDY .....	27
5. EXPERIMENTAL STUDIES OF GLYCEROL ETHERIFICATION REACTIONS.....	29
5.1. CATALYSTS AND CHEMICALS .....	29
5.2. EXPERIMENTAL SETUP .....	31
5.2.1. Experimental Set-up of Etherification of Glycerol with i-butene .....	31
5.2.2. Experimental Set-up of Etherification of Glycerol with 2M2B .....	32
5.2.3. Operating conditions of Gas Chromatography and Calibration Factors .....	35
5.3. REACTION EXPERIMENTS.....	37
5.3.1. Reaction Experiments of Etherification of Glycerol with i-butene.....	37

5.3.2.	Reaction Experiments of Etherification of Glycerol with 2M2B .....	38
6.	EXPERIMENTAL STUDIES FOR SYNTHESIS OF SAPO-34 .....	41
6.1.	SYNTHESIS OF MICROPOROUS SAPO-34 CATALYST .....	41
6.2.	SYNTHESIS OF MESOPOROUS SAPO-34 CATALYSTS.....	43
6.2.1.	Synthesis of Mesoporous SAPO-34,(neutral).....	44
6.2.2.	Synthesis of Mesoporous SAPO-34,acidic .....	45
6.2.3.	Synthesis of Silicotungstic Acid Impregnated Mesoporous SAPO-34, (neutral) .....	45
6.3.	CHARACTERIZATION METHODS APPLIED FOR THE CATALYSTS .....	46
6.3.1.	X-Ray Diffraction (XRD) .....	46
6.3.2.	Nitrogen Physisorption .....	47
6.3.3.	Scanning Electron Microscopy (SEM) .....	47
6.3.4.	Diffuse Reflectance Infrared Fourier Transform Spectroscopy (DRIFTS) of Pyridine Adsorption.....	48
7.	RESULTS OF GLYCEROL ETHERIFICATION WITH I-BUTENE.....	49
7.1.	DRIFTS ANALYSIS RESULTS OF COMMERCIAL SOLID ACID CATALYSTS.....	52
7.2.	ETHERIFICATION OF GLYCEROL WITH i-BUTENE OVER AMBERLYST-36 CATALYST .....	53
7.2.1.	Effect of Temperature on glycerol conversion over Amberlyst-36 .....	54
7.2.2.	Effect of Temperature on Product Selectivity over Amberlyst-36 .....	55
7.3.	ETHERIFICATION OF GLYCEROL WITH i-BUTENE OVER DOWEX DR-2030 CATALYST .....	56
7.3.1.	Effect of Temperature on glycerol conversion over Dowex DR-2030.....	56
7.3.2.	Effect of Temperature on Product Selectivity over Dowex DR-2030 .....	57
7.4.	ETHERIFICATION OF GLYCEROL WITH i-BUTENE OVER SILICOTUNGSTIC ACID (STA) CATALYST .....	58
7.4.1.	Effect of Temperature on glycerol conversion .....	59
7.4.2.	Effect of Temperature on Product Selectivity with STA.....	60
7.5.	ACTIVITY COMPARISON OF DIFFERENT SOLID ACID CATALYSTS.....	61
7.5.1.	Effect of temperature on glycerol conversion obtained with different solid acid catalysts .....	61
7.5.2.	Effect of temperature on product selectivity obtained with different solid acid catalysts .....	64

8. RESULTS OF GLYCEROL ETHERIFICATION WITH 2-METHYL-2-BUTENE(2M2B) .....	67
8.1. GC/MS ANALYSIS RESULTS .....	67
8.1.1. Interpretation of Mass Spectrums from GC/MS Database.....	68
8.1.2. GC/MS analysis results of pure and binary chemical mixtures to obtain retention times.....	69
8.1.3. GC/MS analysis results for etherification of 2M2B (without glycerol) with A-36 .....	69
8.1.4. GC/MS analysis results for etherification of glycerol with 2M2B over A-36 .....	70
8.2. ETHERIFICATION OF GLYCEROL WITH 2M2B OVER COMMERCIAL SOLID ACID CATALYSTS.....	71
8.3. INFLUENCE OF CATALYST TYPE AND CATALYST AMOUNT ON GLYCEROL CONVERSION AND PRODUCT SELECTIVITY .....	73
8.3.1. Influence of catalyst type and catalyst amount on glycerol conversion .....	73
8.3.2. Influence of Catalyst Amount on Product Selectivity over Amberlyst-36 .....	74
8.3.3. Influence of Catalyst Amount on Product Selectivity over Dowex DR-2030 .....	75
8.4. INFLUENCE OF REACTION TEMPERATURE, REACTION TIME AND CATALYST AMOUNT ON GLYCEROL CONVERSION OVER A-36.....	76
8.5. INFLUENCE OF REACTION TEMPERATURE, REACTION TIME AND CATALYST AMOUNT ON PRODUCT SELECTIVITY OVER A-36.....	78
9. CHARACTERIZATION AND ACTIVITY RESULTS OF SAPO-34 CATALYSTS.....	81
9.1. CHARACTERIZATION RESULTS OF MICROPOROUS SAPO-34 CATALYST .....	81
9.1.1. X-Ray Diffraction (XRD) Result .....	81
9.1.2. N <sub>2</sub> Physisorption (BET) Result .....	82
9.1.3. Scanning Electron Microscopy Analysis (SEM).....	85
9.2. CHARACTERIZATION RESULTS OF MESOPOROUS SAPO-34 CATALYSTS .....	86
9.2.1. X-Ray Diffraction (XRD) Result .....	86
9.2.2. N <sub>2</sub> Physisorption (BET) Results.....	88
9.2.3. Scanning Electron Microscopy Analysis (SEM).....	92
9.3. CHARACTERIZATION OF STA@MESOPOROUS SAPO-34, (NEUTRAL).....	94

9.3.1.	N <sub>2</sub> Physisorption (BET) Results .....	94
9.3.2.	Scanning Electron Microscopy Analysis (SEM) .....	96
9.4.	DRIFTS ANALYSIS OF SYNTHESIS SAPO-34 CATALYSTS .....	98
9.5.	ACTIVITY RESULTS OF SYNTHESIS SAPO-34 CATALYSTS .....	99
10.	CONCLUSIONS.....	101
	REFERENCES .....	103
	APPENDICES .....	109
A.	XRD DATA AND PATTERNS .....	109
A1.	XRD DATA OF SAPO-34 .....	109
A2.	XRD PATTERN OF SiO <sub>2</sub> and AlPO <sub>4</sub> .....	110
B.	CALIBRATION FACTORS OF COMPONENTS IN ETHERIFICATION OF GLYCEROL WITH 2M2B.....	113
B1.	CALIBRATION FACTOR OF GLYCEROL FROM GLYCEROL AND ETHANOL MIXTURE (G:EtOH=1/8) .....	113
B2.	CALIBRATION FACTOR OF GLYCEROL AND 2M2B FROM GLYCEROL, ETHANOL AND 2M2B TERNARY MIXTURE .....	115
B2.1.	Calibration factor of glycerol and 2M2B from glycerol, ethanol and 2M2B ternary mixture (G:EtOH:2M2B=1:8:4).....	115
B2.2.	Calibration factor of glycerol and 2M2B from glycerol, ethanol and 2M2B ternary mixture (G:EtOH:2M2B; 0.5:8:2).....	117
B3.	CALIBRATION FACTORS OF REACTION PRODUCTS .....	118
B4.	CALIBRATION FACTOR OF DIMER.....	118
C.	CONVERSION AND SELECTIVITY CALCULATIONS OF ETHERIFICATION OF GLYCEROL WITH I-BUTENE.....	121
D.	GC/MS ANALYSIS RESULTS .....	127
D1.	MASS SPECTRUM OF GLYCEROL, 2M2B AND ETHANOL .....	127
D2.	GC/MS ANALYSIS RESULTS AND RETENTION TIMES .....	129
D3.	GC/MS ANALYSIS RESULTS FOR ETHERIFICATION OF 2M2B (WITHOUT GLYCEROL) OVER A-36.....	132
D3.1.	Matched molecules from the library of GC/MS (Wiley and Nist) for etherification of 2M2B (without glycerol) over A-36 .....	136
D4.	GC/MS ANALYSIS RESULTS FOR ETHERIFICATION OF GLYCEROL WITH 2M2B OVER A-36.....	138
E.	CONVERSION AND SELECTIVITY CALCULATIONS OF ETHERIFICATION OF GLYCEROL WITH 2M2B .....	141

## LIST OF FIGURES

### FIGURES

<b>Figure 1:</b> Transesterification reaction for biodiesel production [7].	4
<b>Figure 2:</b> Global Biodiesel production between 2000 and 2011 [16]	6
<b>Figure 3:</b> Reaction for Glycerol Etherification with tert-Butyl Alcohol (TBA)	10
<b>Figure 4:</b> Reaction for Glycerol Etherification with i-butene	15
<b>Figure 5:</b> Reaction for Glycerol Etherification with C <sub>5</sub> i-olefin (2-Methyl-2-Butene)	19
<b>Figure 6:</b> The crystal structure of Chabazite (CHA) [49]	24
<b>Figure 7:</b> X-Ray diffraction (XRD) pattern of SAPO-34 [53].	26
<b>Figure 8:</b> The experimental Set-up for etherification of glycerol with i-butene	33
<b>Figure 9:</b> The experimental Set-up for etherification of glycerol with 2M2B	34
<b>Figure 10:</b> The synthesis procedure for Microporous SAPO-34.	43
<b>Figure 11:</b> The synthesis procedure for Mesoporous SAPO-34, (neutral).	44
<b>Figure 12:</b> The synthesis procedure for STA impregnated Mesoporous SAPO-34, (neutral)	46
<b>Figure 13:</b> Drift spectrum of pyridine adsorbed solid acid catalysts.	52
<b>Figure 14:</b> Glycerol conversion vs. reaction temperature over Amberlyst-36	54
<b>Figure 15:</b> Product Selectivity vs. reaction temperature over Amberlyst-36	55
<b>Figure 16:</b> Glycerol conversion vs. reaction temperature over Dowex DR-2030.	57
<b>Figure 17:</b> Product Selectivity vs. reaction temperature over Dowex DR-2030.	58
<b>Figure 18:</b> Glycerol conversion vs. reaction temperature over STA.	59
<b>Figure 19:</b> Product Selectivity vs. reaction temperature over STA.	60
<b>Figure 20:</b> Glycerol conversion vs. reaction temperature with different catalysts.	61
<b>Figure 21:</b> Di-i-butene (DIB) selectivity vs. reaction temperature with different catalysts (Reaction time=6h, m <sub>cat</sub> =0.3 g).	64
<b>Figure 22:</b> Monoether selectivity vs. reaction temperature with different catalysts.	65

<b>Figure 23:</b> Diether selectivity vs. reaction temperature with different catalysts .....	66
<b>Figure 24:</b> Tri ether selectivity vs. reaction temperature with different catalysts ....	66
<b>Figure 25:</b> Glycerol conversion vs. catalyst amount (g) with different catalysts .....	73
<b>Figure 26:</b> Product selectivity vs. catalyst amount (g) over Amberlyst-36 catalyst .	75
<b>Figure 27:</b> Product selectivity vs. catalyst amount (g) over Dowex DR-2030 catalyst .....	76
<b>Figure 28:</b> Glycerol conversion values obtained at different; temperatures (120 and 140°C), reaction times (1, 3, 6, 12, 24 h) and catalyst amount ( $m_{cat}=0.3$ or 1 g, A-36) .....	77
<b>Figure 29:</b> Product Selectivity vs. Reaction time with Amberlyst-36 catalyst (Reaction Temperature =120°C, $m_{cat} =0.3$ g).....	79
<b>Figure 30:</b> Product Selectivity vs. Reaction time with Amberlyst-36 catalyst (Reaction Temperature =120°C, $m_{cat}= 1$ g).....	79
<b>Figure 31:</b> Product Selectivity vs. Reaction time with Amberlyst-36 catalyst (Reaction temperature =140°C, $m_{cat} =0.3$ g).....	80
<b>Figure 32:</b> XRD pattern of Microporous SAPO-34.....	82
<b>Figure 33:</b> Nitrogen physisorption isotherm of microporous SAPO-34.....	83
<b>Figure 34:</b> Pore Size Distribution of Microporous SAPO-34.....	84
<b>Figure 35:</b> SEM images of Microporous SAPO-34, (a) with 10000 magnification, (b) with 3000 magnification, (c) with 1500 magnification, (d) with 300000 magnification .....	85
<b>Figure 36:</b> The small angle XRD pattern of Mesoporous SAPO-34, (neutral) .....	86
<b>Figure 37:</b> The small angle XRD pattern of Mesoporous SAPO-34, acidic.....	87
<b>Figure 38:</b> The wide angle XRD pattern of Mesoporous SAPO-34, (neutral and acidic).....	88
<b>Figure 39:</b> Nitrogen physisorption isotherm of mesoporous SAPO-34, (neutral) ...	89
<b>Figure 40:</b> Nitrogen physisorption isotherm of mesoporous SAPO-34, acidic .....	89
<b>Figure 41:</b> Pore Size Distribution of mesoporous SAPO-34, (neutral and acidic) ...	91
<b>Figure 42:</b> SEM images of Mesoporous SAPO-34, (neutral), (a) with 50000 magnification, (b) with 3000 magnification, (c) with 1500 magnification, (d) with 250000 magnification .....	92

<b>Figure 43:</b> SEM images of Mesoporous SAPO-34, acidic, (a) with 120000 magnification, (b) with 2000 magnification, (c) with 1000 magnification, (d) with 240000 magnification.....	93
<b>Figure 44:</b> Nitrogen physisorption isotherm of STA@Mesoporous SAPO-34, (neutral) .....	94
<b>Figure 45:</b> Pore Size Distribution of STA@ Mesoporous SAPO-34, (neutral) .....	96
<b>Figure 46:</b> SEM images of STA@Mesoporous SAPO-34, (neutral), (a) with 120000 magnification, (b) with 15000 magnification, (c) with 2000 magnification, (d) with 250000 magnification.....	97
<b>Figure 47:</b> Drift spectrums of Microporous SAPO-34, Mesoporous SAPO-34, (neutral), Mesoporous SAPO-34, acidic and STA@Mesoporous SAPO-34, (neutral). .....	98
<b>Figure 48:</b> XRD pattern of SiO <sub>2</sub> .....	110
<b>Figure 49:</b> XRD pattern of AlPO <sub>4</sub> .....	111
<b>Figure 50:</b> Mass Spectrum of Glycerol .....	127
<b>Figure 51:</b> Mass spectrum of 2M2B.....	128
<b>Figure 52:</b> Mass spectrum of Ethanol .....	128
<b>Figure 53:</b> GC/MS analysis result of 2M2B to obtain retention time .....	129
<b>Figure 54:</b> GC/MS analysis result of ethanol to obtain retention time.....	130
<b>Figure 55:</b> GC/MS analysis of Glycerol to obtain retention times.....	131
<b>Figure 56:</b> GC/MS analysis results for etherification of 2M2B (without glycerol) over A-36.....	132
<b>Figure 57:</b> GC/MS analysis results for etherification of glycerol with 2M2B over A-36.....	138

## LIST OF TABLES

### TABLES

<b>Table 1:</b> Comparison of physical properties of Diesel and Biodiesel [10-12].....	5
<b>Table 2:</b> Structural properties of aluminophosphate based structures [46, 47].....	23
<b>Table 3:</b> Properties of Chabazite Structure [48].....	24
<b>Table 4:</b> Properties of chemicals used in the study.....	30
<b>Table 5:</b> Physical properties of the catalysts, used in this study.....	31
<b>Table 6:</b> Operating conditions of Gas Chromatograph (Adapted from [57]).....	35
<b>Table 7:</b> Calibration factors of components in etherification of glycerol with i-butene(Adapted from [58]) .....	36
<b>Table 8:</b> Calibration factors of components in etherification of glycerol with 2M2B .....	36
<b>Table 9:</b> Experimental conditions for etherification of glycerol with i-butene.....	37
<b>Table 10:</b> Experimental conditions for etherification of glycerol with 2M2B .....	40
<b>Table 11:</b> Mass/Charge ratio of glycerol, 2M2B and ethanol with the greatest relative abundance.....	68
<b>Table 12:</b> BET and BJH surface area, pore volume and size and micropore volume data of Microporous SAPO-34 .....	83
<b>Table 13:</b> BET and BJH surface area, pore volume and size and micropore volume data of Mesoporous SAPO-34, (neutral and acidic) .....	90
<b>Table 14:</b> BET and BJH surface area, pore volume and size and micropore volume data of Mesoporous SAPO-34 (neutral) and STA@Mesoporous SAPO-34,(neutral). .....	95
<b>Table 15:</b> Generalized X-ray diffraction data of SAPO-34 [51].....	109
<b>Table 16:</b> Area obtained from gas chromatography and calculated calibration factors of glycerol .....	114

<b>Table 17:</b> Area obtained from gas chromatography and calculated calibration factors of glycerol and 2M2B.....	116
<b>Table 18:</b> Area obtained from gas chromatography and calculated calibration factors of glycerol and 2M2B.....	117
<b>Table 19:</b> Calibration factors of components [63].....	118
<b>Table 20:</b> Area obtained from gas chromatography for reaction of 2M2B (without glycerol) with A-36 at T=140°C.....	120
<b>Table 21:</b> Calculated glycerol conversion and product selectivity values at different reaction temperatures over A-36. ....	124
<b>Table 22:</b> Calculated glycerol conversion and product selectivity values at different reaction temperatures over Dowex DR-2030.....	124
<b>Table 23:</b> Calculated glycerol conversion and product selectivity values at different reaction temperatures over STA.....	125
<b>Table 24:</b> Calculated glycerol conversion and product selectivity values at different reaction times over A-36, at T=120 °C, $m_{\text{cat}}=0.3$ g.....	144
<b>Table 25:</b> Calculated glycerol conversion and product selectivity values at different reaction times over A-36, at T=120 °C, $m_{\text{cat}}=1$ g.....	144
<b>Table 26:</b> Calculated glycerol conversion and product selectivity values at different reaction times over A-36, at T=140 °C, $m_{\text{cat}}=0.3$ g.....	145
<b>Table 27:</b> Calculated glycerol conversion and product selectivity values at different reaction times over A-36, at T=140 °C, $m_{\text{cat}}=1$ g.....	145
<b>Table 28:</b> Calculated glycerol conversion and product selectivity values over Dowex DR-2030, at T=120 °C, $m_{\text{cat}}=0.3$ and 1 g.....	146
<b>Table 29:</b> Calculated glycerol conversion and product selectivity values at over A-36, at T=120 °C, $m_{\text{cat}}=0.3$ and 1 g.....	146

## NOMENCLATURE

BET: Nitrogen Physisorption

$\beta$ : Calibration factor

CHA: Chabazite

DRIFTS: Diffuse Reflectance Infrared Fourier Transform Spectroscopy

EtOH: Ethanol

FID: Flame Ionization Detector

G: Glycerol

GC: Gas Chromatography

IB: i-butene

MS: Mass Spectrum

MW: Molecular weight (g/mol)

n: Mole

P: Pressure (bar)

S: Selectivity

SAPO: Silicoaluminophosphate

SEM: Scanning Electron Microscopy

T: Temperature ( $^{\circ}$ C)

TBA: Tert- Butyl alcohol

$X_i$ : Mole fraction of component i

XRD: X-Ray Diffraction



## **CHAPTER 1**

### **INTRODUCTION**

Rapid depletion of petroleum, opened a new and ongoing research for the production of alternative transportation fuels from non-petroleum feedstock [1]. Biodiesel, which is a renewable and environmentally friendly alternative to petroleum based diesel fuel, is produced by trans-esterification of vegetable oils and animal fats with lower molecular weight alcohols (methanol/ethanol), in presence of a basic catalyst. Use of biodiesel in place of petroleum derived diesel provides some advantages such as; being biodegradable, non-toxic, having higher flash point, lower emission of pollutants, and similar or higher cetane number. Glycerol is the main side product of biodiesel production process and one mole of glycerol is produced for every three moles of methyl esters. This corresponds to about 10 % wt of the total biodiesel produced. Production of biodiesel is expected to increase significantly in the coming years, due to the developing economic and environmental policies. Hence, a remarkable surplus of glycerol will be generated as a result of increase in biodiesel production. Economics of biodiesel production strongly depends upon the efficient utilization of its by-product glycerol [2].

In Chapter 2, information about biodiesel and physical properties of biodiesel are presented and compared with petroleum based diesel. Possible alternative ways for glycerol utilization and the most attractive way its etherification for the production of fuel oxygenates are also proposed.

In Chapter 3, the literature survey on the etherification of glycerol with tert-butyl alcohol (TBA), i-butene and also 2-Methyl-2-Butene (2M2B) is given with the aim of oxygenates production.

Heterogeneous solid acid ion exchange resins are very active for etherification reaction because of high acidity however their thermal stability is very low. Acidic mesoporous SAPO-34 can be an alternative to ion exchange resins in etherification reactions due to high thermal stability and less plugging of pores. In Chapter 4, brief information about porous materials is given and detailed literature survey is conducted about SAPO-34 catalyst.

In Chapter 5, detailed information about commercial solid acid catalyst and chemicals used in this study are given. Experimental Set-up and experimental studies carried out for etherification of glycerol with i-butene and 2M2B are represented.

The synthesis procedure of Microporous, Mesoporous SAPO-34, and Silicotungstic acid (STA) impregnated Mesoporous SAPO-34 are explained and the characterization techniques applied in this study are presented in Chapter 6.

In Chapter 7, results corresponding to etherification of glycerol with i-butene over commercial solid acid catalysts namely; A-36, Dowex DR-2030 and STA are given. Besides activity of commercial solid acid catalysts were compared. In Chapter 8, GC/MS analysis results are given in order to determine product properties by the etherification of glycerol with 2M2B. Besides results of glycerol etherification with 2M2B over commercial catalysts are presented. Characterization results of the synthesized catalyst and their activity test in etherification of glycerol with i-butene are given in Chapter 9. Finally, conclusions of this study are displayed in Chapter 10.

## CHAPTER 2

### BIODIESEL AS A TRANSPORTATION FUEL ALTERNATE

Transportation and industry are the biggest energy consumption sectors. As a result of fast growth of population, energy consumption grows at an extremely fast rate. International Energy Agency (IEA) reported that in 2030, the world will need 50% more energy than nowadays [3]. World energy demand is mostly provided by limited fossil fuel sources such as oil, natural gas and coal. Fossil fuel sources are not endless and decreases from day to day. As a result, CO<sub>2</sub> emissions from combustion of fossil fuels are also increasing at a fast rate.

To meet worlds growing energy needs and to decrease environmental consequences as well as difficulties in the supply and variability of oil prices, opened a new and ongoing research area for the production of alternative transportation fuels from non- petroleum feedstock [1,4]. As an alternative to fossil fuels, biomass has drawn attention especially in growing countries, to decrease petroleum dependence. Biomass is an abundant and renewable energy source and has a potential to verify economic development and clean environment [5]. Using biomass as fuel resource may contribute to decrease carbon dioxide, SO<sub>x</sub> and NO<sub>x</sub> emissions and may have an important effect on reducing landfills.

Diesel is the most used fossil based transportation fuel and has harmful effects on environment and also human health. Biodiesel is a well-known biomass based alternative fuel and has a potential to replace petroleum diesel. Biodiesel can be used directly in modified motor vehicles or may also be used by blending with

petroleum diesel or gasoline [5]. In Europe, objective and arrangements consistent with the energy statute law (Directive 2009/28/EC) declare that, by the end of 2020 transportation fuels should contain 10% from renewable energy sources [6]. This type of policy and being eco-friendly will result in increase of biodiesel production in future years.

Biodiesel is a mixture of monoalkyl esters, produced by transesterification of vegetable oils and animal fats with alcohols, in the presence of a basic catalyst. The transesterification reaction, which produces biodiesel, is given in Figure 1.

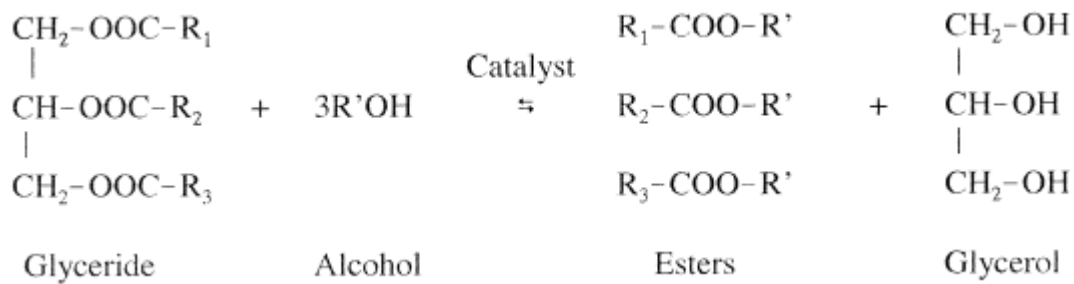


**Figure 1:** Transesterification reaction for biodiesel production [7].

As shown in this reaction stoichiometry, one mole of glycerol is produced as a side product, together with three moles of esters. Transesterification reaction occurs in three consecutive reaction steps. The first step is formation of diglycerides from triglycerides, second step is formation of monoglycerides from diglycerides and the last step is formation of glycerol from monoglycerides. Various alcohols can be used in transesterification reactions. Due to their low cost, methanol and ethanol are widely used in transesterification reactions [8].

Using biodiesel instead of petroleum-derived diesel as fuel alternative has drawn attention due to its attractive fuel characteristics. In Table 1, physical properties of diesel and biodiesel are given. Cetane number of biodiesel is 51.5, which is higher than petroleum based diesel. Cetane number is an important fuel characteristic and higher cetane number means better combustion quality, lower noise and long motor

life [9]. Higher oxygen content and its sulfur free nature are important fuel properties of biodiesel, in reducing emission and smokeless combustion.

**Table 1:** Comparison of physical properties of Diesel and Biodiesel [10-12]

<b>Properties</b>	<b>Diesel</b>	<b>Biodiesel</b>
Chemical Formula	$C_{10.8}H_{18.7}$	$C_{18.74}H_{34.43}O_2$
Molecular weight (g/mol)	148.3	291.62
Density ( $g/cm^3$ @20°C)	0.84	0.8814
Cetane Number	45	51.5
Boiling Point (°C)	180-330	315-350
Flash Point (°C)	62	146
Carbon content (wt %)	87.4	77.10
Oxygen content (wt %)	-	10.97
Sulphur content (wt %)	~ 0.0476	~ 0

The advantages of using biodiesel as an alternative fuel can be listed as follows; biodegradable, renewable energy source, high efficiency in combustion due to oxygen content, almost no  $CO_x$  and  $SO_x$  emission, blending ability with gasoline and petroleum diesel. Such advantages and country policies has increased biodiesel production sharply. Figure 2 represents Global Biodiesel production between 2000 and 2011. In the early 2000s, biodiesel production was negligibly small. However, in 2011 biodiesel production reached to 21 Billion Liters. Glycerol is the main side product of Biodiesel production and one mole of glycerol is produced for every three moles of methyl esters in transesterification reaction [13]. This corresponds to about 10 wt.% of the total biodiesel produced. Production of biodiesel is expected to increase significantly, due to economic and environmental policies of countries. Hence, a remarkable surplus of glycerol will be generated as a result of increase of biodiesel production. Economics of biodiesel production strongly depends upon the efficient utilization of its byproduct glycerol [2, 14, 15].

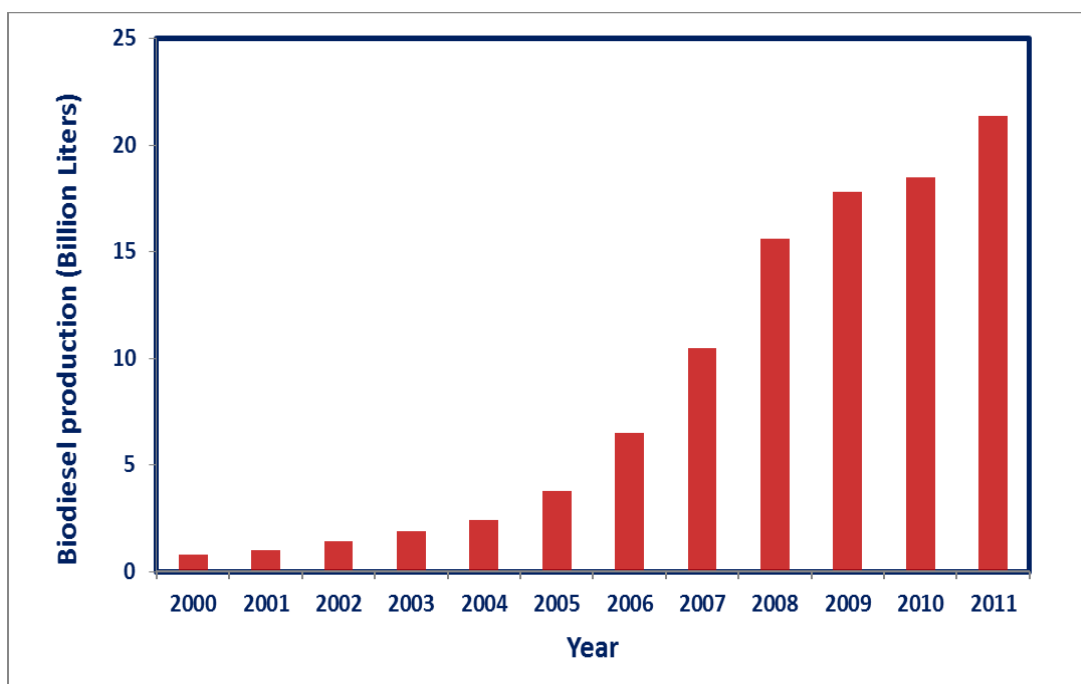


**Figure 2:** Global Biodiesel production between 2000 and 2011 [16]

Glycerol (1,2,3-propanetriol) is a non-toxic, viscous, colorless, odorless alcohol having a chemical formula of  $C_3H_8O_3$ . Glycerol is a highly viscous liquid at standard pressure and temperature and it is soluble in alcohols and water [17]. Glycerol can be used as a heating fuel due to its flammability property but the high viscosity, high ignition temperature and low calorific value limit its widespread use as a fuel. Nowadays glycerol is used in various applications including, food, medicine, cosmetics and polymers.

Some of the possible alternative ways for glycerol utilization are; acrolein production by dehydration, hydrogen and synthesis gas production by reforming, selective oxidation for dihydroxyacetone, production of 1,3-propanediol, and its esterification/etherification [18].

Glycerol can be used in acrolein production by its dehydration. Acrolein is a remarkable raw material for medicines, super absorber polymers, acrylic acid esters and detergents. Dehydration of glycerol has a potential to contribute positive effects

on biodiesel production process economy besides it can be recommended as an alternative to the present acrolein technology based on fossil fuel derived propylene [19-22].

Another attractive way for glycerol utilization is hydrogen production by reforming. Hydrogen is a clean, renewable energy source and an important fuel for fuel cell applications which has a potential to be the energy source of the future. Steam reforming, liquid phase reforming, supercritical water reforming, photocatalytic conversion, autothermal reforming are main routes for production of hydrogen from glycerol. The utilization of biodiesel by-product glycerol to produce synthesis gas or hydrogen could be an important renewable input for petrochemical industry [23-27].

In biotechnological application, glycerol can be used in 1,3-propanediol production by bacteria in fermentation reactions. 1, 3-propanediol has a wide use in chemical and pharmaceutical industries, for instance; production of polymers such as polyesters, polypropylene and polyurethanes and as an additive/solvent for lubricants. Nowadays 1,3-propanediol is produced from acrolein but this process is difficult, inefficient and costly. Fermentation of glycerol to 1,3-propanediol has a potential to reduce excessive glycerol and also polymers which are produced from glycerol are biodegradable [28,29].

Among these possible glycerol utilization processes, its etherification with C<sub>4</sub> olefin (i-butene) or tert-butyl alcohol (TBA) is considered as an attractive route for the production of fuel oxygenates. Etherification of glycerol with i-butene or tert-butyl alcohol can produce two mono-tert-butyl glycerol ether isomers (3-tert-butoxy-1,2-propanediol (MTBG1) and 2-tert-butoxy-1,3-propanediol (MTBG2)), two di-tert-butyl glycerol ether isomers (2,3-ditert-butoxy-1-propanol (DTBG1) and 1,3-ditert-butoxy-2-propanol (DTBG2)), and a tri-tert-butyl glycerol ether (1,2,3-tritert-butoxy-propane (TTBG)). Glycerol tertiary ethers were published to have high octane numbers between 91-99 (BMON, "blending motor octane number") and 112-128 (BRON, "blending research octane number") and can be used as gasoline

additives for octane enhancement. They can also be mixed with biodiesel to increase its amount and improve the economics. The solubility of mono ethers (MTBG) in diesel is quite low. Whereas di-ethers (DTBG) and tri-ethers (TTBG) are highly soluble in diesel and gasoline. They are considered as excellent fuel components which can be added to gasoline, instead of current commercial oxygenate additives, such as MTBE, ETBE and TAME. Blending of these ethers with diesel has an important positive effect in terms of reduction of particular matter, carbon monoxide and hydrocarbons emissions. Furthermore these ethers can lower the cloud point and viscosity of the fuels [2, 14, 15].

## CHAPTER 3

### ETHERIFICATION OF GLYCEROL

As mentioned in the previous chapter, glycerol is the main side product in the biodiesel production process. The economic aspect of biodiesel production strongly depends on effective utilization of its by-product glycerol. In this chapter, the literature survey on the etherification of glycerol with tert-butyl alcohol (TBA), i-butene and also 2-Methyl-2-Butene (2M2B) is given with the aim of oxygenates production.

#### 3.1. ETHERIFICATION OF GLYCEROL WITH TERT-BUTYL ALCOHOL (TBA)

Etherification of glycerol with tert-butyl alcohol (TBA) in the presence of an acid catalyst is expected to produce two mono-tert-butyl glycerol ether isomers (3-tert-butoxy-1,2-propanediol (MTBG1) and 2-tert-butoxy-1,3-propanediol (MTBG2)), two di-tert-butyl glycerol ether isomers (2,3-ditert-butoxy-1-propanol (DTBG1) and 1,3-ditertbutoxy- 2-propanol (DTBG2)), and a tri-tert-butyl glycerol ether (1,2,3-tritert-butoxy-propane (TTBG)). The reaction steps are shown in Figure 3. Besides these main reactions, dehydration of tert-butyl alcohol (TBA) to i-butene may also take place as a side reaction. The main advantage of using tert-butyl alcohol (TBA) instead of isobutene, in the etherification reactions is that glycerol is highly soluble in TBA and solvent is required. Disadvantage of etherification of glycerol with tert-butyl alcohol (TBA) is formation of water as the second product during the reaction

process. Water negatively affects the equilibrium by decreasing glycerol conversion and also adsorption of water on the acid sites of the catalyst may cause deactivation. Parameters such as; catalyst type, reaction temperature, molar ratio of reactants, and reaction time, can affect etherification reaction rate, glycerol conversion and product distribution. In the literature, etherification of glycerol was studied in presence of homogeneous or heterogeneous catalysts.

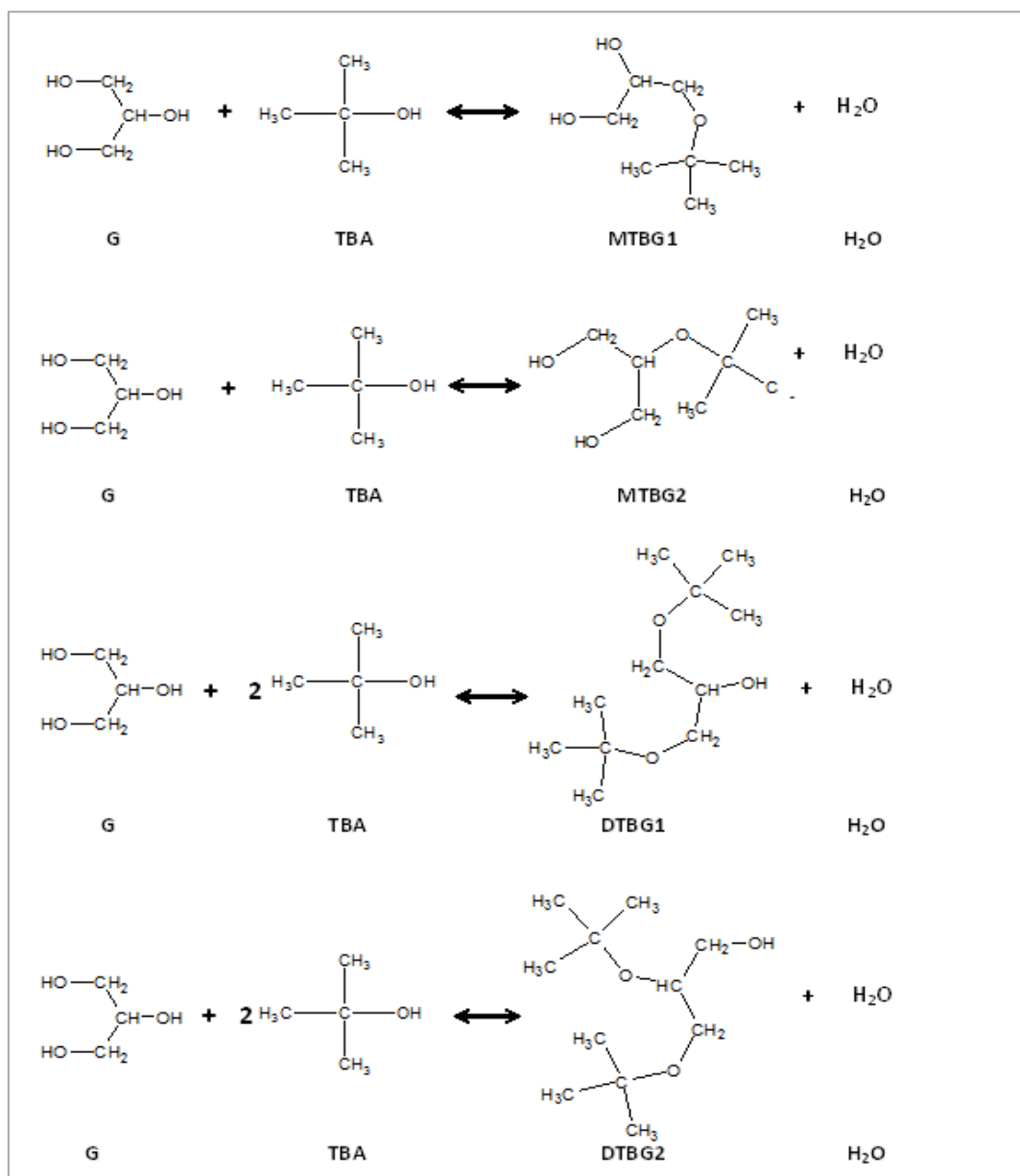


**Figure 3:** Reaction for Glycerol Etherification with tert-Butyl Alcohol (TBA)

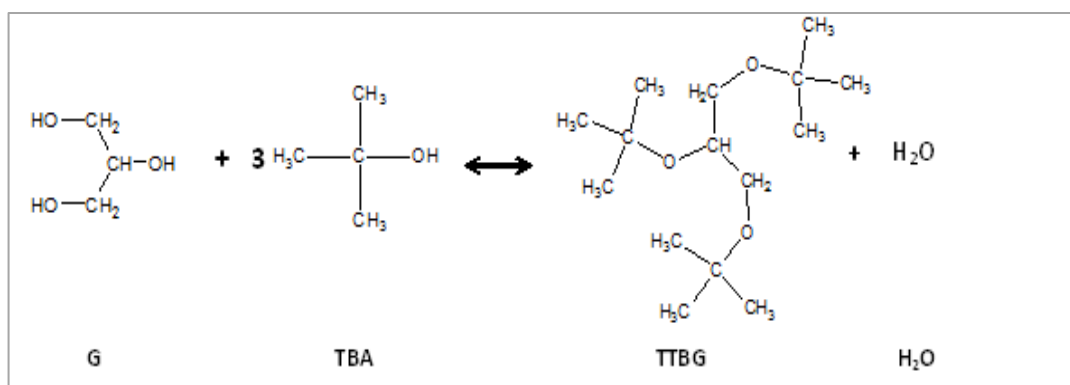


**Figure 3:** Reaction for Glycerol Etherification with tert-Butyl Alcohol (TBA)  
(continued)

Etherification of glycerol with tert-butanol (TBA) in a fixed bed continuous flow reactor was first investigated by Özbay et al. [14]. Activities of commercial solid acid catalysts, such as Amberlyst-15 (A-15), Amberlyst-16 (A-16) and Amberlyst-35 (A-35), Nafion-SAC-13 and  $\gamma$ -alumina were compared. In short residence time of about 20 seconds, nearly 50 % glycerol conversion was recorded with Amberlyst-15 (A-15) at 110°C. Comparison of catalytic activities of Amberlyst type polymeric ion exchange resins was found as A-15>A-35>A-16. At higher temperatures activity of Nafion-SAC-13 was increased.

Özbay et al.[15] also investigated the effect of feed composition, temperature (70-110°C) and reaction pressure (1-5 atm) on glycerol conversion and product distribution during etherification of glycerol with TBA. Reaction was carried out with acidic ion-exchange resin Amberlyst-15 (A-15) in a fixed bed continuous flow and autoclave reactors. In the fixed bed continuous flow reactor glycerol conversion was recorded as 66%, at 110°C with a TBA/G molar ratio of 8/1 and at a space time of 18 s.g.cm<sup>-3</sup>. In the case of autoclave reactor with the same conditions mentioned above, glycerol conversion reached to 90% after 400 minutes of reaction time. Results showed the advantages of flow reactor to achieve quite high glycerol conversion values in very short residence times. To adsorb the water produced with

dehydration of tert-butanol (TBA), Zeolite 4A and 5A were physically mixed with the catalyst. Results showed that performance of Zeolite 4A was better than 5A.

Importance of Bronsted acidity of the catalyst used for etherification of glycerol with tert-butanol (TBA) reaction is also discussed in a study of Gonzales et al. [30]. They studied etherification of glycerol with tert-butanol (TBA) over commercial mordenite, beta and ZSM-5 zeolites and zeolites were modified with several different methods to increase the acidity. Reactions were carried out in autoclave reactor at 75 and 90°C and the activity of zeolites were compared with Amberlyst-15 (A-15) resin. They reported that activity comparison was in order as A-15 > beta > ZSM-5 > mordenite and in a good agreement with their Bronsted acid sites strength. Formation of glycerol tri-ether were sterically hindered.

Another comprehensive study was made by Ozbay et al. [2] on etherification of glycerol with tert-butanol (TBA) in continuous flow and batch reactors catalyzed by commercial solid acid catalysts, Amberlyst-15, Amberlyst-35, Amberlyst-36, Amberlyst-16, Lewatit K2629, Relite EXC8D, H-Beta, H-Mordenite and Nafion SAC-13. Considering the stability of the catalysts, reaction temperature was selected between 80°C and 200°C. Results proved the advantages of flow reactors in terms of achieving very high conversions at quite low residence times. Amberlyst 15 showed the highest glycerol conversion at 90 and 100°C and this result was consistent with its highest Bronsted acidity. Lewatit K2629, Amberlyst-35 and Amberlyst-36 had similar Bronsted acidity and glycerol conversion values were nearly same for these three resins. Between 110 and 130°C highest glycerol conversion recorded with Amberlyst-36 was due to lower crosslinking degree/higher accessibility of reactants to the active sites. Ether selectivity was mainly towards mono-ethers and most of the resin catalysts gave similar mono- and di-ether selectivities.

Klepacova et al. [31] studied etherification of glycerol with tert-butanol in an autoclave reactor and activity of Amberlyst-15 (A-15) resins, and two large pore zeolites namely H-Beta and H-Y were compared at 90°C with TBA/G molar ratio 4:1. Maximum glycerol conversion was recorded in case of Amberlyst -15 (A-15) as

96%. At the same reaction conditions di-ether selectivity was 45% with H-Beta and 25% with A-15. Zeolite H-Y was not so active as the other two catalysts.

Frusteri et al.[32] studied etherification of glycerol with tert-butanol (TBA) in a batch reactor and tested activity of lab made silica supported solid acid catalysts and commercial acid ion-exchange resins, Nafion on amorphous silica and Amberlyst-15 (A-15). Due to high acidity of Amberlyst-15 (A-15), glycerol conversion values were relatively high compared with other catalysts. Low catalyst/glycerol ratio (1.2 wt. %) was sufficient to achieve high glycerol conversion.

### 3.2. ETHERIFICATION OF GLYCEROL WITH *i*-BUTENE

Etherification of glycerol with C<sub>4</sub> *i*-olefin (*i*-butene) occurs following three consecutive reversible reaction steps over the solid acid catalysts. The reaction steps giving the products; mono-*tert*-butyl glycerol ether isomers (3-*tert*-butoxy-1,2-propanediol; MTBG1 and 2-*tert*-butoxy-1,3-propanediol; MTBG2), two di-*tert*-butyl glycerol ether isomers (2,3-ditert-butoxy-1-propanol; DTBG1 and 1,3-ditertbutoxy-2-propanol; DTBG2), and tri-*tert*-butyl glycerol ether (1,2,3-tritert-butoxy-propane; TTBG), are shown in Figure 4. Besides these reactions; oligomerization and the hydration of C<sub>4</sub> *i*-olefin (*i*-butene) are two side reactions, which might take place in the reactor [33]. Oligomerization of *i*-butene is not desired and has a negative effect on ether yields. However, as a result of hydration of *i*-butene, TBA may form, which may also react with glycerol to produce the ethers. Solubility of glycerol in *i*-butene is quite low and as a result, mass transfer resistances play a significant role on the observed rate of etherification. Use of a solvent has been recommended to enhance the rate of etherification of glycerol with *i*-butene.

Parameters such as; catalyst type, reaction temperature, molar ratio of reactants, reaction time, solvent type can affect etherification reaction rate, glycerol conversion and product selectivity values. In the literature, etherification of glycerol was studied by using homogeneous or heterogeneous catalysts and all of these studies were performed in batch reactors.

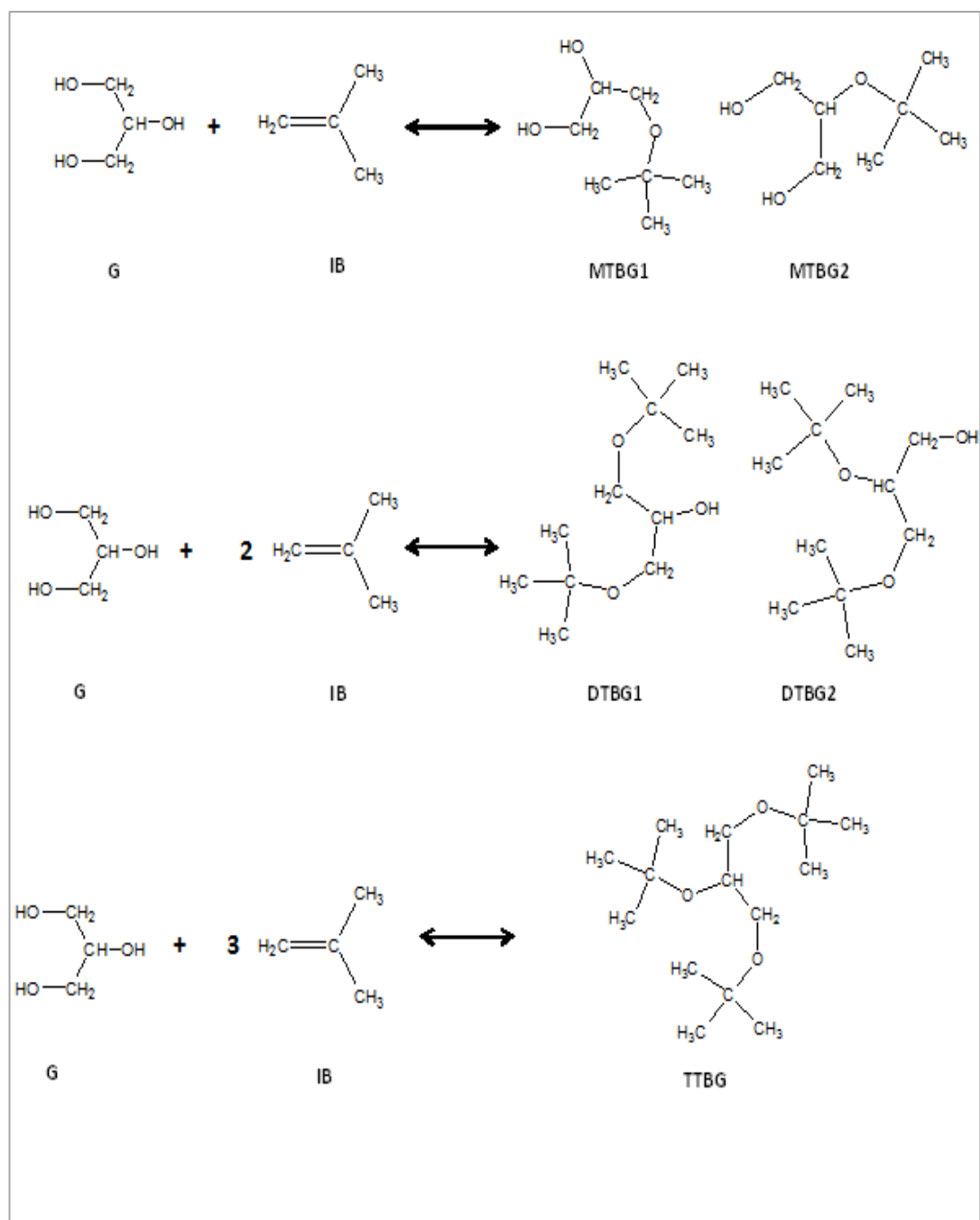


**Figure 4:** Reaction for Glycerol Etherification with i-butene

Melero et al. [34] conducted etherification of glycerol with i-butene over two sulfonic acid modified mesostructured silicas namely, Propylsulfonic and Arenesulfonic-acid-functionalized mesostructured silica. At 75°C with IB:G molar ratio of (4/1) in an autoclave reactor up to 100% glycerol conversion 54% di-ether and 41% tri-ether selectivity values were obtained with arenesulfonic-acid. In the case of Propylsulfonic acid, 90% glycerol conversion 56% di-ether and 35% tri-ether selectivity were achieved. I-butene oligomerization was not observed under any reaction conditions.

Increase of the catalytic performance of commercial HY zeolite as a result of acid treatment was reported by Xiao et al. [35]. Compared to commercial HY, both nitric acid and of citric acid treatments increased glycerol conversion and selectivities to DTBG and TTBG. One molar citric acid treatment and 0.5 M nitric acid treatment resulted in the same glycerol conversion of nearly 84%.

Karinen et al. [36] conducted etherification of glycerol with i-butene in the presence of Amberlyst-35, in a batch reactor. Effects of reaction temperature and IB/GLY molar ratio on product distribution were studied. Best diether selectivity (above 60 %) was recorded at 80°C with an IB/GLY molar ratio of 3. Oligomerisation reaction rates increased more rapidly as a function of temperature than etherification reaction rates and therefore above 80°C, selectivity to ethers decreased.

Klepacova et al.[37] observed the effect of solvent, catalyst type and temperature on the etherification of glycerol with i-butene, catalyzed by strong acidic ion-exchange resins Amberlyst-15 and -35, p-toluenesulfonic acid and by two large-pore zeolites H-Y and H-Beta. The etherification over zeolite H-Y was slower, equilibrium state was not achieved during first 8 h and formation of dimers was very low and as a result the highest glycerol conversion of 88.7% was achieved. Over zeolite H-Beta, formations of di-ethers were maximum but tri-ethers were sterically hindered. As temperature increased, oligomerization reaction rates to form C<sub>8</sub> alkenes increased and caused some decrease of glycerol conversion. Different solvents (dioxane,

dimethyl sulfoxide and sulfolane) were tested to eliminate or reduce mass transfer effects. Maximum solubility of C<sub>4</sub> i-olefin (i-butene) was obtained in dioxane.

Frusteri et al.[33] prepared different solid acid catalysts using different silica sources namely, spherical silica (MS3030,ES70Y) and Fumed silica (LM50) and as acid precursors Hyflon Ion S4X perfluorosulfonic ionomers. These catalysts were tested in etherification of glycerol with i-butene and activity results were compared with Amberlyst-15 resin. Results indicated that catalysts prepared by using spherical silica were the most active catalyst in glycerol conversion and also di and tri-ether selectivity. Optimal reaction conditions were recorded with A-15 as, IB/GLY molar ratio (3:1) at 70°C and 6 h reaction time.

Etherification of glycerol with i-butene with Amberlyst-15 (powder and beads) ionic resin, p-toluenesulfonic acid, silicotungstic acid, cesium salt of silicotungstic acid, and ionic liquid containing sulfonic acid groups was studied by Lee et al.[38]. Compared to Amberlyst-15 beads, Amberlyst-15 powder gave better results, showing complete glycerol conversion within 30 minutes. Among homogeneous catalysts, silicotungstic acid showed higher yield in di-i-butene (DIB) formation. High acidity and characteristic Keggin structure of silicotungstic acid increased di-i-butene (DIB) formation.

### 3.3. ETHERIFICATION OF GLYCEROL WITH 2-METHYL-2-BUTENE (2M2B)

Etherification of glycerol with 2-Methyl-2-Butene is another possible route for producing fuel oxygenates. Nearly 10% C<sub>5</sub> reactive olefins are present in FCC gasoline. In the literature, there are some studies for the etherification of these olefins with methanol or ethanol to produce some octane enhancing oxygenates [39]. However, to our knowledge there is no published work for the investigations of experimental conditions on glycerol conversion and product distributions in etherification of glycerol with C<sub>5</sub> reactive olefins. Etherification of glycerol with C<sub>5</sub> i-olefins (2M2B and 2M1B) is considered to contribute positively to the economics of biodiesel production and also decrease the harmful effects on environment and human health of these olefins.

Etherification of glycerol with C<sub>5</sub> i-olefin (2-Methyl-2-Butene) is an acid catalyzed and sequential reaction. With the standpoint of etherification of glycerol with tert-butyl alcohol (TBA) and C<sub>4</sub> i-olefin (i-butene), it is expected to form five ethers. These ethers are two monoethers [(2-(tert-pentyloxy)propane-1,3-diol and 3-(tert-pentyloxy)propane-1,2-diol], two diethers [(2,3-bis(tert-pentyloxy)propan-1-ol and 1,3-bis(tert-pentyloxy)propan-2-ol] and one triether [2-[(1,3-bis(tert-pentyloxy)propan-2-yl]oxy-2-methylbutane]. The reaction steps are shown in Figure 5 [18]. We denote these ethers herein as ME1, ME2, DE1, DE2 and TE, respectively.

Izquierdo et al.[18] used a molecular behavior simulation program to investigate the properties of the possible ethers produced with C<sub>5</sub> i-olefins (2M2B). Compared with ethers derived from i-butene, ethers derived from C<sub>5</sub> i-olefins (2M2B) had higher boiling, melting temperature and lower enthalpy of formation. Results recommended that formation of ethers produced from etherification of C<sub>5</sub> i-olefins (2M2B) were more exothermic.

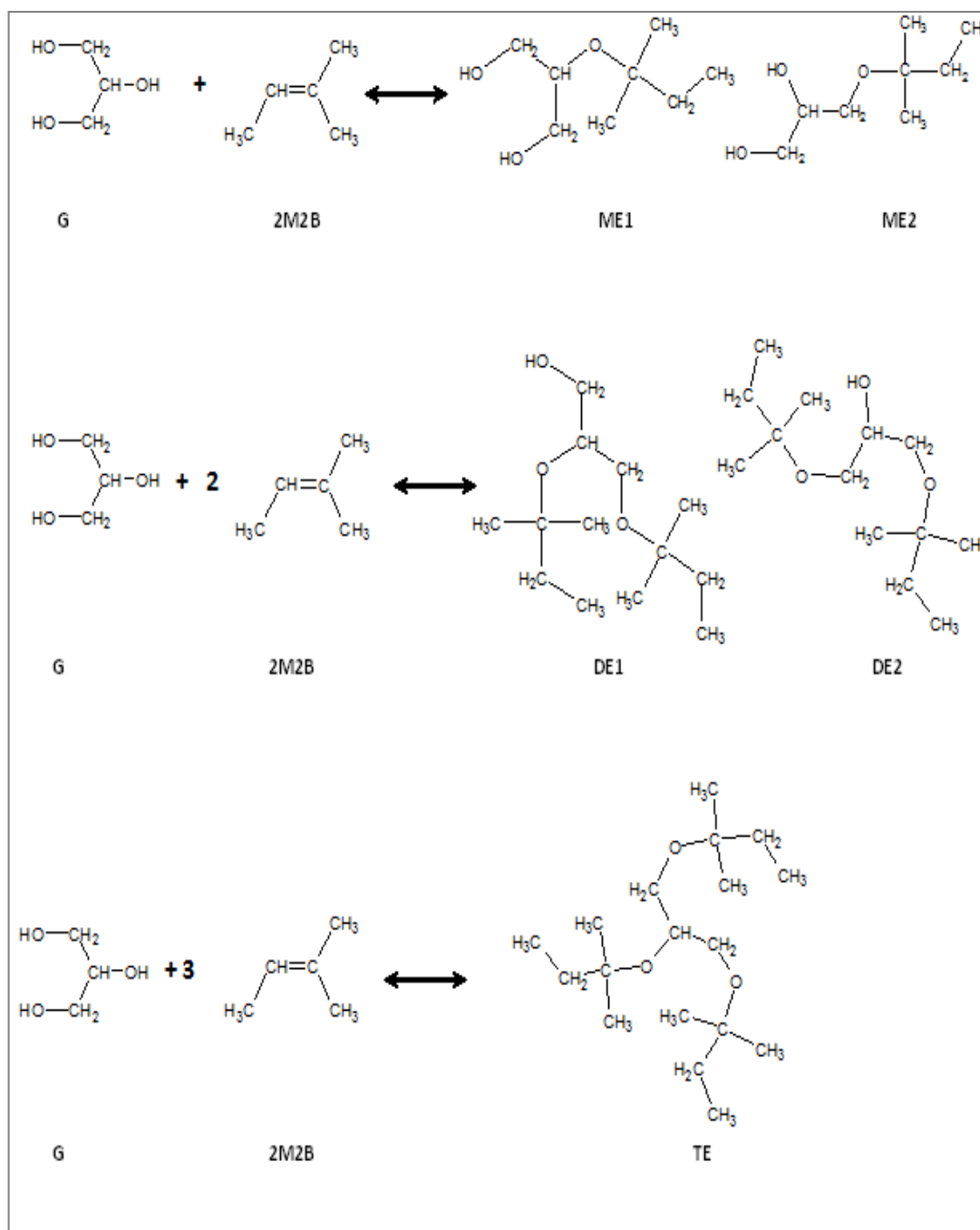


**Figure 5:** Reaction for Glycerol Etherification with C<sub>5</sub> i-olefin (2-Methyl-2-Butene)



## CHAPTER 4

### POROUS MATERIALS

Etherification of glycerol can be carried out using heterogeneous solid acid ion exchange resins. These resins are very active for etherification reaction because of high acidity however their thermal stability is very low. Acidic mesoporous SAPO-34 can be an alternative to ion exchange resins in etherification reactions due to high thermal stability and less plugging of pores. In this chapter brief information about porous materials is given and detailed literature survey is conducted about SAPO-34 catalysts.

Microporous, mesoporous and macroporous materials are the classification of porous materials according to IUPAC definition. Microporous materials have pore diameter less than 2 nm, mesoporous materials have pore diameter between 2 nm and 50 nm and macroporous materials have pore diameter larger than 50 nm [40].

Microporous materials, particularly zeolites, draw great attention in industrial areas such as; oil refining, petrochemistry and chemical synthesis and their usage as adsorbents is also significant.

Their great performance in catalysis depend on [41];

- High surface area and adsorption capacity
- Controlled adsorption properties; between hydrophobic and hydrophilic
- Generation of active sites (acid sites) in the framework

- Strong electric fields and electronic confinement are accountable for a preactivation of the reactants
- Their complex channel structure can be shape selective to assist the given catalytic reaction towards the desired product, avoiding the side reactions

Catalytic activities listed below made zeolites benefit only for applications which requires molecules lower than 1-1.2 nm pore diameters. Besides microporous materials involve some problems such as; diffusion limitations on the observed reaction rate and rapid deactivation due to coke formation. Therefore zeolites with larger pore diameters became an important research area and bring researchers to a new region called 'mesoporous'. Researchers at Union Carbide find out  $\text{AlPO}_4$  structures which includes aluminum and phosphorous in a pore size range between 1.3-1.5 nm. After a short time related materials such as SAPO's (silicoaluminophosphates) and MeAPOs (metal aluminophosphates) were synthesized [40].

#### **4.1. SILICOALUMINOPHOSPHATE-34 (SAPO-34)**

Aluminophosphate molecular sieves (AIPO) are important materials due to wide usage in catalytic applications. Substitution of silicon into  $\text{AlPO}_4$  framework create SAPO's [42]. SAPO's comprised of three dimensional networks of silicon, aluminum, and phosphorous. Si substitution into the neutral framework of AIPOs molecular sieve resulted in unbalanced electric charges. Brønsted acid sites are formed with neutralization of these negative charges and increase the acidity. Substitution of silicon into aluminophosphate framework can occur in three different ways. In the first way silicon instead of aluminum, in the second way silicon instead of phosphorus, and in the third way instead of two silicons for one aluminum and one phosphorus. Studies has shown that silicon substitution in first way was not efficient. The second way resulted only in Brønsted acid sites whereas in the third way acid strength increased [43-45].

Aluminophosphate-based molecular sieves are shown as  $\text{AlPO}_4\text{-n}$ . ‘n’ is a number and gives information about structure type. Without considering the framework composition same number is used for same structure type. Pore size and structure type for  $\text{AlPO}_4$  based materials are given in Table 2. For instance, SAPO-34 and  $\text{AlPO}_4\text{-34}$  have the same structure type with small pore size and 8 tetrahedral atoms in largest ring [46].

**Table 2:** Structural properties of aluminophosphate based structures [46, 47]

<b>Pore Size</b>	<b>Number of Tetrahedral atoms in largest ring</b>	<b>Type of Structure</b>
Very large	18	VPI-5
Large	12	5,36,37,40,46,50
Medium	10	11,31,41
Small	8	14,17,18,22,26,33,34,35,39,42, 43,44,47,52
Very Small	6	16,20

SAPO-34 is an acidic silicoaluminophosphate molecular sieve with chabazite structure (CHA) and nearly 0.43 nm pore size. Chabazite (CHA) structure consist double 6-rings and one cavity formed per unit cell. This cavity is open through three-dimensional eight-ring pore system. The framework of chabazite structure is rhombohedral. Properties of Chabazite structure is given in Table 3. Figure 6 shows the crystal structure of Chabazite (CHA) [48].

**Table 3:** Properties of Chabazite Structure [48]

Chemical Formula	$[\text{Ca}_6^{2+}(\text{H}_2\text{O})_{40}][\text{Al}_{12}\text{Si}_{24}\text{O}_{72}]$
Space Group	Rhombohedral
Pore Structure	Three-dimensional eight-ring
Mineral forms	Chabazite, wilhendersonite
Synthetic forms	AIPO-34, CoAPO-44, CoAPO-47, DAF-5, GaPO-34, Linde D, Linde R, LZ-218, MeAPO-47, MeAPSO-47, (Ni(deta)2)-UT-6, Phi, SAPO-34, SAPO-47, UiO-21, ZK-14, ZYT-6

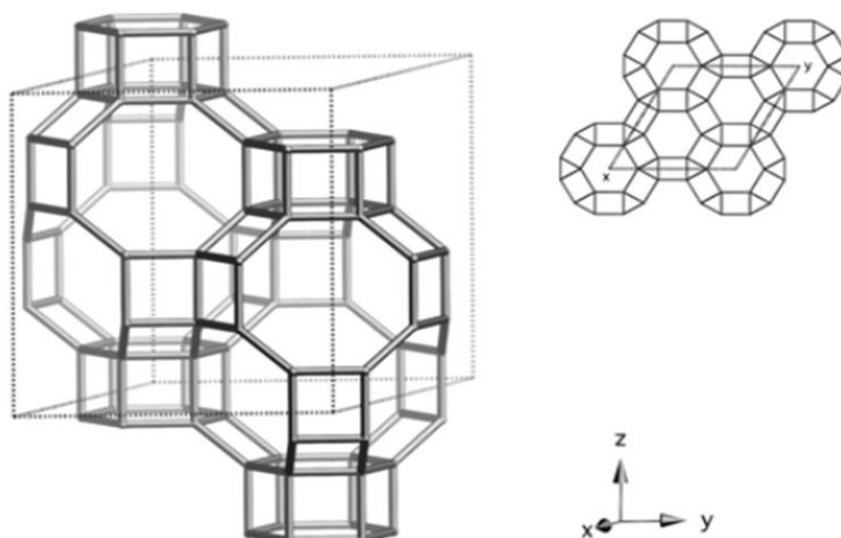


**Figure 6:** The crystal structure of Chabazite (CHA) [49]

SAPO-34 is the most attractive catalysts for methanol to olefin (MTO) reaction due to their hydrothermal stability, porous structure and middle acidity. Besides, it is important on account of production of non-oil based chemicals, high selectivity to  $\text{C}_2\text{-C}_4$  olefins, and as an cost-effective solution for the increasing require of propylene [45].

SAPO-34 could be synthesized with different organic amines such as; tetraethylammonium hydroxide (TEAOH), dipropylamine, iso-propylamine, piperidine, morpholine, triethylamine (TEA), and diethylamine (DEA) [50]. Some studies in the literature about synthesis of SAPO-34 are given below.

Liu et al.[45] hydrothermally synthesized SAPO-34 with Diethylamine (DEA) as template and examine the crystallization process. Diffraction of X-ray results showed that at the beginning of crystallization (t=0 h) solid sample was mainly amorphous boehmite and as crystallization time increased diffraction peaks of SAPO-34 became obviously. SEM images were in compliance with Diffraction of X-ray. After 0.5 h crystallization time cubic-like rhombohedra crystals were seen. According to EDS results Si capacity on the surface of SAPO-34 increased with increasing crystallization time.

Guangyu et al.[51] worked on optimal synthesis conditions for hydrothermal synthesis of SAPO-34 with Diethylamine (DEA) as template and different templates such as Triethylamine (TEA) and morpholine (MOR) compared. Optimal condition for pure SAPO-34 achieved in the range of  $0.7 \leq n(\text{P}_2\text{O}_5) \leq 1.2$ , and  $15 \leq n(\text{H}_2\text{O}) \leq 300$ . Highest Si content and crystallinity obtained with DEA and lowest with TEA.

Si incorporation mechanism is important in synthesis of SAPO-34. Number and distribution of Si atoms affects directly the structure, acidity and catalytic performance. Observation the effect of Si contents on Si incorporation mechanism was studied by Xu et al.[52]. They prepared starting gels with different  $\text{SiO}_2/\text{Al}_2\text{O}_3$  molar ratios. As a result starting gels with  $\text{SiO}_2/\text{Al}_2\text{O}_3 > 0.075$  formed SAPO-34 molecular sieve with CHA structure.

Dubois et al.[53] synthesized SAPO-34 according to the procedure of SAPO-34 patent. They used tetraethylammonium hydroxide (TEAOH) as surfactant. X-Ray Diffraction (XRD) pattern of SAPO-34 has peaks at  $2\theta$  values between  $10 - 50^\circ$  (Figure 7). The most intense peaks observed at  $2\theta = 9.65, 20.9$  and  $30.7^\circ$ . The X-

ray Diffraction (XRD) raw datas from SAPO-34 pattern are given in Appendix A1 [54].

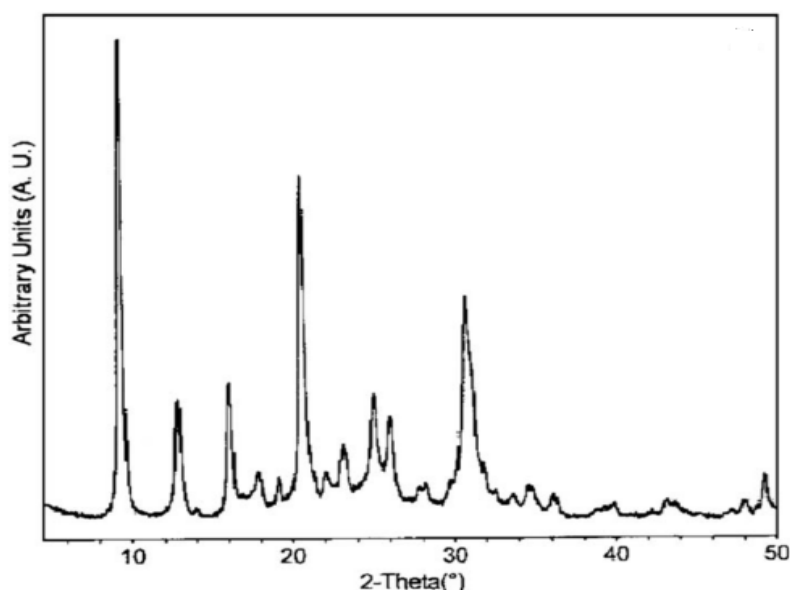


**Figure 7:** X-Ray diffraction (XRD) pattern of SAPO-34 [53].

Conventional SAPO-34 is a microporous material with zeolite structure. Diffusion limitations on the observed reaction rate and deactivation due to coke formation are important problems in such acidic microporous materials. However, mesoporous materials with ordered pore structures are considered to be less prone to coking and transport limitations. Below some studies in the literature on the synthesis of mesoporous SAPO-34 is given.

Yang et al.[55] used TEAOH as template and synthesized mesoporous SAPO-34 with different microwave heating times and compared them with traditionally hydrothermal synthesis method in methanol to olefin (MTO) conversion reaction. X-ray Diffraction patterns indicated that all samples indicated the same characteristic peaks but as microwave heating time increased intensity of XRD peaks increased. A peak seen at  $2\theta=1.1$  shows the mesoporous in the catalyst.  $N_2$  adsorption/desorption isotherms demonstrate IUPAC classification of Type 1 and 4 also meso- and

microporous are together. SEM images resulted in; after 2 h of microwave heating particle size became stationary.

Liu et al.[56] synthesized mesoporous SAPO-34 with SBA-15 as silica source and activity tests were made in Methanol to olefins reactions. SAPO-34 was synthesized with hydrothermal method and SBA-15 added to the mixture. XRD patterns showed characteristic SAPO-34 peaks at wide angle and sharp peak deal with mesoporosity was between  $2\theta = 0.5-1$ . SEM images represent a bulk particle with 15  $\mu\text{m}$  and TEM images shows hexagonal pore structure. Due to SBA-15 as silica source and also as template (P123) BJH results indicate large pore size distribution between 7-30 nm.

#### **4.2. OBJECTIVE OF THE STUDY**

Glycerol is the main side product of biodiesel production process and one mole of glycerol is produced for every three moles of methyl esters. Production of biodiesel is expected to increase significantly in the coming years. Hence, a remarkable surplus of glycerol will be generated as a result of increase of biodiesel production. Economics of biodiesel production strongly depends upon the efficient utilization of its byproduct glycerol. Etherification of glycerol with  $\text{C}_4$  i-olefin (i-butene) or tert-butyl alcohol (TBA) is considered as an attractive route for the production of fuel oxygenates. Another possible route may be etherification of glycerol with  $\text{C}_5$  i-olefins [2-Methyl-1-butene (2M1B) or 2-Methyl-2-butene (2M2B)]. Thus, conversion of glycerol, which is the byproduct of biodiesel, to value added fuel additives is the main objective of the presented study.

In the first part of this study etherification of glycerol with i-butene over commercial solid acid catalysts were studied in order to produce fuel oxygenates.

There is no published work in the literature for the production of fuel additives by the etherification of glycerol with  $\text{C}_5$  reactive olefins. In the second part of this study

etherification of glycerol with 2M2B was studied firstly, with the aim of production fuel additives.

In the third part of this study mesoporous SAPO-34 like solid acid catalysts were synthesized in order to bring a new dimension to commercial solid acid catalysts and tested in etherification of glycerol with *i*-butene reaction.

## CHAPTER 5

### EXPERIMENTAL STUDIES OF GLYCEROL ETHERIFICATION REACTIONS

In this chapter detailed information about commercial solid acid catalyst and chemicals used in this study are given. Experimental set-up and experimental studies carried out for etherification of glycerol with i-butene and 2M2B are reported. Etherification of glycerol with 2M2B is a new research area. To obtain information about products GC/MS analysis was applied before the reaction experiments and details are given in this chapter.

#### 5.1. CATALYSTS AND CHEMICALS

The chemicals used in this study were C<sub>4</sub> i-olefin (i-butene), Glycerol, 1, 4 Dioxane, C<sub>5</sub> i-olefin (2- Methyl- 2 Butene ) and Ethanol. Properties of chemicals used are given in Table 4. Three ion exchange resin catalysts, namely Amberlyst-36, Dowex DR-2030, and silicotungstic acid (STA) (H<sub>4</sub>SiW<sub>12</sub>O<sub>40</sub>) were used as solid acid catalysts. Ion exchange resin catalysts are copolymers in macroreticular structure and functionalized with sulfonic acid groups. Silicotungstic acid (STA) is a Keggin type heteropolyacid with very high proton mobility. Before the experiments these catalyst were dried according to their maximum heat treatment temperature. Some of the physical properties of these catalysts are given in Table 5. Diffuse Reflectance Fourier Transform IR Spectroscopy (DRIFTS) analysis of pyridine adsorbed samples

was performed to determine the relative strengths of the Brønsted and Lewis acid sites on the surface of the commercial solid acid catalysts used in this study. In part 6.3.4 under Characterization Methods Applied for Catalysts details for Fourier Transform Infrared Spectroscopy (FT-IR) is given.

**Table 4:** Properties of chemicals used in the study

<b>Chemical</b>	<b>Chemical Formula</b>	<b>Boiling Point, °C</b>	<b>Purity, %</b>	<b>Density, (g/ml)</b>	<b>Molecular weight, (g/mol)</b>	<b>Company</b>
<b>Glycerol</b>	C <sub>3</sub> H <sub>8</sub> O <sub>3</sub>	290	≥ 99.5	1.26	92.1	Merck
<b>i-butene</b>	C <sub>4</sub> H <sub>8</sub>	-7	≥ 98	0.59	56.1	Air Products
<b>2M2B</b>	C <sub>5</sub> H <sub>10</sub>	39	≈85	0.66	70,1	Merck
<b>1,4 Dioxane</b>	C <sub>4</sub> H <sub>8</sub> O <sub>2</sub>	101	≥ 99	1.03	88.1	Merck
<b>Ethanol</b>	C <sub>2</sub> H <sub>6</sub> O	78	≥ 99.5	0.79	46.1	Merck

**Table 5:** Physical properties of the catalysts, used in this study

Property	A-36 <sup>[a]</sup>	Dowex DR-2030 <sup>[b]</sup>	Silicotungstic acid (STA) <sup>[c]</sup>
Exchange Capacity, (meq H <sup>+</sup> /g)	5.4	4.7	-
Surface Area,(m <sup>2</sup> /g )	33	30	7.8
Porosity,(cc/g)	0.2	0.35	0.03
Average Pore Diameter,(nm)	24	20	-
Particle Diameter, ( cm)	0.06-0.085	0.043-0.0525	Powder
Max. Operating Temperature,(C <sup>0</sup> )	150	130	400 <sup>[19]</sup>

<sup>a</sup> Data obtained from Sigma-Aldrich Chemistry

<sup>b</sup> Data obtained from The Dow Chemical Company

<sup>c</sup> Measured by Quantachrome Corporation, Autosorb-6 device in Central Laboratory in METU.

## 5.2. EXPERIMENTAL SETUP

Etherification reactions of glycerol with i-butene and 2M2B were performed in a stainless steel autoclave batch reactor (75 ml), equipped with a PID temperature controller, magnetic stirrer, heating jacket and a pressure gauge. Two valves for liquid extraction/feeding and two for gas extraction/feeding were disposed on the reactor.

### 5.2.1. Experimental Set-up of Etherification of Glycerol with i-butene

Etherification of glycerol with i-butene started with placing (0.055 mole) glycerol, (0.3 g) catalyst and (30 ml) 1,4 dioxan (solvent) in to the autoclave reactor. Then the

reactor was closed and (0.446 mole) i- butene was fed to the system from gas feeding valve which was disposed on the reactor. The amount of i-butene was determined with weighting. At the end of the reaction test, the reactor was cooled to room temperature, until the system pressure reached to atmospheric. The schematic representation of the reaction set-up for etherification of glycerol with i-butene is displayed in Figure 8.

### **5.2.2. Experimental Set-up of Etherification of Glycerol with 2M2B**

Etherification of glycerol with 2M2B started also with placing (0.033 mole) glycerol, (0.3 or 1 g) catalyst and (0.261 mole) 2M2B into the autoclave reactor. Due to low boiling point of 2M2B (BP=39°C) the reactor closed as quickly as possible and reactor heated to reaction temperature. After the completion of a reaction run, the reactor was cooled to room temperature, until the system pressure reached to atmospheric. Glycerol is insoluble in 2M2B and after reaction two phases obtained. Therefore many chemicals such as; 1,4 Dioxan, tert-butyl alcohol (TBA) and ethanol tried as solvent to achieve a single phase of reactants and products mixture. As a result ethanol was chosen as solvent in etherification of glycerol with 2M2B. As soon as the reactor was opened, 50 ml of ethanol was added to achieve a single phase of glycerol, 2M2B and the reaction products mixture. This mixture was stirred until it became homogenous. The schematic representation of the reaction set-up for etherification of glycerol with 2M2B is displayed in Figure 9.

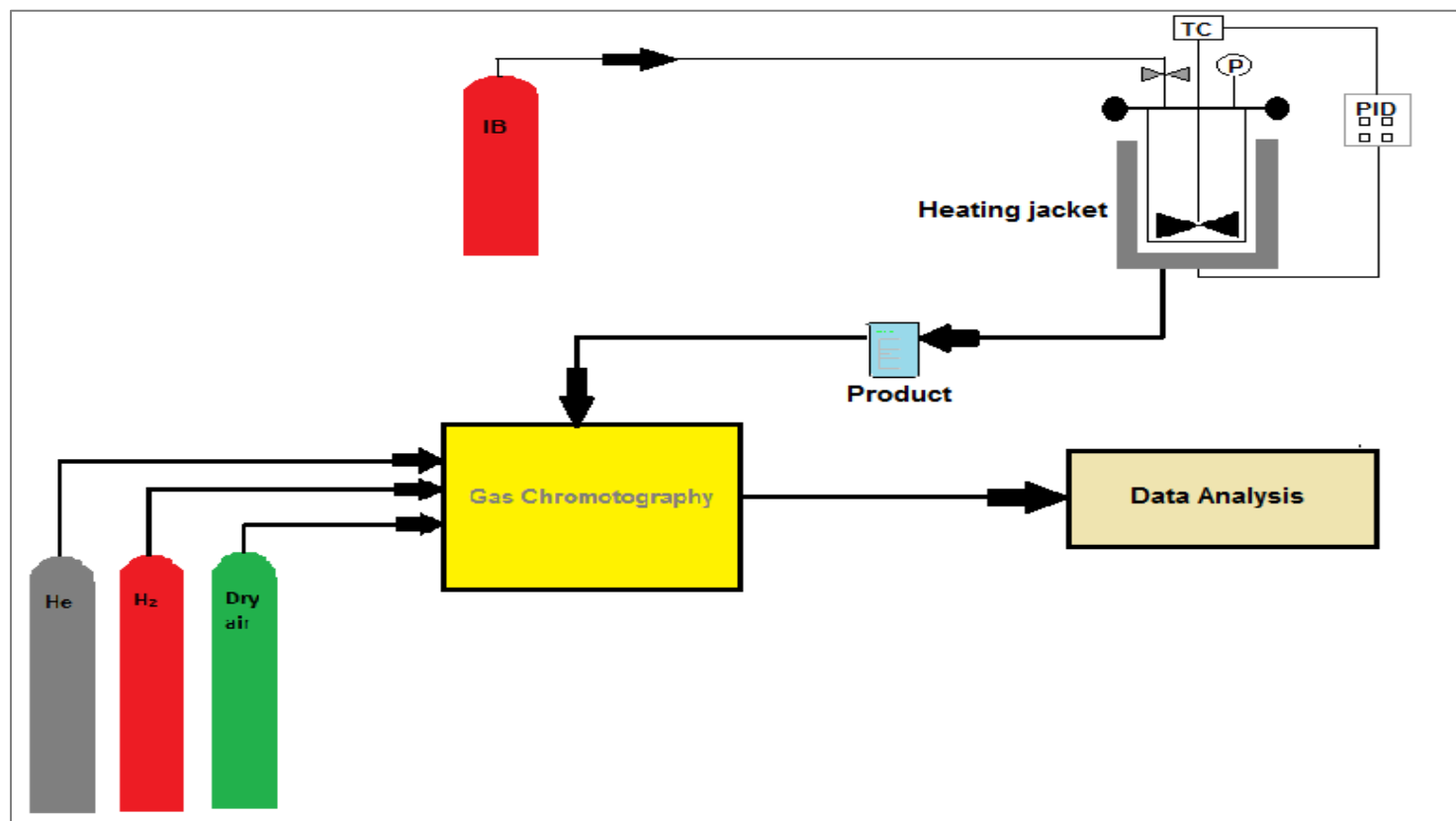


**Figure 8:** The experimental Set-up for etherification of glycerol with i-butene

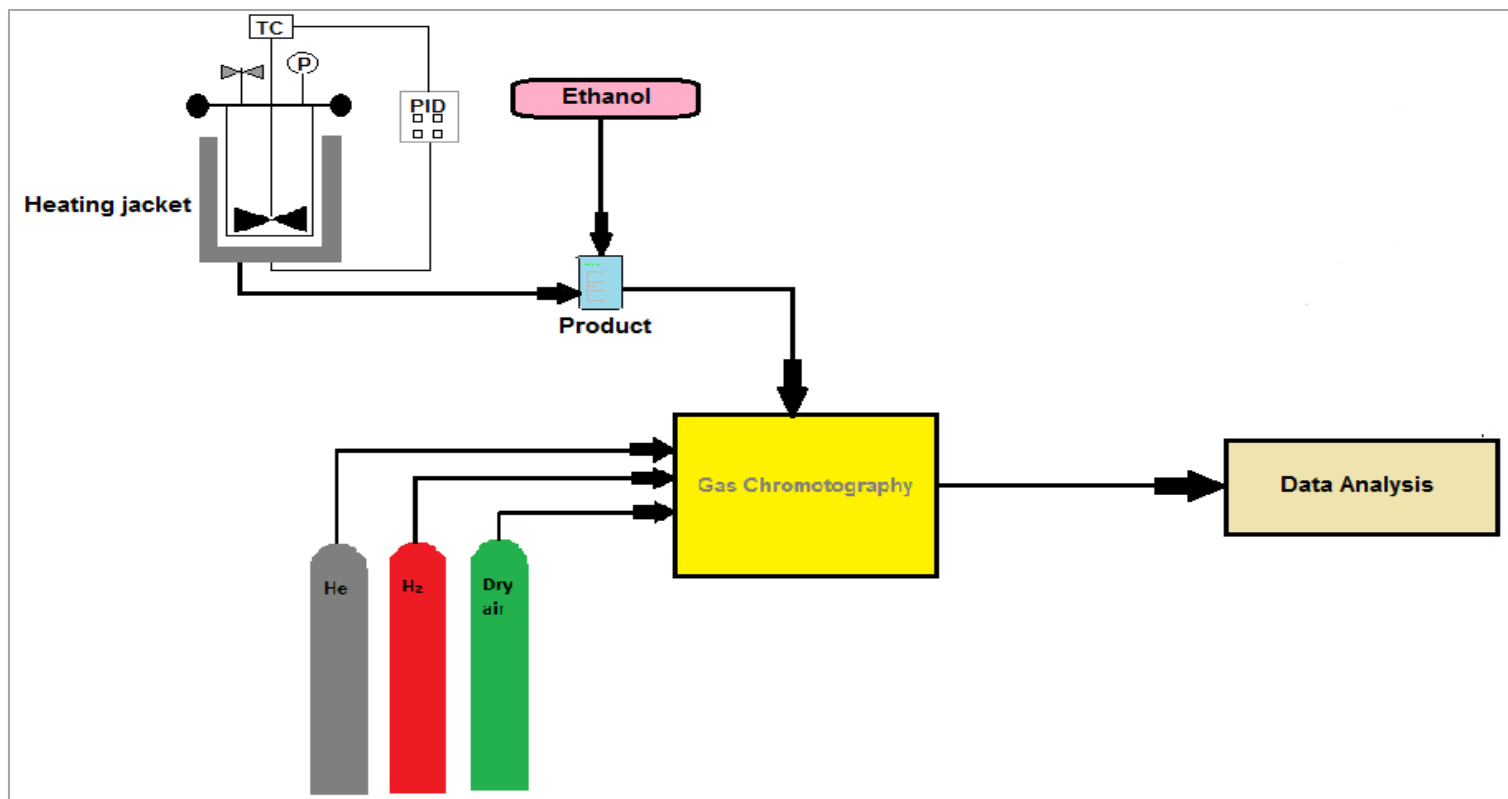


**Figure 9:** The experimental Set-up for etherification of glycerol with 2M2B

### 5.2.3. Operating conditions of Gas Chromatography and Calibration Factors

At the end of each run, chemical composition of the product mixture was analyzed by a gas chromatograph (Agilent 6890N), which was equipped with a capillary HP Innowax column and a flame ionization detector (FID) Before each analysis the column was conditioned for 1 hour with He gas to prevent impurities. Flow rate of dry air and hydrogen were set to 300 ml/min and 30 ml/min respectively and peak distinction was observed when the detector temperature was 270°C. Operating conditions of Gas Chromatograph is given in Table 6.

**Table 6:** Operating conditions of Gas Chromatograph (Adapted from [57])

Detector	FID
Column	Hp Innowax
Carrier gas (He) flow rate, (ml/min)	1.4
Column Temperature Program	10 minute 50°C 4°C/min 115°C 15°C/min 250°C
Detector Temperature, °C	270
Injection Temperature, °C	295
Amount of Injection, µl	0.5

In order to obtain quantitative results from the gas chromatography, calibration factors were calculated. Calibration factors of components in etherification of glycerol with i-butene are presented in Table 7. In order to determine the calibration factors of components in etherification of glycerol with 2M2B related mixtures was prepared. Calibration factors of components in etherification of glycerol with 2M2B are presented in Table 8 and calculations are given in Appendix B.

**Table 7:** Calibration factors of components in etherification of glycerol with i-butene(Adapted from [58])

<b>Component</b>	<b>Calibration Factor,(<math>\beta</math>)</b>
i-butene	0.282
di-i-butene	0.113
TBA	0.273
TTBG	0.296
DTBG	0.364
MTBG	0.434
G	1

**Table 8:** Calibration factors of components in etherification of glycerol with 2M2B

<b>Component</b>	<b>Calibration Factor, (<math>\beta</math>)</b>
2M2B	0.31
Ethanol	1
Dimers	0.76
TE	0.46
DE	0.56
ME	0.67
Glycerol	1.4

### 5.3. REACTION EXPERIMENTS

#### 5.3.1. Reaction Experiments of Etherification of Glycerol with i-butene

In this context etherification reactions with i-butene were performed over commercial solid acid resins, A-36, Dowex DR-2030, and Silicotungstic acid (STA). With taking the stability of resin catalyst into account reaction temperature was selected between 70-120°C. In each experiment 0.055 mole of glycerol, 0.3 g of catalyst, 0.446 mole i-butene and 30 ml 1,4 dioxane (solvent) were introduced to the reactor. Effect of reaction temperature on glycerol conversion and product selectivity was studied. In Table 9 the experimental conditions for etherification of glycerol with i-butene reaction carried out over commercial solid acid catalysts are given.

**Table 9:** Experimental conditions for etherification of glycerol with i-butene

<b>Catalyst</b>	<b>Amount of catalyst ,(g)</b>	<b>Reaction Temperature,(°C)</b>	<b>Reaction time,(h)</b>
<b>Amberlyst-36</b>	0.3	70, 80, 90, 120	6
<b>Dowex DR-2030</b>	0.3	70, 80, 90, 120	6
<b>STA</b>	0.3	70, 80, 90, 120	6

### **5.3.2. Reaction Experiments of Etherification of Glycerol with 2M2B**

Etherification of glycerol with C<sub>5</sub> i-olefin (2M2B) is a new research area. There is no published work for the production and product properties of fuel additives by the etherification of glycerol with 2M2B. To obtain some preliminary information about products, GC/MS analysis was applied before the reaction experiments.

#### **5.3.2.1. GC/MS Analysis**

Mass Spectroscopy is an analysis technique in order to identify unknown molecules. A typical mass spectrometer has three parts; ion source, mass analyzer and the detector. The ion source produce molecular ions (radical cations) from compounds. The Mass analyzer classified ions according to their mass to charge ratios. Ions with different mass to charge ratios calculated by the detector. Number of peaks in a mass spectrum data, depends on the structure of compound, ionization potential and type of ionization. Electron ionization and Chemical ionization are two types of ionization. In Electron ionization radical ions in Chemical ionization protonated molecules are formed from the molecule. Mass spectrum plotted mass to charge ratio (x axis) against relative abundance (y axis) of fragment ions [59,60].

Gas chromatography/Mass Spectrometer (GC/MS) of Salih Research Group (SAREG) from Hacettepe University, Department of Chemistry was used for Mass spectrum analysis.

GC/MS analysis was performed to identify the production and product properties of fuel additives by the etherification of glycerol with 2M2B. In order to interpret GC/MS analysis of glycerol etherification with 2M2B reaction results many preliminary mass spectral analysis were performed. Firstly mass spectra of the chemicals which we have been used during this study were taken from the database of the GC/MS device. Afterwards pure and binary mixtures of chemicals were analyzed in GC/MS and retention times determined. According to etherification of glycerol with 2M2B a wide range of products observed. Some of these products were

thought to occur due to oligomerization (mainly dimerization) of 2M2B. In order to prove this initial experiments performed by using only 2M2B as the reactant (without glycerol) with Amberlyst-36 as catalyst and GC/MS analyses of this experiment were done. Finally GC/MS analysis for etherification of glycerol with A-36 reaction was examined to obtain information about reaction products.

### **5.3.2.2.Reaction Experiments**

Etherification of glycerol with 2M2B was performed using A-36 and Dowex DR-2030 under different reaction conditions. In the case of using A-36 experiments were repeated with different amounts of catalyst, namely 0.3 and 1 g. Also, a set of experiments were performed at different reaction times (1, 3, 6, 12, 24 h). Initial experiments performed with 2M2B indicated that the reaction temperature should be higher than the experiments performed with i-butene to achieve sufficiently high glycerol conversions. Hence, reaction temperatures were selected as 120° and 140°C. Due to the instability of the resin type catalysts at higher temperatures, maximum temperature was selected as 140°C. During the reaction runs the pressure in the reactor was recorded as 6-8 bars. In Table 10, the experimental conditions for etherification of glycerol with 2M2B carried out over commercial solid acid catalysts are given.

**Table 10:** Experimental conditions for etherification of glycerol with 2M2B

<b>Catalyst</b>	<b>Amount of catalyst, (g)</b>	<b>Reaction Temperature, (°C)</b>	<b>Reaction time, (h)</b>
<b>Dowex DR- 2030</b>	0.3	120	6
	1		
<b>Amberlit-36</b>	0.3	120	6
	1		
<b>Amberlit-36</b>	0.3	120	1,3,6,12,24
	1		
<b>Amberlit-36</b>	0.3	140	1,3,6,12,24
	1		

## CHAPTER 6

### EXPERIMENTAL STUDIES FOR SYNTHESIS OF SAPO-34-LIKE MATERIALS

In this chapter the synthesis procedure of microporous SAPO-34, mesoporous SAPO-34, neutral and acidic and Silicotungstic acid (STA) impregnated mesoporous SAPO-34 is given in detail. The characterization techniques applied in this study are also explained in detail.

#### 6.1. SYNTHESIS OF MICROPOROUS SAPO-34-LIKE CATALYST

Microporous SAPO-34 catalyst was synthesized via a hydrothermal route. The synthesis procedure is similar to the one described by Guangyu et al.[51]. The chemicals listed below were used for the synthesis;

- Surfactant Source: Diethylamine (DEA), $[C_4H_{11}N]$ , (Merck)
- Silica Source: Ludox AS-40 colloidal silica, 40 wt % suspension in water,  $SiO_2$ , (surface area:  $220\text{ m}^2/\text{g}$ , Sigma Aldrich)
- Aluminum Source: Aluminumtriisopropylate (Aluminum isopropoxide),  $Al[OCH(CH_3)_2]_3$ , (Merck)
- Phosphorus Source: Ortho-phosphoric acid,  $H_3PO_4$  (85 %)(Merck)
- Solvent: Deionized water

For the synthesis of microporous SAPO-34 catalyst, five important steps: preparation of synthesis solution, hydrothermal synthesis, centrifuging, drying, and calcination were followed respectively.

✓ **Preparation of Synthesis Solution:** 74.38 g aluminum isopropoxide was dissolved in 149.98 ml deionized water. Solution was stirred at 400 rpm for 45 minutes at room temperature. 12.7 ml Ludox was added dropwise to the mixture. After mixing at 500 rpm for 15 minutes 19.64 ml phosphoric acid added to the mixture dropwise and at least stirred for 2 hours. Finally 37.66 ml surfactant (DEA) added slowly to the mixture and stirred for 1 hour. pH of the mixture remains constant around 8.7. pH of the solution was made 7.4 with adding a few drops of phosphoric acid.

✓ **Hydrothermal synthesis:** Hydrothermal synthesis was performed at 200°C under autogenic pressure for 24 h.

✓ **Centrifuging:** The white aqueous mixture was washed with deionized water with centrifugation until the pH of the wash water remained constant.

✓ **Drying:** The solid material recovered by centrifugation was placed into the oven and dried at 120°C for 4 hours.

✓ **Calcination:** Solid product was placed into a quartz tube equipped with a membrane filter. Calcination was performed in a tubular furnace with a heating rate of 1°C/min from ambient temperature to 550°C and kept at 550°C for 5 hours under the flow of dry air. At the end of calcination, solid material inside the quartz tube was cooled down to ambient temperature under the flow of dry air. Finally, microporous SAPO-34 material was obtained.

Steps of microporous SAPO-34 synthesis are shown in Figure 10.

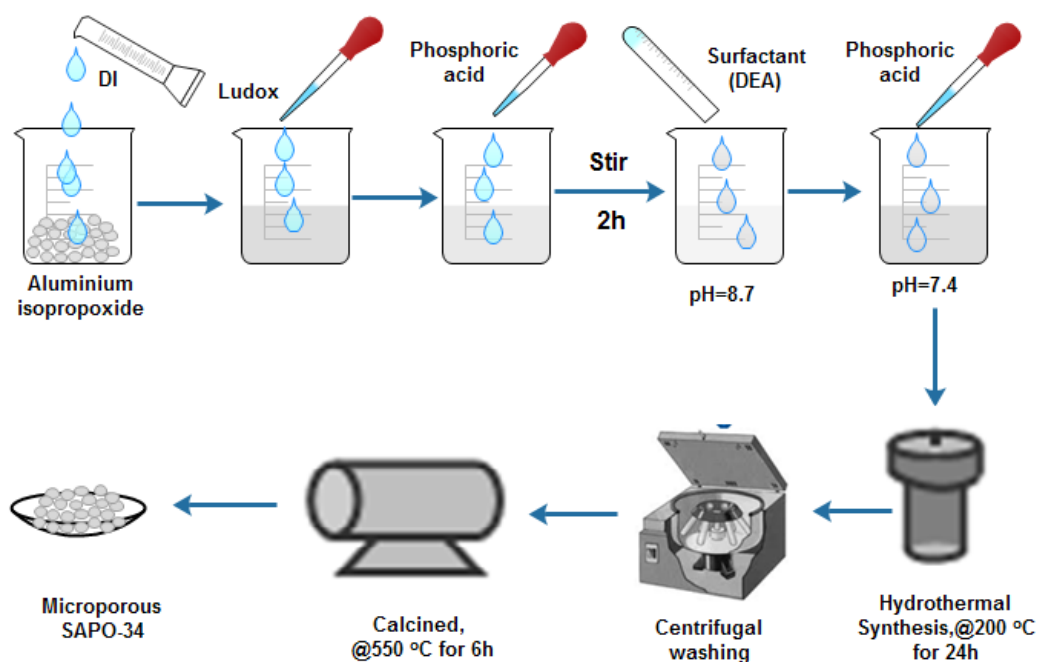


**Figure 10:** The synthesis procedure for Microporous SAPO-34

## 6.2. SYNTHESIS OF MESOPOROUS SAPO-34-LIKE CATALYSTS

In order to observe the effect of solution pH on synthesis of mesoporous SAPO-34 two different solutions were prepared. One of the solution was with a pH value of 7.4 (neutral) and the other one with pH value of 2.4 (acidic). Both of them were synthesized via hydrothermal route. The chemicals listed below were used for the synthesis;

- Surfactant Source: Pluronic P123, Poly(ethylene glycol) - block - poly(propylene glycol) - block - poly(ethylene glycol), EO20PO70EO20, MW = 5800 – Sigma-Aldrich
- Silica Source: Ludox AS-40 colloidal silica, 40 wt % suspension in water, SiO<sub>2</sub>, (surface area:220 m<sup>2</sup>/g, Sigma Aldrich)
- Aluminum Source: Aluminumtriisopropylate (Aluminum isopropoxide), Al[OCH(CH<sub>3</sub>)<sub>2</sub>]<sub>3</sub>, (Merck)
- Phosphorus Source: Ortho-phosphoric acid, H<sub>3</sub>PO<sub>4</sub> (85 %) (Merck)

- Solvent: Deionized water
- Base source: 1N Sodium hydroxide, NaOH (Merck)

### 6.2.1. Synthesis of Mesoporous SAPO-34,(neutral)

Approximately 4.0 g of (EO)<sub>20</sub>(PO)<sub>70</sub>(EO)<sub>20</sub> triblock copolymer (Pluronic P123) was dissolved in 125 ml deionized water and allowed to stir for 2 h. Temperature of this solution increased from room temperature to 40°C and 1.9 ml silica source (Ludox) was added dropwise to the solution and stirred for another hour. 11.17 g aluminum isopropoxide added slowly to the mixture. The combined solution was allowed to continue stirring for 2 h. Phosphoric acid added also to the solution and pH of the solution measured as 2.4. The pH of the combined solution made neutral (pH=7.4) with NaOH solution. Hydrothermal Synthesis, Centrifuging, Drying and Calcination steps were the same as microporous SAPO-34 in Section 6.1.

Steps of mesoporous SAPO-34, (neutral) synthesis are shown in Figure 11.

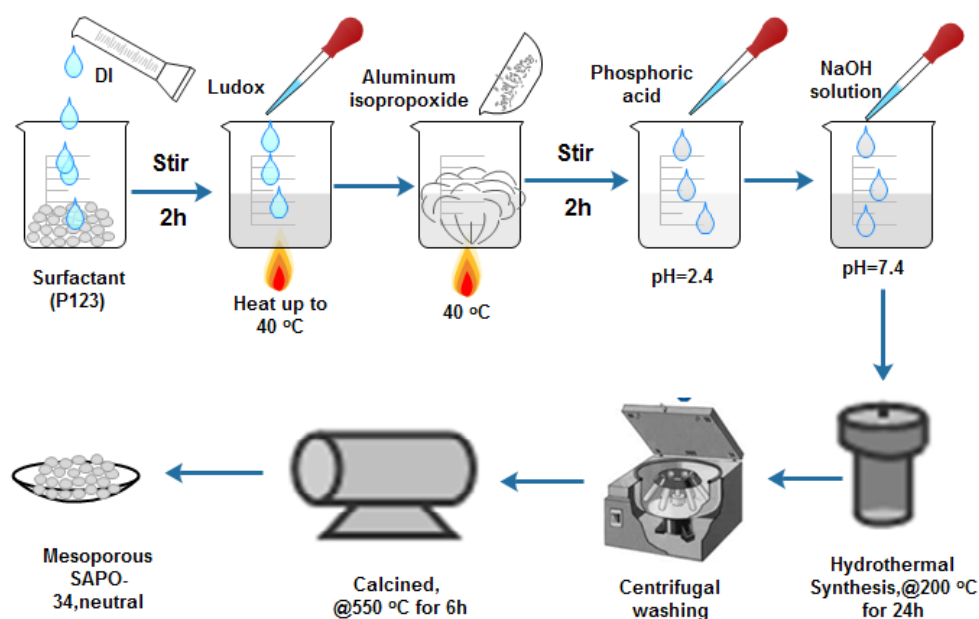


**Figure 11:** The synthesis procedure for Mesoporous SAPO-34, (neutral)

### **6.2.2. Synthesis of Mesoporous SAPO-34,acidic**

Mesoporous SAPO-34, (acidic) was synthesized likewise the procedure for Mesoporous SAPO-34, (neutral) which was given in Section 6.2.1. However the only difference was; synthesis was completed with adding phosphoric acid and the final pH was recorded as 2.4.

Hydrothermal Synthesis, Centrifuging, Drying and Calcination steps were the same as microporous SAPO-34 in Section 6.1.

### **6.2.3. Synthesis of Silicotungstic Acid Impregnated Mesoporous SAPO-34, (neutral)**

Silicotungstic acid (STA) was impregnated on synthesized mesoporous SAPO-34 (neutral) according to procedure presented in study of Varışlı et al. [61]. The weight percent of STA to mesoporous SAPO-34 is adjusted to 20 %.The chemicals listed below were used for impregnation;

- Heteropolyacid: Silicotungstic acid hydrate 99.9%,  $H_4SiW_{12}O_{40}$  – Sigma-Aldrich
- Solvent: Deionized water
- Solvent: Ethanol 99.5%,  $C_2H_5OH$ , Merck

3 g of mesoporous SAPO-34(neutral) was stirred continuously in 60 mL of deionized water and in an another vessel; 0.6 g of STA was dissolved in 15 mL of pure ethanol. STA solution was added on mesoporous SAPO-34(neutral) solution and the resultant mixture was stirred at 30°C for 60 hours. Then, the mixture was heated to 50°C and stirred for another 24 hours. Then, the mixture was dried at 110°C to evaporate the water and ethanol without mixing.

The obtained catalyst was named as STA@Mesoporous SAPO-34, (neutral). The impregnation procedure was summarized schematically in Figure 12.

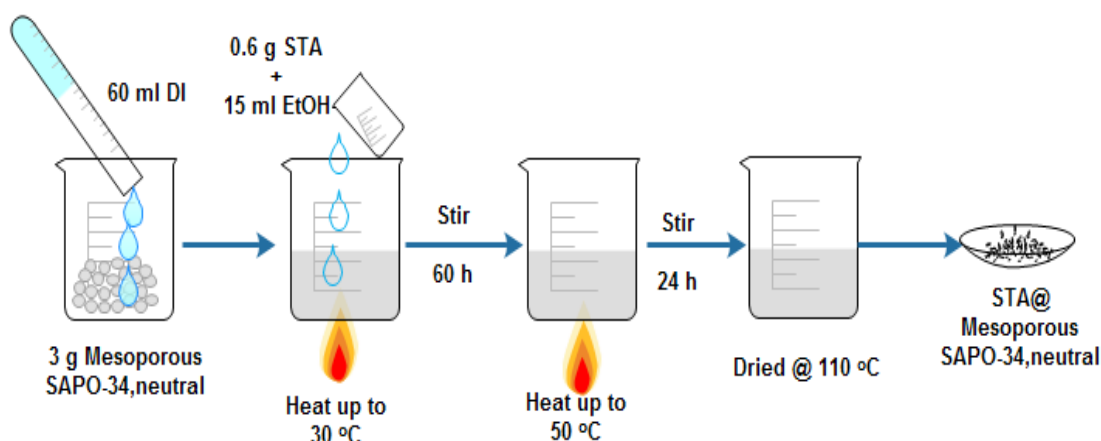


**Figure 12:** The synthesis procedure for STA impregnated Mesoporous SAPO-34, (neutral)

### 6.3. CHARACTERIZATION METHODS APPLIED FOR THE CATALYSTS

In order to characterize the synthesis catalyst, X-ray diffraction (XRD), nitrogen physisorption (BET), Scanning Electron Microscopy (SEM), Fourier Transform Infrared Spectroscopy (FT-IR) were employed.

#### 6.3.1. X-Ray Diffraction (XRD)

X-Ray Diffraction is one of the basic characterization technique, which provides information about particle size and crystalline phases. X-ray made a  $\theta$  angle with lattice plane and reflected with the same angle. Bragg's Law which is given in equation 6.1.is used to calculate the distance between reflection angle and lattice plane.

$$n \lambda = 2d \sin \theta \quad (n=1,2,3..) \quad 6.1.$$

$\lambda$ , Wavelength

d, distance between lattice planes

$\theta$ , diffraction angle between the incoming X-rays

The XRD Rigaku Ultima-IV X-Ray diffractometer in the METU-Central laboratory was used to obtain the XRD pattern of the synthesized microporous SAPO-34. Besides, the XRD Panalytical Empyrean X-Ray diffractometer in the Bilecik Şeyh Edabali University -Central laboratory was used to obtain the XRD pattern of the synthesized mesoporous SAPO-34, catalysts.

### **6.3.2. Nitrogen Physisorption**

Nitrogen Physisorption characterization technique gave information about Multipoint BET surface area, BJH adsorption/desorption pore diameters and pore volumes of synthesized catalysts. Different models such as BET (Bruanauer, Emmett, Teller) and BJH (Barrett, Joyner, Halenda) have been developed to calculate surface areas and pore sizes distributions. Nitrogen adsorption-desorption analyses were made by Quantachrome Corporation, Autosorb-6 device in METU Central Laboratory. Degassing process was done at 120 °C for 6 hours and the samples were analyzed at a relative pressure range of 0.05 to 0.99 at liquid nitrogen (N<sub>2</sub>).

### **6.3.3. Scanning Electron Microscopy (SEM)**

The topographical and compositional information about the synthesized catalysts were obtained by JSM-6400 Electron Microscope (JEOL) equipped with NORAN System 6 X-ray Microanalysis System & Semafore Digitizer in Metallurgical and Material Engineering in METU.

#### **6.3.4. Diffuse Reflectance Infrared Fourier Transform Spectroscopy (DRIFTS) of Pyridine Adsorption**

Diffuse Reflectance Infrared Fourier Transform Spectroscopy (DRIFTS) analysis of pyridine adsorbed catalyst samples was performed by using a Perkin Elmer Spectrum One instrument in Middle East Technical University Kinetic Laboratory. The samples were pretreated at 110°C for 12 hours to remove water adsorbed on the acid sites. After the adsorption of 1 ml pyridine, samples were dried at 40°C for 2 hours before the DRIFTS analysis. A background spectrum was recorded with KBr. FT-IR spectrum of the sample which was not treated by pyridine was subtracted from the spectrum of pyridine-adsorbed sample for the detection of adsorbed surface species. Acidic strengths of Lewis and Brønsted sites were then determined from the differences of these spectra.

Distinctive bands, which appear at 1540 and 1640  $\text{cm}^{-1}$  correspond to the Brønsted acid sites. However, for the Lewis acid sites, bands are expected at 1450 and 1598.

## CHAPTER 7

### RESULTS OF GLYCEROL ETHERIFICATION WITH *i*-BUTENE

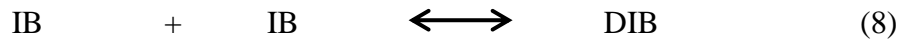
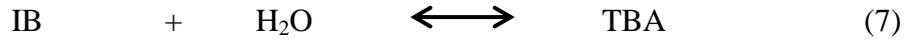
In this chapter, results corresponding to etherification of glycerol with *i*-butene over commercial solid acid catalysts namely; A-36, Dowex DR-2030 and STA are given. To determine the relative strengths of the Brønsted and Lewis acid sites on the surface of the solid acid catalysts used in this study Diffuse Reflectance Fourier Transform IR Spectroscopy (DRIFTS) analysis results are given. Effect of reaction temperature on glycerol conversion and product selectivity is presented for each catalyst. Besides, activity of commercial solid acid catalysts were compared.

Etherification of glycerol with *i*-butene takes place in three consecutive reversible reaction steps which are represented in reactions (1)-(6). Reaction (1) and (2), are for producing mono-*tert*-butyl glycerol ether isomers (3-*tert*-butoxy-1,2-propanediol; MTBG1 and 2-*tert*-butoxy-1,3-propanediol; MTBG2), (3) and (4) for di-*tert*-butyl glycerol ether isomers (2,3-ditert-butoxy-1-propanol; DTBG1 and 1,3-ditertbutoxy-2-propanol; DTBG2), (5) and (6) for producing tri-*tert*-butyl glycerol ether (1,2,3-tritert-butoxy-propane; TTBG). Besides these reactions; the hydration of *i*-butene (7) and oligomerization (8) are two side reactions, which may take place in the reactor. [33]. Oligomerization of *i*-butene is not desired and has a negative effect on ether yields. However, as a result of hydration of *i*-butene TBA may form, which may also react with glycerol to produce the ethers.

### Main Reactions



### Side Reactions



One of the major aims of this study is to achieve high glycerol conversion and product selectivity. Within products the solubility of mono ethers (MTBG) in diesel fuel is quite low. On the other hand, di-ethers (DTBG) and tri-ethers (TTBG) are highly soluble in diesel and gasoline. They are considered as excellent fuel components which can be added to gasoline, instead of current commercial oxygenate additives, such as MTBE, ETBE and TAME. These ethers were reported to have high octane numbers and can be used as gasoline additives for octane enhancement. They can also be mixed with biodiesel to increase its amount and improve the economics [2].

The total conversion of glycerol ( $X_G$ ) to mono-, di- and tri-ethers was calculated using equation 7.1. In this equation  $X_{MTBG1}$ ,  $X_{MTBG2}$ ,  $X_{DTBG1}$ ,  $X_{DTBG2}$ ,  $X_{TTBG}$  are mole fractions of mono-, di- and tri-ethers.

$$X_G = \frac{X_{MTBG1} + X_{MTBG2} + X_{DTBG1} + X_{DTBG2} + X_{TTBG}}{X_G + X_{MTBG1} + X_{MTBG2} + X_{DTBG1} + X_{DTBG2} + X_{TTBG}} \quad 7.1.$$

Selectivity of mono-ethers to glycerol was calculated according to 'proportion of produced mono-ethers to converted glycerol' with using equation 7.2.

$$S_{\text{MTBG/G}} = \frac{X_{\text{MTBG1}} + X_{\text{MTBG2}}}{X_{\text{MTBG1}} + X_{\text{MTBG2}} + X_{\text{DTBG1}} + X_{\text{DTBG2}} + X_{\text{TTBG}}} \quad 7.2.$$

Selectivity of di-ethers to glycerol was calculated according to 'proportion of produced di-ethers to converted glycerol' with using equation 7.3.

$$S_{\text{DTBG/G}} = \frac{X_{\text{DTBG1}} + X_{\text{DTBG2}}}{X_{\text{MTBG1}} + X_{\text{MTBG2}} + X_{\text{DTBG1}} + X_{\text{DTBG2}} + X_{\text{TTBG}}} \quad 7.3.$$

Selectivity of tri-ethers to glycerol was calculated according to 'proportion of produced tri-ethers to converted glycerol' with using equation 7.4.

$$S_{\text{TTBG/G}} = \frac{X_{\text{TTBG}}}{X_{\text{MTBG1}} + X_{\text{MTBG2}} + X_{\text{DTBG1}} + X_{\text{DTBG2}} + X_{\text{TTBG}}} \quad 7.4.$$

Selectivity of di-i-butene (DIB) was calculated according to 'proportion of produced di-i-butene (DIB) to reacted i-butene' with using equation 7.5.

$$S_{\text{DIB/IB}} = \frac{2 * X_{\text{DIB}}}{X_{\text{MTBG1}} + X_{\text{MTBG2}} + 2 * X_{\text{DTBG1}} + 2 * X_{\text{DTBG2}} + 3 * X_{\text{TTBG}} + X_{\text{TBA}} + 2 * X_{\text{DIB}}} \quad 7.5.$$

Etherification reactions with i-butene were performed in a temperature range of 70-120°C using A-36, Dowex DR-2030 and STA as the solid acid catalysts. Due to low solubility of glycerol in i-butene 1,4 Dioxane is used as solvent in each reaction. Effect of temperature on glycerol conversion and product selectivity was investigated for each catalyst. Also activity of catalyst was compared at different reaction

temperatures. Results will be discussed in the following sections. Sample conversion and selectivity calculations are given in Appendix C.

### 7.1. DRIFTS ANALYSIS RESULTS OF COMMERCIAL SOLID ACID CATALYSTS

Diffuse Reflectance Fourier Transform IR Spectroscopy (DRIFTS) analysis of pyridine adsorbed samples was performed to determine the relative strengths of the Brønsted and Lewis acid sites on the surface of the solid acid catalysts used in this study (Figure 13). Distinctive bands, which appear at 1540 and 1640  $\text{cm}^{-1}$  correspond to the Brønsted acid sites. However, for the Lewis acid sites, bands are expected at 1450 and 1598  $\text{cm}^{-1}$  [2].

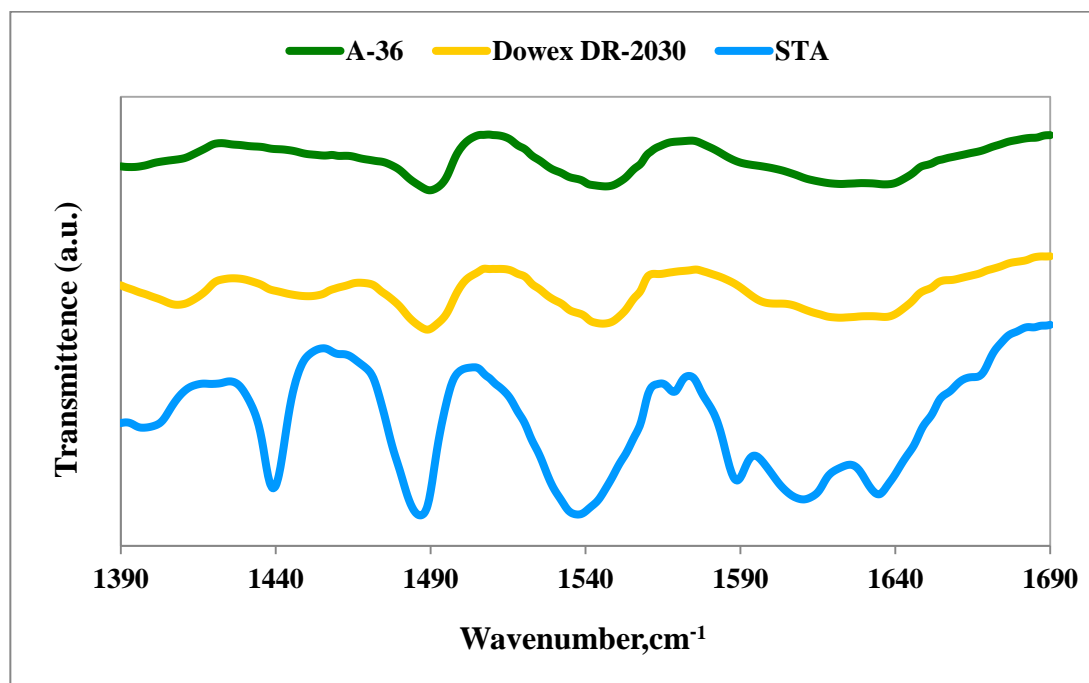


**Figure 13:** Drift spectrum of pyridine adsorbed solid acid catalysts.

According to DRIFTS results given in Figure 13, for Amberlyst-36 and Dowex DR - 2030 acidic resins, the Lewis bands at 1450 and 1598  $\text{cm}^{-1}$  are quite weak. However,

the intensities of the bands at 1540 and 1640  $\text{cm}^{-1}$  were quite strong, indicating strong Brønsted acidity. Sulfonic acid functionality on the catalyst surface for the acidic resins is the cause of Brønsted acidity [2]. Contribution of Brønsted and Lewis acid sites gives a band at 1490  $\text{cm}^{-1}$  which can be visibly seen for Amberlyst-36 and Dowex DR-2030. Because of low Lewis acidity of these resins, it can be considered that the band at 1490  $\text{cm}^{-1}$  was also mainly due to Brønsted acid sites. Although the hydrogen exchange capacity of A-36 was higher than that of Dowex DR-2030 (Table 5), DRIFTS analysis indicated somewhat higher intensity of Brønsted acid sites for Dowex DR-2030. This was considered to be due to higher porosity of DR-2030 than A-36, which allowed better penetration of pyridine into the catalyst to be adsorbed on the active sites. In fact, higher porosity was also expected to cause less diffusional resistance also in the reaction tests.

The DRIFT spectrum of pyridine adsorbed silicotungstic acid (STA) showed the presence of both Lewis and Brønsted acid sites (Figure 13). However, to comparison of the intensities of the bands showed that the Brønsted acidity of STA was much more intense than Lewis acidity. Strong Brønsted acidity is due to high proton mobility of STA. Heteropolyacids are known to have acidities even higher than sulphuric acid and they are considered as super acids [62].

## **7.2. ETHERIFICATION OF GLYCEROL WITH *i*-BUTENE OVER AMBERLYST-36 CATALYST**

In order to observe the effect of reaction temperature on glycerol conversion and product selectivity etherification of glycerol with *i*-butene was performed over Amberlyst-36 in a temperature range of 70-120°C. Amount of Amberlyst-36 was 0.3 g and 1.4 Dioxan was used as solvent in each reaction.

### 7.2.1. Effect of Temperature on glycerol conversion over Amberlyst-36

Glycerol conversion values obtained at different temperatures by using Amberlyst-36 catalyst is reported in Figure 14.

At 70°C glycerol conversion was nearly 40 %. As temperature increased to 80 and 90°C glycerol conversion increased and at 90°C glycerol conversion reached to maximum value of about 100%. Amberlyst-36 is a copolymer of divinylbenzene and its active site is  $-\text{SO}_3\text{H}$ . Divinylbenzene gives information about crosslinking degree and rigidity. Swelling capacity and divinylbenzene amount is inversely proportional. Increase in temperature increased swelling of catalyst in polar solvents due to separation of hydrogen bonded acid groups. Amberlyst-36 has lower crosslinking degree as a result high swelling capacity. Increasing of glycerol conversion with reaction temperature up to 90°C is due to; higher swelling capacity of Amberlyst-36 higher is the accessibility of reactants to the active sites [2].

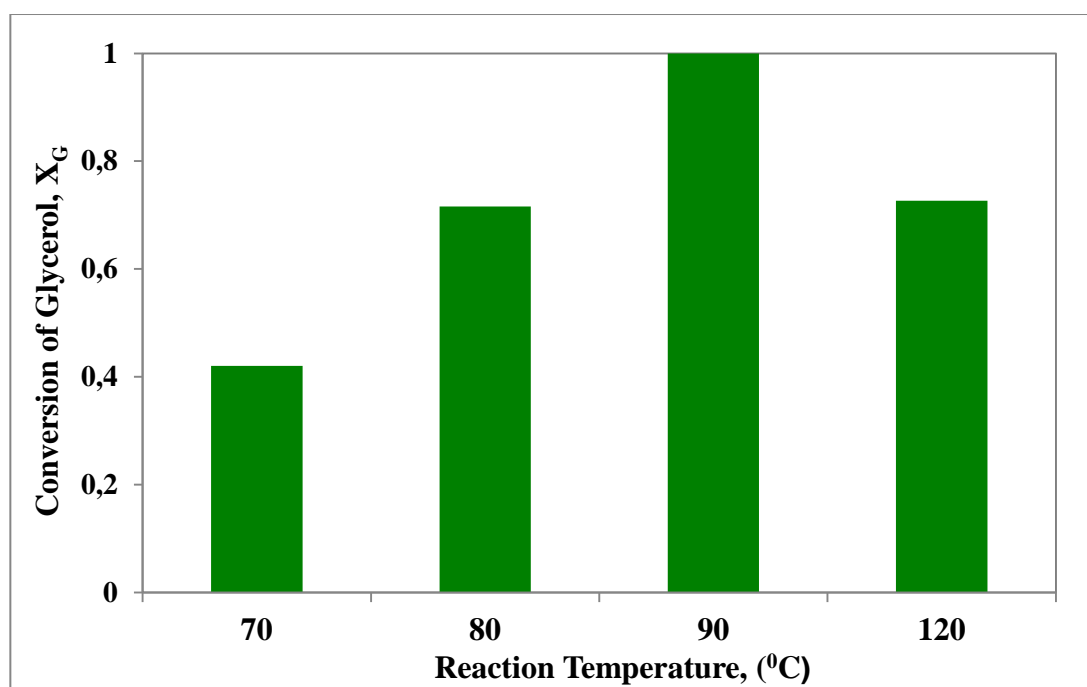


**Figure 14:** Glycerol conversion vs. reaction temperature over Amberlyst-36  
(Reaction time=6h,  $m_{\text{cat}}=0.3$  g)

When reaction temperature increased to 120°C glycerol conversion decreased to 70 %. Increase in temperature is also expected to increase the etherification reaction rate. However, rate of i-butene oligomerization (mainly C<sub>8</sub>, di-i-butene, (DIB)) was also expected to increase with an increase in temperature. Apparently the increase of the rate of i-butene oligomerization was more rapid than the glycerol etherification reaction rate.

### 7.2.2. Effect of Temperature on Product Selectivity over Amberlyst-36

Product selectivity values obtained at different temperatures by using Amberlyst-36 catalyst is reported in Figure 15.

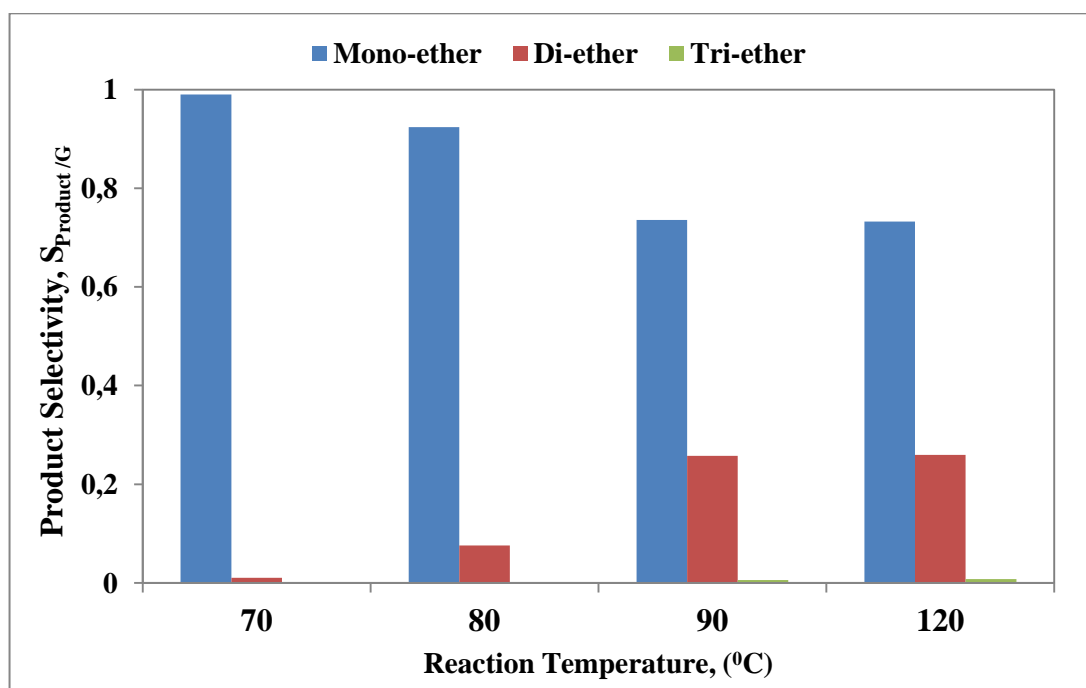


**Figure 15:** Product Selectivity vs. reaction temperature over Amberlyst-36

(Reaction time=6h,  $m_{\text{cat}}=0.3$  g)

Di- and tri-ethers of glycerol (DTBG and TTBG) are preferred products due to their high solubility in diesel and gasoline. Product selectivity is mainly towards monoethers at 70°C and selectivity value is approximately 0.99. As temperature increased to 80 and 90°C monoether selectivity decreased diether selectivity increased. Tri ether selectivity was low at all temperatures. Tri-ether as a branched structure occupies more volume than mono- and di-ethers of glycerol, which decreases its formation compared to the others.

### **7.3. ETHERIFICATION OF GLYCEROL WITH i-BUTENE OVER DOWEX DR-2030 CATALYST**

In order to observe the effect of reaction temperature on glycerol conversion and product selectivity, etherification of glycerol with i-butene was performed over Dowex DR-2030 resin in a temperature range of 70-120°C. Amount of Dowex DR-2030 was 0.3 g and 1,4 Dioxane was used as solvent in each reaction.

#### **7.3.1. Effect of Temperature on glycerol conversion over Dowex DR-2030**

Glycerol conversion values obtained at different temperatures by using Dowex DR-2030 catalyst is reported in Figure 16.

At 70°C glycerol conversion was nearly 60 %. As temperature increased to 80 and 90°C glycerol conversion increased and at 90°C glycerol conversion reached to maximum value of about 100%. When reaction temperature increased to 120°C glycerol conversion decreased compared with 90°C. Increase in temperature is also expected to increase the etherification reaction rate. However, rate of i-butene oligomerization (mainly C<sub>8</sub>, di-i-butene, (DIB)) was more rapid than the glycerol etherification reaction rate.

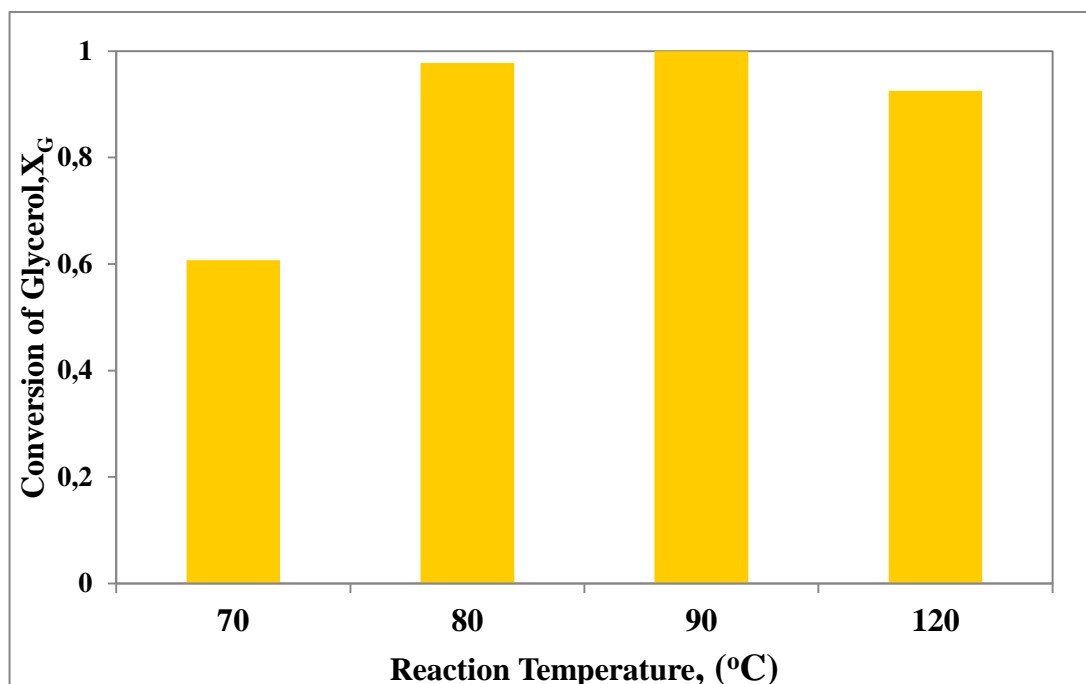


**Figure 16:** Glycerol conversion vs. reaction temperature over Dowex DR-2030  
(Reaction time=6h,  $m_{\text{cat}}=0.3$  g)

### 7.3.2. Effect of Temperature on Product Selectivity over Dowex DR-2030

Product selectivity values obtained at different temperatures by using Dowex DR-2030 catalyst is reported in Figure 17.

Product selectivity is mainly towards monoethers at 70°C and selectivity value is approximately 0.99. As temperature increased to 80 and 90°C monoether selectivity decreased di and tri-ether selectivity increased. At 90°C di- and triether selectivity reaches to maximum among studied temperatures. Di and tri-ether selectivity values were 0.6 and 0.1 respectively. Due to di- and tri-ethers of glycerol (DTBG and TTBG) are preferred products in diesel and gasoline this result is highly promising.

Decrease of di and tri-ether selectivities observed with Dowex DR-2030 with a further increase of temperature to 120°C may be related to the decrease of i-butene concentration in the reactor due to formation of di-i-butene (DIB).

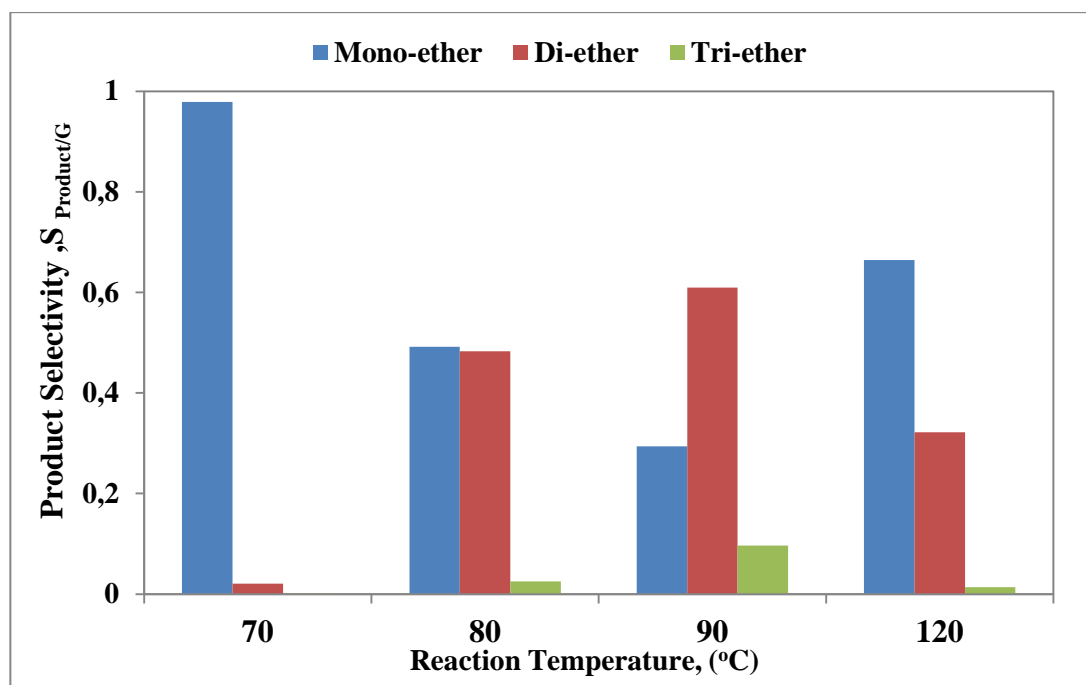


**Figure 17:** Product Selectivity vs. reaction temperature over Dowex DR-2030

(Reaction time=6h,  $m_{\text{cat}}=0.3$  g)

#### 7.4. ETHERIFICATION OF GLYCEROL WITH i-BUTENE OVER SILICOTUNGSTIC ACID (STA) CATALYST

In order to observe the effect of reaction temperature on glycerol conversion and product selectivity etherification of glycerol with i-butene was performed over Silicotungstic acid in a temperature range of 70-120°C. Amount of Silicotungstic acid was 0.3 g and 1,4 Dioxane was used as solvent in each reaction.

#### 7.4.1. Effect of Temperature on glycerol conversion

Glycerol conversion values obtained at different temperatures by using Silicotungstic acid catalyst is reported in Figure 18.

At 70°C glycerol conversion was nearly 80 %. Silicotungstic acid is a heteropolyacid and considered as a pseudo liquid, indicating easy penetration of reactants to the acid sites. As temperature increased to 80 and 90°C glycerol conversion increased with increasing reaction rate. Further increase in temperature to 120°C decreased glycerol conversion compared with 90°C. At 120°C glycerol conversion decreased to 0.5. Apparently, higher acidity of STA also facilitates the oligomerization of i-butene. Due to quite high chemical attraction of i-butene to Keggin anion of STA is expected to cause protonation of i-butene and formation of the alkoxy state on the surface. This may couple with a next i-butene molecule producing di-i-butene (DIB) [38].

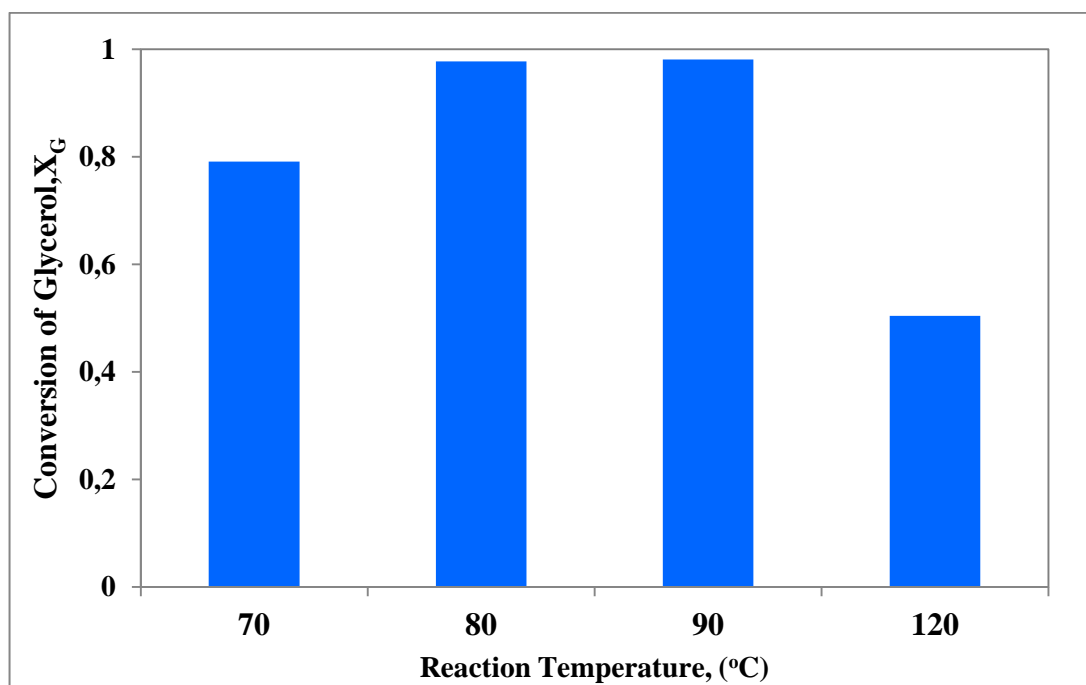


**Figure 18:** Glycerol conversion vs. reaction temperature over STA

(Reaction time=6h,  $m_{\text{cat}}=0.3$  g)

#### 7.4.2. Effect of Temperature on Product Selectivity with STA

Product selectivity values obtained at different temperatures by using Silicotungstic acid catalyst is reported in Figure 19.

Product selectivity is mainly towards monoethers at 70°C and selectivity value is approximately 0.99. As temperature was increased to 80°C monoether selectivity decreased sharply di and tri-ether selectivity increased. Diether selectivity reaches to maximum at 80°C and is nearly 0.6. Further increase in temperature causes decreasing of di and tri ether selectivity and mono ether selectivity increased. Decrease of di and tri-ether selectivities may be related to the decrease of i-butene concentration in the reactor due to formation of di-i-butene (DIB).

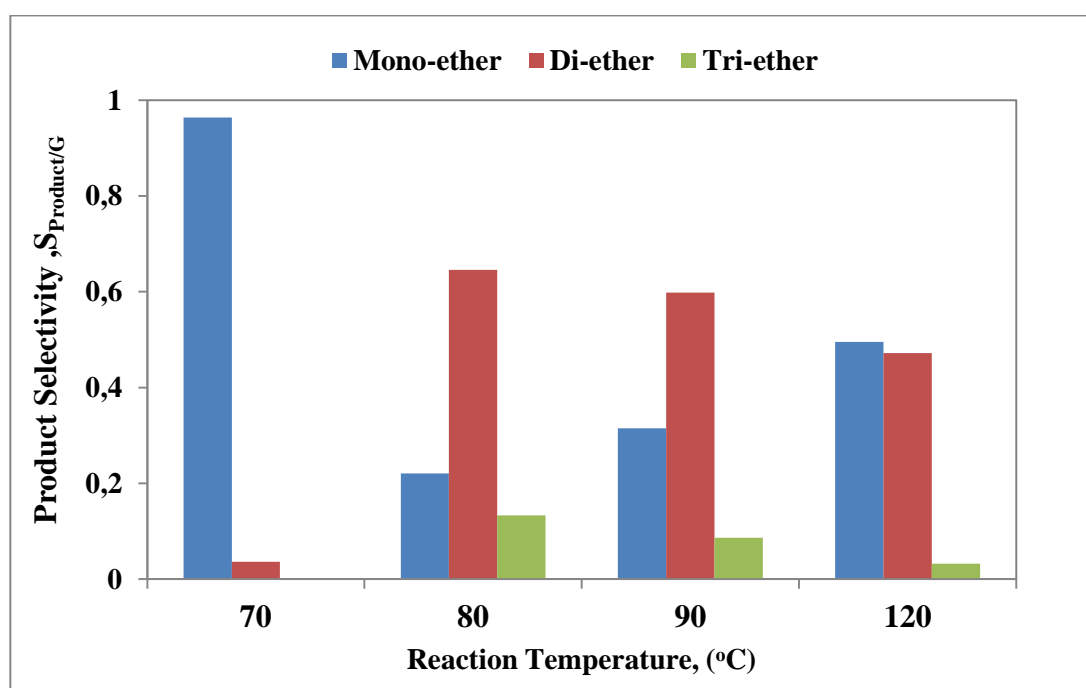


**Figure 19:** Product Selectivity vs. reaction temperature over STA

(Reaction time=6h,  $m_{\text{cat}}=0.3$  g)

## 7.5. ACTIVITY COMPARISON OF DIFFERENT SOLID ACID CATALYSTS

Activity of solid acid catalysts used in this study namely; Amberlyst-36, Dowex DR-2030 and Silicotungstic acid compared in a temperature range of 70-120°C. Effect of temperature on glycerol conversion and product selectivity is represented.

### 7.5.1. Effect of temperature on glycerol conversion obtained with different solid acid catalysts

Glycerol conversion values obtained as a result of its etherification with i-butene are reported in Figure 20. Results obtained at different temperatures by using Amberlyst-36, Dowex DR-2030 and STA catalysts in the presence of 1,4 Dioxan as solvent are reported in this figure.

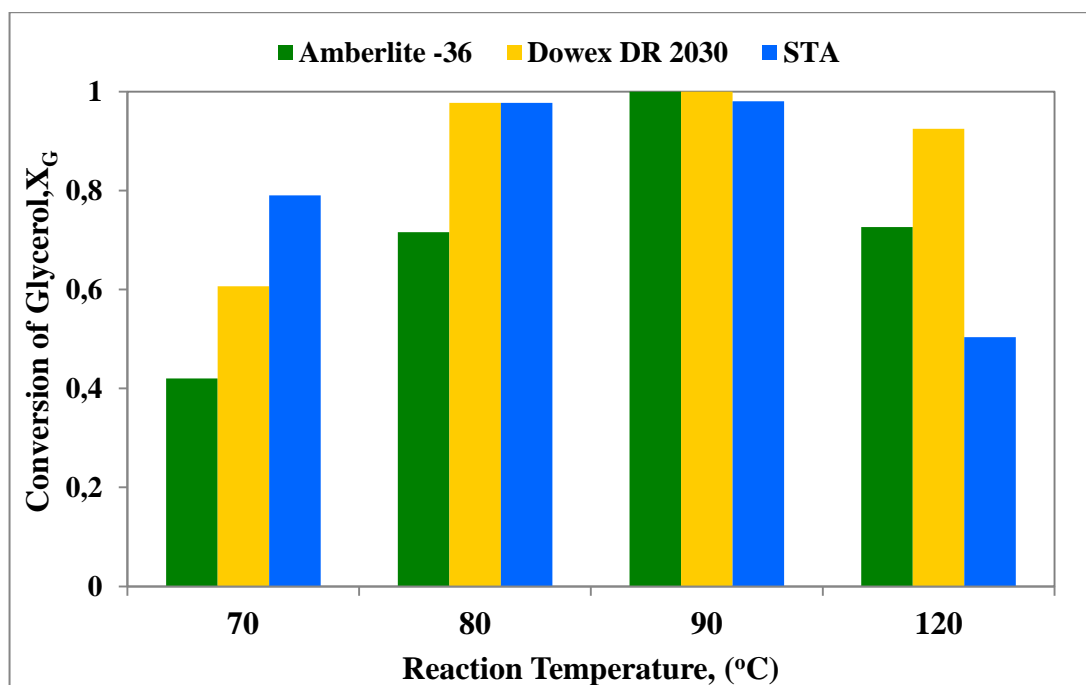


**Figure 20:** Glycerol conversion vs. reaction temperature with different catalysts  
(Reaction time=6h,  $m_{\text{cat}}=0.3$  g)

At 70 and 80°C, maximum glycerol conversion values were obtained by using STA as the catalyst. Considering that the Brønsted acidity of STA was higher than the other resin type solid acid catalysts, this is an expected result. Heteropolyacids are sometimes considered as pseudo liquids, indicating easy penetration of reactants to the acid sites. In this temperature range, catalytic performance of Dowex DR-2030 was also higher than the performance of Amberlyst-36. Comparison of the activities of the two resin catalysts was also in concordance with the Brønsted acidity results (Figure 13). Dowex DR-2030 was also more porous than Amberlyst-36, which facilitates transport of reactants to the active sites within the catalyst. Pore diffusion resistances are expected to be significant in this reaction system. Apparently, diffusion resistance within Dowex DR-2030 was less than Amberlyst-36. Although the hydrogen exchange capacity of Amberlyst-36 was somewhat higher than Dowex DR-2030 (Table 5) and penetration of the reactants to the active sites within Amberlyst-36 was more difficult than Dowex DR-2030. These acidic resins include  $-\text{SO}_3\text{H}$  groups which are directly related to hydrogen exchange capacity. A dense network of  $-\text{SO}_3\text{H}$  groups were formed within the micro-grains of the resins. Penetration of pyridine into the resin catalysts during DRIFTS analysis might also be hindered due to diffusional effects. Hence, DRIFTS results indicated higher Brønsted acidity for Dowex DR-2030, which correspond to the sites near to the external surface of the catalysts, up to a depth that pyridine had penetrated. Ozbay et al. [2] had also reported in a recent publication on etherification of glycerol with TBA that, mainly the acid sites near the outer surface of the acidic resins contributed to the Brønsted acidity measured by DRIFTS analysis of pyridine adsorbed samples and also to the etherification reaction at low temperatures. As reaction temperature increased to 90°C glycerol conversion catalyzed with both Amberlyst-36 and Dowex DR-2030 increases and reached to a maximum value of about 100%. With both of these resin type catalysts, nearly the same glycerol conversion was obtained at 90°C. This is due to the increase of the etherification rate with an increase in temperature.

When reaction temperature increased to 120°C, glycerol conversion decreased with all of the catalysts used in this work. All three of these catalysts are expected to be

stable at 120°C. Increase in temperature is also expected to increase the etherification reaction rate. However, rate of *i*-butene oligomerization (mainly C<sub>8</sub>, di-*i*-butene, (DIB)) was also expected to increase with an increase in temperature. Apparently the increase of the rate of *i*-butene oligomerization was more rapid than the glycerol etherification reaction rate. Similar results were also reported in the literature with different catalysts [36, 37]. Especially over 90°C, this caused a negative effect on glycerol conversion. To prove this conclusion, di-*i*-butene mole fractions in the product mixtures obtained at different temperatures were also determined. Influence of temperature on selectivity of di-*i*-butene (DIB), obtained with the three catalysts used in this study is given in Figure 21. As seen in this figure, at 70°C, almost no di-*i*-butene (DIB) was formed. However, as the temperature was increased to 80 and 90°C, selectivity of di-*i*-butene (DIB) increased sharply especially in case of silicotungstic acid (STA). At 90°C, the selectivity of di-*i*-butene (DIB) reached to 0.26 with STA. As temperature was increased to 120°C, selectivity of di-*i*-butene (DIB) was further increased with all of the catalyst used in this study. Especially in case of silicotungstic acid (STA) di-*i*-butene (DIB) selectivity was recorded as nearly 0.5. Apparently, higher acidity of STA also facilitates the oligomerization of *i*-butene. Due to quite high chemical attraction of *i*-butene to Keggin anion of STA is expected to cause protonation of *i*-butene and formation of the alkoxy state on the surface. This may couple with a next *i*-butene molecule producing di-*i*-butene (DIB) [38]. Decrease of glycerol conversion at 120°C is a direct consequence of increase of di-*i*-butene (DIB) formation.

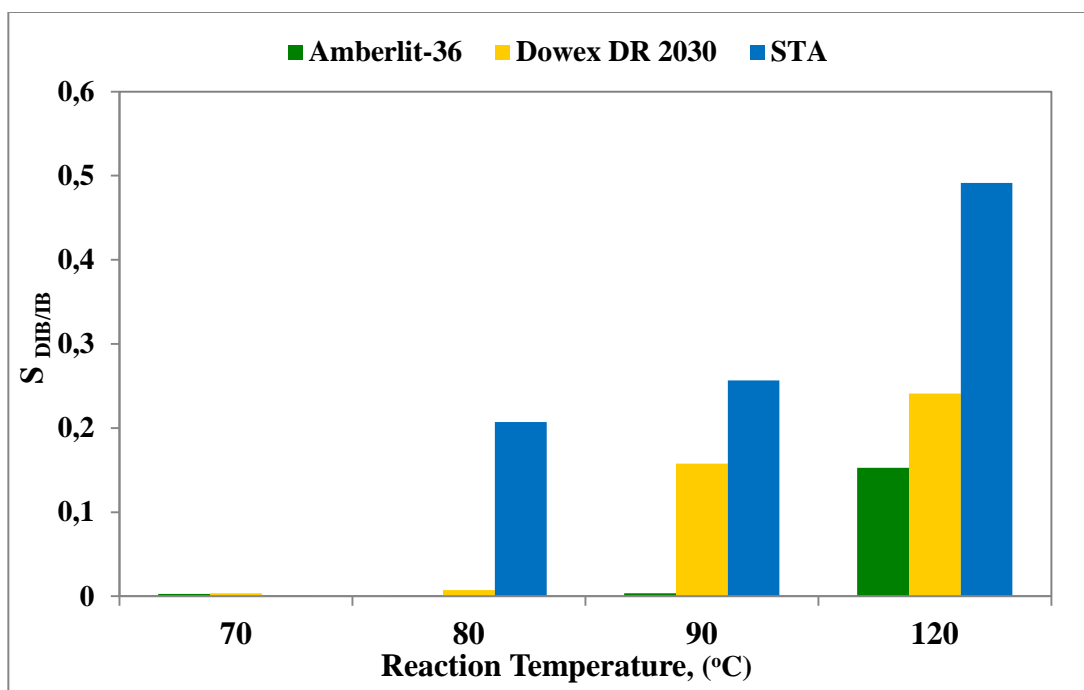


**Figure 21:** Di-i-butene (DIB) selectivity vs. reaction temperature with different catalysts (Reaction time=6h,  $m_{\text{cat}}=0.3$  g)

### 7.5.2. Effect of temperature on product selectivity obtained with different solid acid catalysts

Mono, di and tri ether selectivities obtained as a result of glycerol etherification with i-butene in the presence of Amberlyst-36, Dowex DR-2030 and STA are shown in Figure 22, 23, 24 respectively.

Because of their low solubility in diesel and gasoline monoethers of glycerol (MTBG) are not preferred as oxygenate additives. Therefore, di and tri ethers of glycerol (DTBG and TTBG) are preferred products. Product selectivity is towards mono ethers at 70°C and selectivity values are approximately 0.9 with all three of the acidic catalyst used in this study. As temperature was increased to 80°C, a drastic decrease in mono ether selectivity was observed, especially with silicotungstic acid (STA) catalyst. Di and tri ether selectivities reached to a maximum in this

temperature with STA. As temperature was increased to 90°C, di and tri ether selectivities obtained in the presence of Dowex DR-2030 and silicotungstic acid (STA) were quite similar. However, for Amberlyst-36, mono-ether selectivity was higher than di and tri ether selectivity. This was considered to be due to the lower porosity of A-36 than Dowex DR-2030, which created much higher diffusion resistance for the penetration of reactants to the active sites. In the case of STA, the pseudo-liquid character of this catalysts allows easier penetration of the reactants to the acid sites. Decrease of di and tri-ether selectivities observed with STA and Dowex DR-2030 with a further increase of temperature to 120°C may be related to the decrease of i-butene concentration in the reactor due to formation of di-i-butene (DIB)

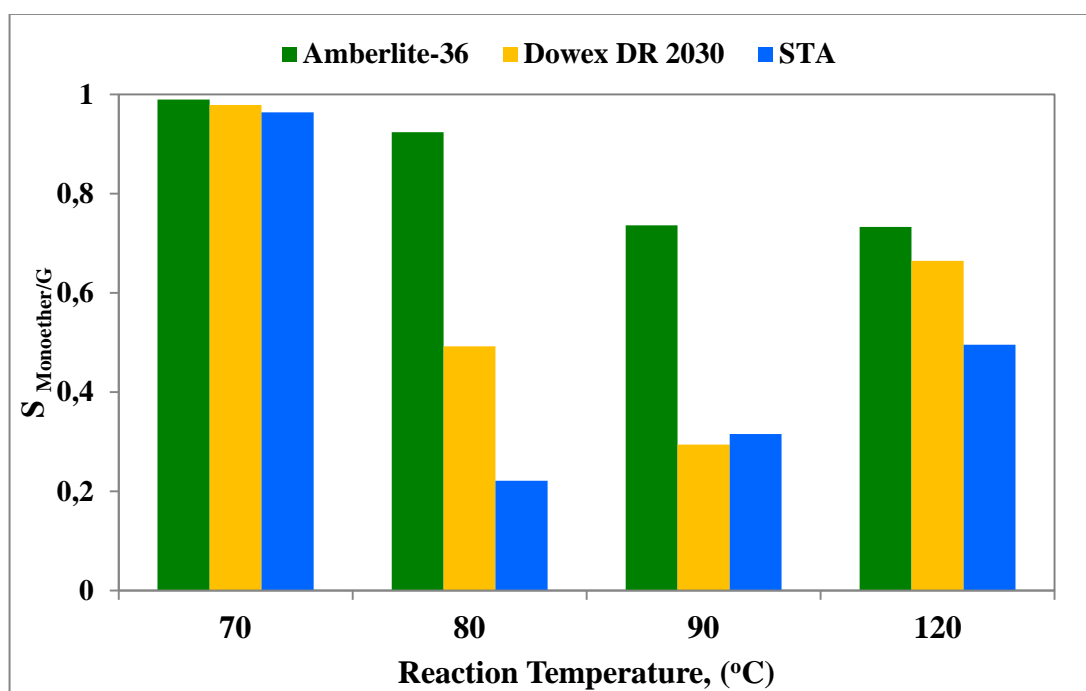


**Figure 22:** Monoether selectivity vs. reaction temperature with different catalysts  
(Reaction time=6h , $m_{cat}$ = 0.3 g)

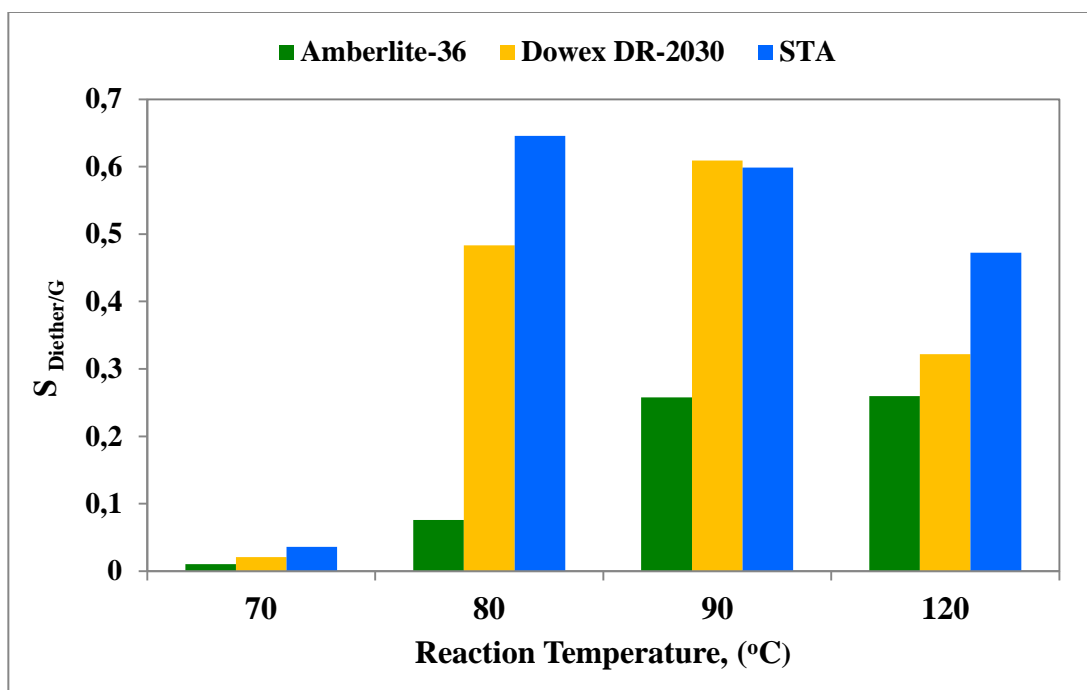


**Figure 23:** Diether selectivity vs. reaction temperature with different catalysts  
(Reaction time=6h,  $m_{cat}=0.3$  g)

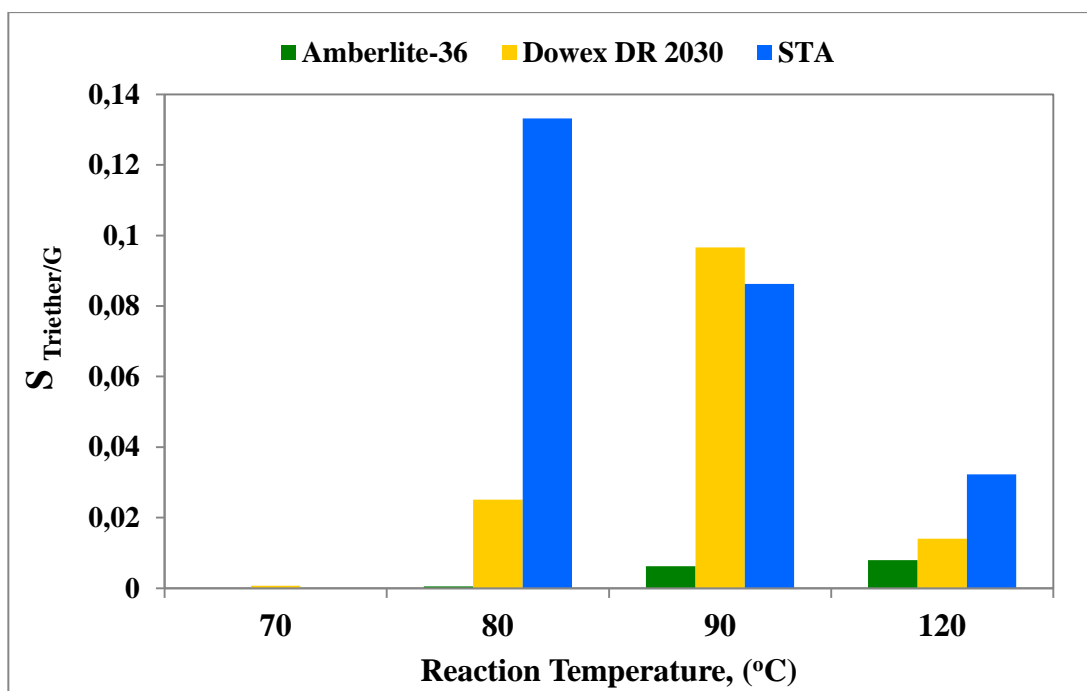


**Figure 24:** Tri ether selectivity vs. reaction temperature with different catalysts  
(Reaction time=6h,  $m_{cat}=0.3$  g)

## CHAPTER 8

### RESULTS OF GLYCEROL ETHERIFICATION WITH 2-METHYL-2-BUTENE (2M2B)

In this chapter GC/MS analysis results are given in order to determine product properties by the etherification of glycerol with 2M2B. Besides results corresponding to etherification of glycerol with 2M2B over commercial solid acid catalysts namely; A-36 and Dowex DR-2030 are presented.

#### 8.1. GC/MS ANALYSIS RESULTS

Etherification of glycerol with C<sub>5</sub> i-olefin (2M2B) is a new research area. There is no work published for the production and product properties of fuel additives by the etherification of glycerol with 2M2B. To obtain information about products, before the reaction experiments GC/MS analysis was applied.

Results of GC/MS analysis was composed of four parts. In the first part, mass spectra of the chemicals which we have been used during this study were taken from the database of the GC/MS device. These spectra were interpreted in order to separate reactants from products. In the second part, pure and binary mixtures of chemicals were analyzed in GC/MS and retention times were determined. According to etherification of glycerol with 2M2B a wide range of products were observed. Some of these products were thought to occur due to oligomerization (mainly dimerization) of 2M2B. In order to prove this, initial experiments were performed by using only

2M2B as the reactant (without glycerol) with Amberlyst-36 as catalyst. In the third part, GC/MS analysis result of this experiment was investigated. At least GC/MS analysis for etherification of glycerol with A-36 was examined to obtain information about reaction products.

### 8.1.1. Interpretation of Mass Spectras from GC/MS Database

Mass spectra of Glycerol, 2M2B and ethanol were taken from database of GC/MS device and are given in Appendix D1. In these spectra information about Relative Abundance (%) against Mass/Charge ratio is given. In Table 11 Mass/Charge (m/z) ratio of the first 10 peaks with the greatest relative abundance is represented.

**Table 11:** Mass/Charge ratio of glycerol, 2M2B and ethanol with the greatest relative abundance

Chemical	Molecular weight (g/mol)	mass/charge (m/z)									
		61	43	44	31	29	15	60	42	27	28
Glycerol	92.09	61	43	44	31	29	15	60	42	27	28
2M2B	70.13	55	70	41	42	39	29	27	53	43	56
Ethanol	46.06	31	45	29	27	46	43	26	30	15	42

After ionization of samples in the mass spectrometer, ions are separated according to their mass / charge (m/z) ratio. Accordingly, glycerol with a molecular weight of 92.09 g/mol gives main peaks at 61, 43, 44, 31, 29, 15, 60, 42, 27 and 28 mass/charge (m/z) ratio. With this information, behavior of reactants in GC/MS was identified.

### **8.1.2. GC/MS analysis results of pure and binary chemical mixtures to obtain retention times**

In order to obtain the retention times of pure 2M2B and a binary mixture of ethanol and glycerol with Glycerol/Ethanol molar ratio of 1/8 were analyzed in GC/MS. Retention times are given below.

#### **➤ *Pure 2M2B***

GC/MS analysis result of pure 2M2B is given in Appendix D2. As a result of this analysis, retention time of 2M2B was determined as  $t=0.54$  min.

#### **➤ *Glycerol and Ethanol binary mixture with a molar ratio of (G/EtOH=1/8)***

GC/MS analysis result of glycerol and ethanol binary mixture with a molar ratio of (G/EtOH=1/8) is given in Appendix D2. Retention times of ethanol and glycerol were recorded as  $t=0.52$  and  $t=17.4-20.9$  minute, respectively.

### **8.1.3. GC/MS analysis results for etherification of 2M2B (without glycerol) with A-36**

Initial experiments of etherification of glycerol with 2M2B had indicated that some side reactions such as oligomerization (mainly dimerization) of 2M2B could occur. In order to prove this experiments were performed by using only 2M2B as the reactant (without glycerol) with Amberlyst-36 as the catalyst. Mass spectra of this reaction and the matched molecules with these spectra from the library of GC/MS (Wiley and Nist) are given in Appendix D3.

Dimerization of 2M2B, formed  $C_{10}H_{20}$  with a molecular weight of 140 g/mol. Analyzing of mass spectra demonstrated that the relative abundance of mass/charge (m/z) ratio with 140 g/mol was were small among others. Maximum relative abundance was recorded between 55-83 g/mol. Broken down to smaller molecules during ionization is regarded as the cause of this result. Therefore, too much

conclusive information could not be obtained from these mass spectra. Another way was writing the molecular formulas of each component which matched with the molecules from the library of GC/MS. The molecules with molecular formulas  $C_{10}H_{20}$  were considered as a result of dimerization. Retention time was recorded between  $t=1.12-2.7$  minute.

From GC/MS results, occurrence of dimerization was established. However the column of GC/MS and the gas chromatography within our laboratory were different from each other. As a result, retention times and location of peak were not same. Therefore this reaction was analyzed in our gas chromatograph, retention times and location of possible oligomers were determined.

#### **8.1.4. GC/MS analysis results for etherification of glycerol with 2M2B over A-36**

GC/MS analysis for etherification of glycerol with 2M2B over A-36 catalyst was taken in order to investigate reaction products. The GC/MS result of this reaction is given in Appendix D4. At the beginning spectra of reactants and oligomerization products were determined. The products of etherification of glycerol with 2M2B (Figure 5) have molecular weights of 162, 232, 302 g/ mol respectively. But when the mass spectra were analyzed the relative abundances of these molecular weight were less than expected. As mentioned in the previous part, decomposition of these products to smaller molecules during ionization is regarded as the main cause of this result. Besides, due to lack of information about the products no information could be obtained from the matched molecules of GC/MS library.

As a solution, etherification of glycerol with tert-butanol (TBA) which has been studied previously by our group was used as a reference. At the same reaction conditions, etherification of glycerol with 2M2B and TBA were performed separately. At the end of each run, chemical composition of the product mixture was analyzed by the gas chromatography within our laboratory. Similar product

distribution was considered to occur with both reactants. According to the gas chromatogram results, peak observed at t=23, between 26-30 and 31-35 minutes were determined as tri, di and mono-ethers respectively.

## 8.2. ETHERIFICATION OF GLYCEROL WITH 2M2B OVER COMMERCIAL SOLID ACID CATALYSTS

After observing some ideas about the products, reaction experiments were performed. In this part, results corresponding to etherification of glycerol with 2M2B over commercial solid acid catalysts namely; A-36, Dowex DR-2030 is given. Effect of reaction temperature, reaction time and catalyst amount on glycerol conversion and product selectivity are presented.

Etherification of glycerol with 2M2B is also an acid catalyzed reaction. Formations of five ethers were expected as a result of consecutive etherification reactions which are represented in reactions (1)-(6). Reaction (1) and (2), are for producing mono-glycerol ethers isomers (ME1 and ME2), (3) and (4) for di-glycerol ether isomers (DE1 and DE2), (5) and (6) for producing tri-glycerol ether (TE).

### Main Reactions



The total conversion of glycerol ( $X_G$ ) to mono-, di- and tri-ethers was calculated using equation 8.1. In this equation  $X_{\text{Monoether}}$ ,  $X_{\text{Diether}}$ ,  $X_{\text{Triether}}$  are mole fractions of mono-, di- and tri-ethers.

$$X_G = \frac{X_{\text{Monoether}} + X_{\text{Diether}} + X_{\text{Triether}}}{X_{\text{Glycerol}} + X_{\text{Monoether}} + X_{\text{Diether}} + X_{\text{Triether}}} \quad 8.1.$$

Selectivity of mono-ethers to glycerol was calculated according to 'proportion of produced mono-ethers to converted glycerol' with using equation 8.2.

$$S_{\text{Monoether/G}} = \frac{X_{\text{Monoether}}}{X_{\text{Monoether}} + X_{\text{Diether}} + X_{\text{Triether}}} \quad 8.2.$$

Selectivity of di-ethers to glycerol was calculated according to 'proportion of produced di-ethers to converted glycerol' with using equation 8.3.

$$S_{\text{Diether/G}} = \frac{X_{\text{Diether}}}{X_{\text{Monoether}} + X_{\text{Diether}} + X_{\text{Triether}}} \quad 8.3.$$

Selectivity of tri-ethers to glycerol was calculated according to 'proportion of produced tri-ethers to converted glycerol' with using equation 8.4.

$$S_{\text{Triether/G}} = \frac{X_{\text{Triether}}}{X_{\text{Monoether}} + X_{\text{Diether}} + X_{\text{Triether}}} \quad 8.4.$$

Etherification of glycerol with 2M2B was performed using A-36 and Dowex DR-2030 under different reaction conditions. In the case of using A-36 experiments were repeated with different amounts of catalyst, namely 0.3 and 1 g. Also, a set of experiments were performed at different reaction times (1, 3, 6, 12, 24 h). Reaction temperatures were selected as 120° and 140°C. Activity of A-36 and Dowex DR-2030

was compared with different catalyst amounts. Effect of catalyst amount and reaction temperature on glycerol conversion and product selectivity was studied over A-36. Sample conversion and selectivity calculations are given in Appendix E

### 8.3. INFLUENCE OF CATALYST TYPE AND CATALYST AMOUNT ON GLYCEROL CONVERSION AND PRODUCT SELECTIVITY

#### 8.3.1. Influence of catalyst type and catalyst amount on glycerol conversion

In order to determine the influence of catalyst type and catalyst amount on glycerol conversion, etherification of glycerol was studied with 2M2B over Amberlyst-36 and Dowex DR-2030 resins. Maximum allowable operating temperatures of catalysts were taken into account and reaction temperature was selected as 120°C. Glycerol conversion results obtained at the end of a 6 h reaction period indicated that the activities of these catalysts were quite comparable at this temperature (Figure 25).

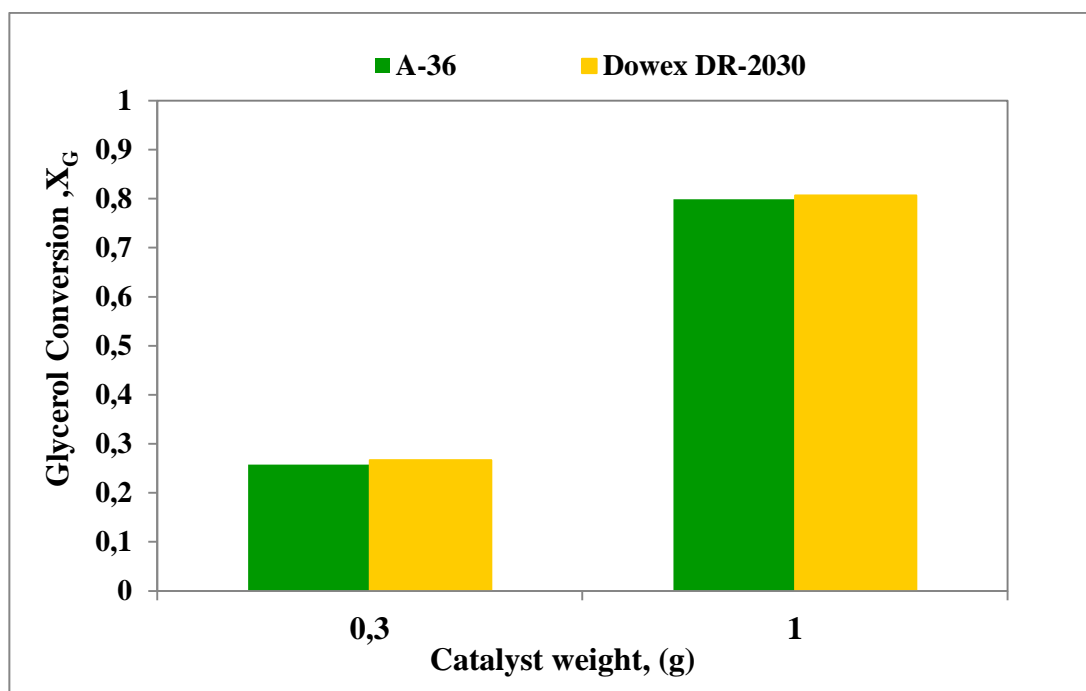


**Figure 25:** Glycerol conversion vs. catalyst amount (g) with different catalysts  
(Reaction time=6 h, Reaction temperature = 120°C)

A significant increase was observed in conversion values, with an increase in catalyst amount. This is due to the increased number of active sites per unit volume of the reaction mixture. The glycerol conversion values observed as a result of its reaction with 2M2B were less than the corresponding values obtained with i-butene as the reactant. This is considered to be mainly due to the larger molecular size of 2M2B than i-butene, which causes higher pore diffusion resistance, as well as more steric effects. Besides, initial experiments performed at the same conditions by using only 2M2B as the reactant (without glycerol) had indicated formation of some undesired side reactions, such as its oligomerization.

### **8.3.2. Influence of Catalyst Amount on Product Selectivity over Amberlyst-36**

Effect of catalyst amount on product distributions obtained at 120°C was illustrated in Figure 26, for Amberlyst-36 catalyst, results indicated that mono-ethers were the main product for both catalyst amounts (0.3 and 1 g). Monoether selectivity was nearly 0.7 with 0.3 g Amberlyst-36 however when catalyst amount increased to 1 g monoether selectivity decreased to 0.6. Decrease of mono-ether selectivity with catalyst amount was accompanied with an increase in di-ether and tri-ether selectivity values. This is due to the production of these ethers through a consecutive reaction path. Di-ether selectivity values of about 0.3 and 0.4 obtained with 0.3 and 1.0 g catalyst respectively were highly promising.

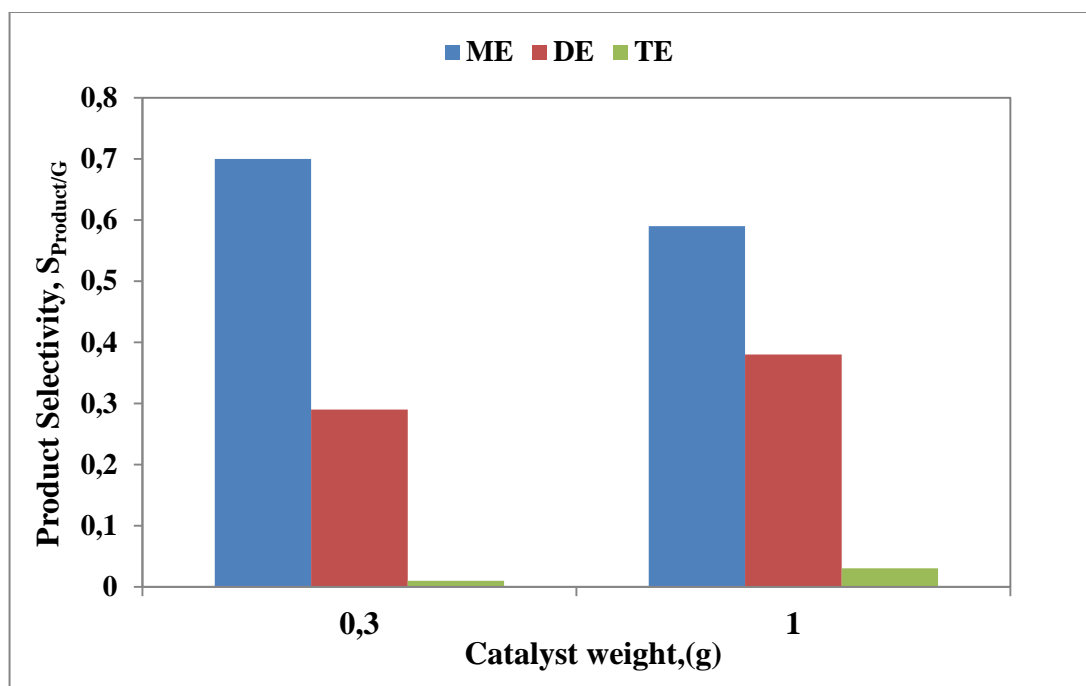


**Figure 26:** Product selectivity vs. catalyst amount (g) over Amberlyst-36 catalyst  
(Reaction time=6 h, Reaction temperature = 120°C)

### 8.3.3. Influence of Catalyst Amount on Product Selectivity over Dowex DR-2030

Effect of catalyst amount on product distributions obtained at 120°C was illustrated in Figure 27, for Dowex DR-2030 catalyst. As mentioned in the previous part results indicated that mono-ethers were the main product for both catalyst amounts (0.3 and 1 g). Mono ether selectivity was 0.8 with 0.3 g Dowex DR-2030 however when catalyst amount increased to 1 g mono ether selectivity decreased to 0.5. This is due to the production of these ethers through a consecutive reaction path. Di-ether selectivity values of about 0.2 and 0.5 obtained with 0.3 and 1.0 g catalyst respectively were highly promising.

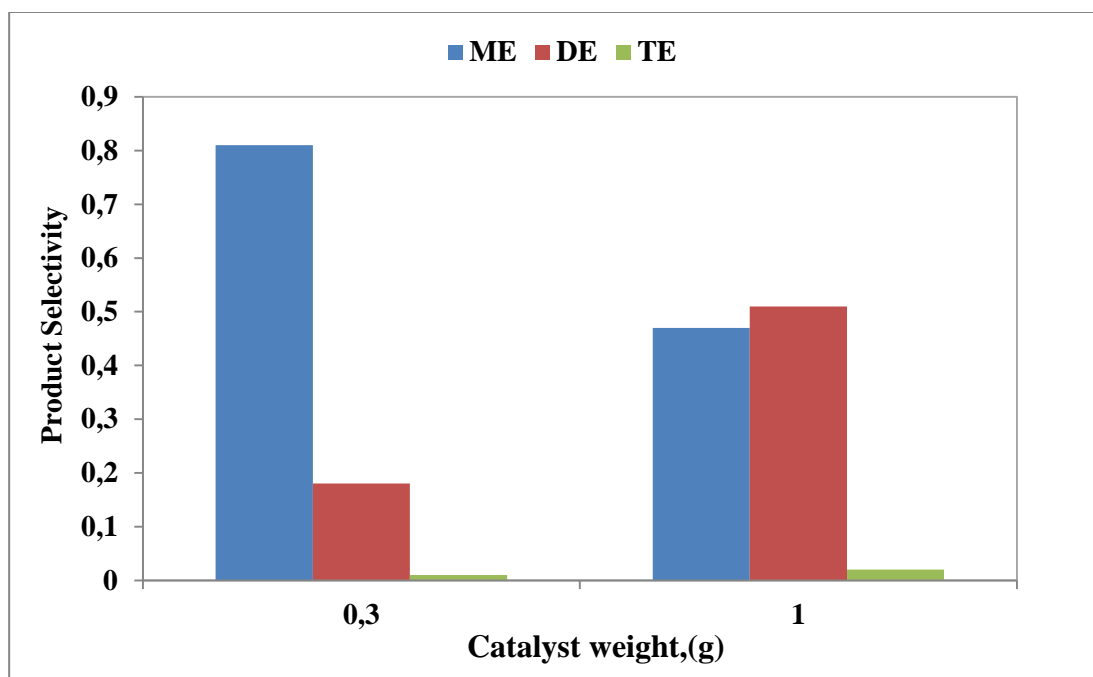


**Figure 27:** Product selectivity vs. catalyst amount (g) over Dowex DR-2030 catalyst  
(Reaction time=6 h, Reaction temperature = 120°C)

Considering that the catalytic activities of A-36 and Dowex DR-2030 were quite similar, detailed investigation of effects of reaction conditions on the catalytic performance and product distributions were continued with A-36, which is more stable at high temperatures.

#### **8.4. INFLUENCE OF REACTION TEMPERATURE, REACTION TIME AND CATALYST AMOUNT ON GLYCEROL CONVERSION OVER A-36**

Etherification of glycerol with 2M2B was investigated at 120 and 140°C over A-36 in the batch reactor. Effects of reaction time on glycerol conversion and product distributions were evaluated. In order to determine the effect of reaction time and

catalyst amount, experiments were repeated at 1, 3, 6, 12, 24 h reaction periods and using 0.3 and 1 g catalyst loadings. Results are illustrated in Figure 28.

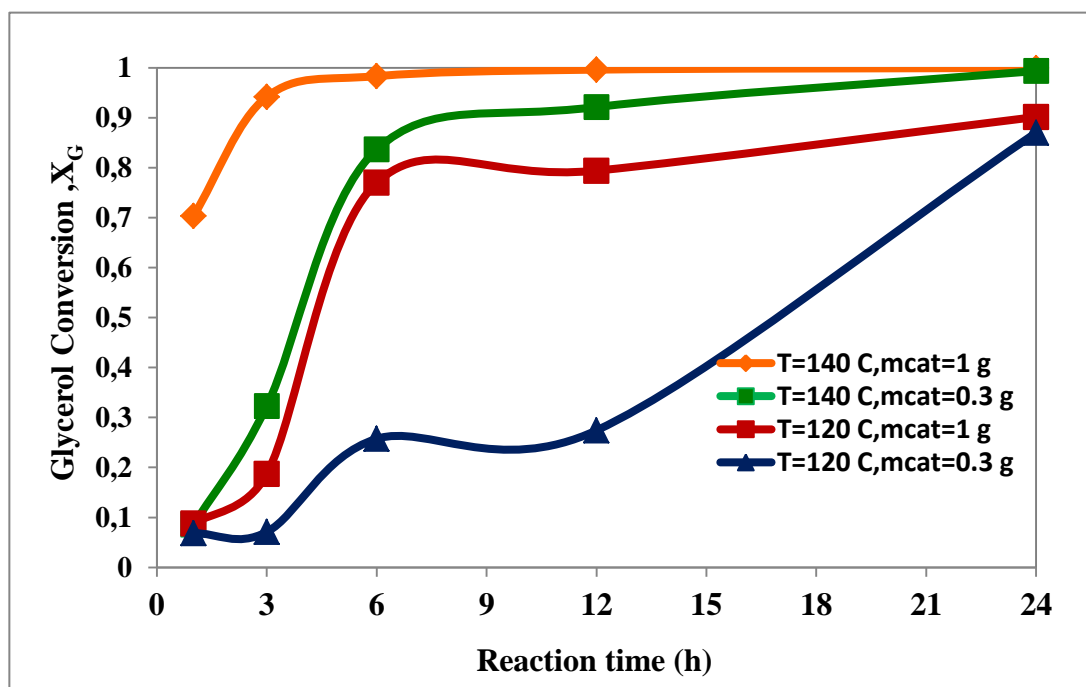


**Figure 28:** Glycerol conversion values obtained at different; temperatures (120 and 140°C), reaction times (1, 3, 6, 12, 24 h) and catalyst amount ( $m_{\text{cat}}=0.3$  or 1 g, A-36)

At 140°C with 1 g of catalyst, the reaction was very fast in the first hour and glycerol conversion value reached to 70%. As the reaction time increased, glycerol conversion increased until the 6' th hour of reaction time, approaching to almost complete conversion. After this point no significant change in terms of glycerol conversion was observed.

As, it was seen in, Figure 28 glycerol conversion rate was slower in the case of using less amount of catalyst at 140°C. In the first hour of reaction period, glycerol conversion was only 10%, in case of using 0.3 g of catalyst. As the reaction time increased glycerol conversion increased sharply until 6'th hour of reaction time, and approached to almost complete conversion only after 24 h of reaction time. Glycerol conversion values also varied drastically with the amount of catalyst loading in the

reactions conducted at 120°C. Glycerol conversion values after 24 h of reaction time at 120°C in the case of using 0.3 and 1 g of catalyst reached to nearly 90%. As expected, lower reaction rates were observed at 120°C than the corresponding values obtained at 140°C.

### **8.5. INFLUENCE OF REACTION TEMPERATURE, REACTION TIME AND CATALYST AMOUNT ON PRODUCT SELECTIVITY OVER A-36**

Effect of reaction period on product distributions obtained at 120°C was illustrated in Figure 29 and 30, for different amounts of catalyst (A-36) charged to the reactor. Both of these figures indicated that mono-ethers were the main product at initial reaction times. Decrease of mono-ether selectivity with reaction time was accompanied with an increase in di-ether and tri-ether selectivity values. This is due to the production of these ethers through a consecutive reaction path. As it is shown in Figure 29 and 30 increase of catalyst amount from 0.3 g to 1.0 g, significantly enhanced the etherification reactions, causing much sharper decrease of mono-ether selectivity and much higher di- and tri-ether selectivity values at longer reaction times. Di-ether selectivity values of about 0.7 and tri-ether selectivities approaching to 0.1 obtained with 1.0 g catalyst at reaction times longer than 12 h were highly promising. Effect of reaction temperature on ether selectivity values is illustrated in Figure 31. Comparison of the results reported in this figure with the corresponding results given in Figure 29 clearly showed the positive effect of increase of temperature from 120°C to 140°C on the di-ether and tri-ether selectivity values obtained by using 0.3 g of catalyst. Much sharper decrease of mono-ether selectivity and a much sharper increase of di- and tri-ether selectivity values were obtained by increasing the temperature to 140°C. Considering that di- and tri-ethers of glycerol were more soluble in diesel fuel and gasoline, this is an attractive result

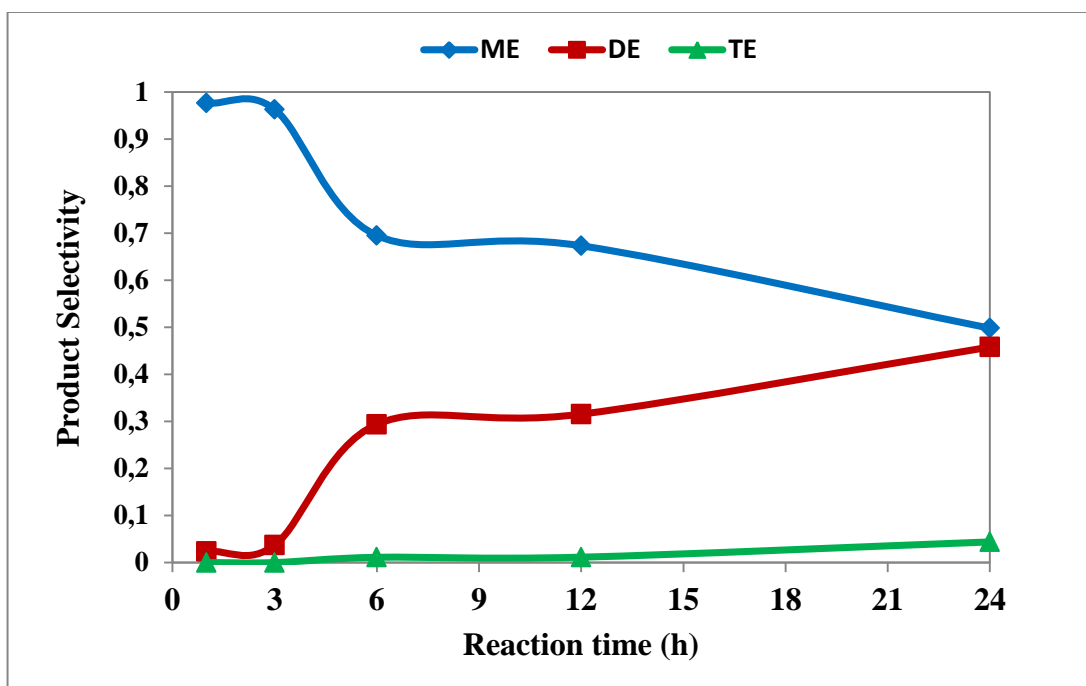


**Figure 29:** Product Selectivity vs. Reaction time with Amberlyst-36 catalyst  
(Reaction Temperature =120°C,  $m_{\text{cat}}=0.3$  g)

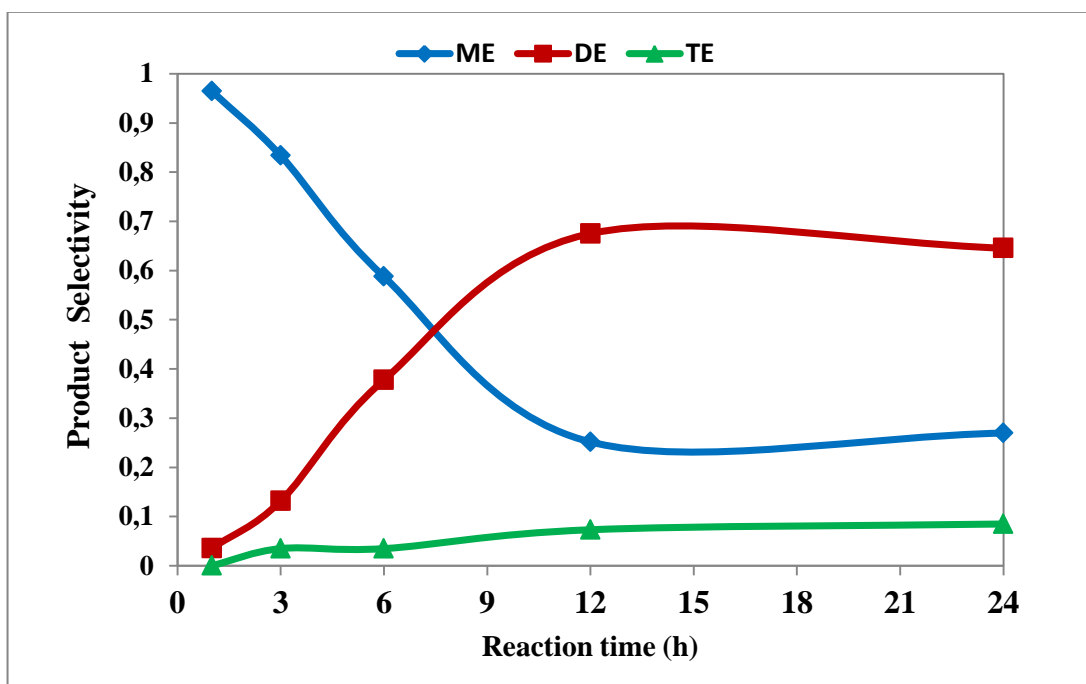


**Figure 30:** Product Selectivity vs. Reaction time with Amberlyst-36 catalyst  
(Reaction Temperature =120°C,  $m_{\text{cat}}=1$  g)

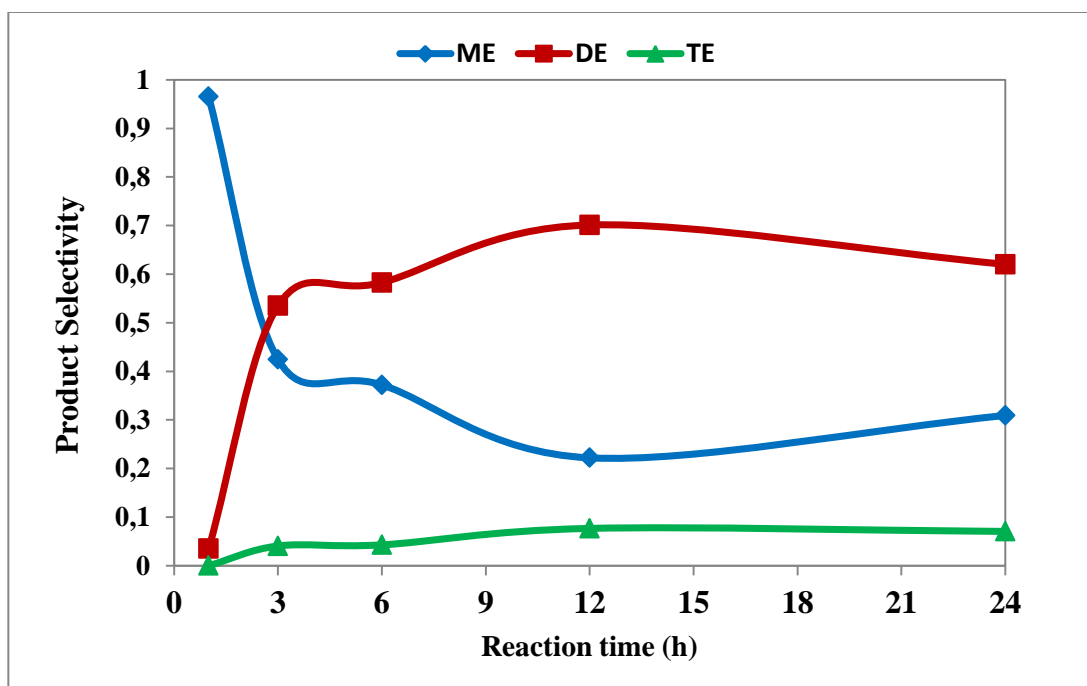


**Figure 31:** Product Selectivity vs. Reaction time with Amberlyst-36 catalyst  
(Reaction temperature =140°C,  $m_{\text{cat}} = 0.3 \text{ g}$ )

## **CHAPTER 9**

### **CHARACTERIZATION AND ACTIVITY RESULTS OF SAPO-34-LIKE CATALYSTS**

In this study, microporous SAPO-34, mesoporous SAPO-34, and Silicotungstic acid (STA) impregnated mesoporous SAPO-34-like materials were synthesized. Mesoporous SAPO-34 and Silicotungstic acid (STA) impregnated mesoporous SAPO-34 were tested in etherification of glycerol with i-butene. In this chapter, characterization results of the synthesized SAPO-34 catalysts are presented. X-Ray diffraction (XRD), nitrogen physisorption (BET), Scanning Electron Microscopy (SEM), and Diffuse Reflectance Infrared Fourier Transform Spectroscopy of pyridine adsorption techniques were used for the characterization of these materials. In addition to characterization results, activity results in etherification of glycerol are also explained.

#### **9.1. CHARACTERIZATION RESULTS OF MICROPOROUS SAPO-34-LIKE CATALYST**

##### **9.1.1. X-Ray Diffraction (XRD) Result**

The XRD pattern of microporous SAPO-34 is given in Figure 32.

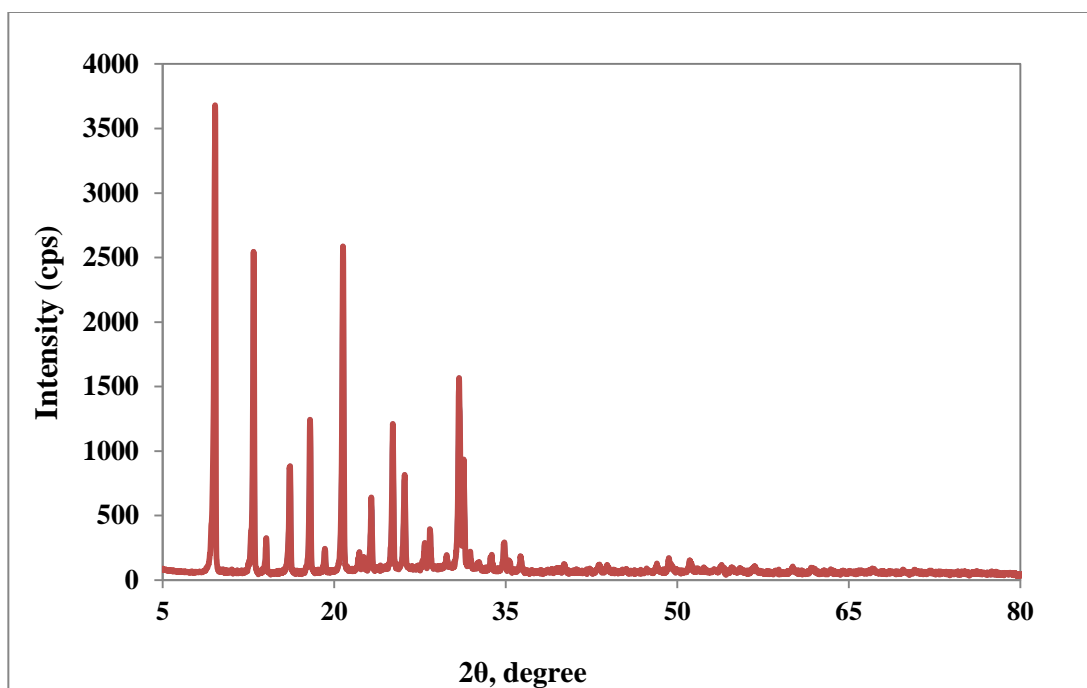


**Figure 32:** XRD pattern of microporous SAPO-34

According to XRD pattern shown in Figure 32, identical characteristic peaks corresponding to the Chabasite structure (CHA) of SAPO-34 based on literature (See Figure 7) are observed. The major peak at  $2\theta = 9.58^\circ$ , minor peaks at  $12.94^\circ$ ,  $16.08^\circ$ ,  $17.86^\circ$ ,  $20.76^\circ$ ,  $25.12^\circ$ ,  $25.18^\circ$ , and a double peak at  $2\theta \approx 27$  and  $31^\circ$  correspond to  $\text{Al}(\text{PO}_4)$  and  $\text{SiO}_2$  crystals. XRD pattern of pure  $\text{Al}(\text{PO}_4)$  and  $\text{SiO}_2$  are given in Appendix A.

### 9.1.2. $\text{N}_2$ Physisorption (BET) Result

Nitrogen adsorption desorption isotherms, surface area, average pore diameter, pore volume and pore size distributions were determined by nitrogen physisorption results. Nitrogen physisorption isotherm of microporous SAPO-34, which is given in Figure 33, showed a Type IV isotherm, as described by the IUPAC classification, indicating mesoporous structure. However, the isotherms are not exactly the same as

Type IV. The difference could be due to existence of non-ordered mesoporous and microporous structures.

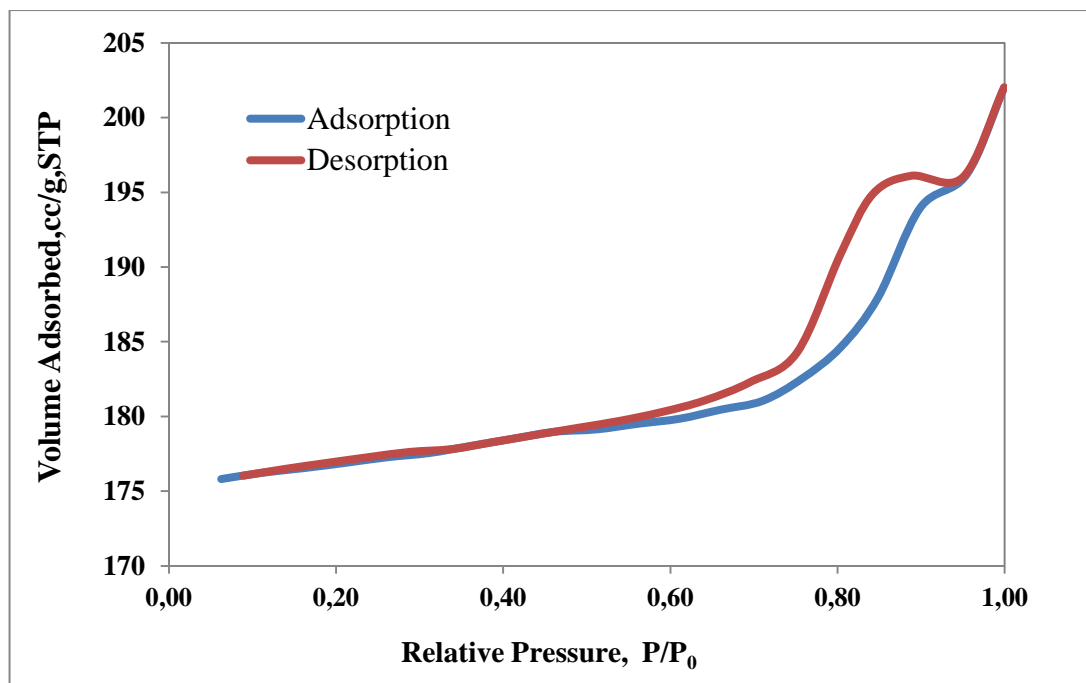


**Figure 33:** Nitrogen physisorption isotherm of microporous SAPO-34

BET surface area, pore volume, pore diameter and micropore volume values of microporous SAPO-34 are listed in Table 12. The surface area was recorded as 579 m<sup>2</sup>/g. According to Table 12, the surface area and micropore volume of the synthesized Microporous SAPO-34 are obtained as expected in the literature [50].

**Table 12:** BET and BJH surface area, pore volume and size and micropore volume data of Microporous SAPO-34

Catalyst	BET Surface Area, (m <sup>2</sup> /g)	BJH Desorption Pore Volume (cm <sup>3</sup> /g)	BJH Desorption Pore Diameter (nm)	DR Micropore Volume, (cm <sup>3</sup> /g)
Microporous SAPO-34	579	0.047	9.7	0.28

Pore size distribution curve of microporous SAPO-34 is given in Figure 34. As shown in Figure 34, pores are mainly in a range of nearly 5-15 nm, but there are also pores with nearly 3 nm in size. This analysis indicated presence of both mesopores and micropores in the structure of this material.

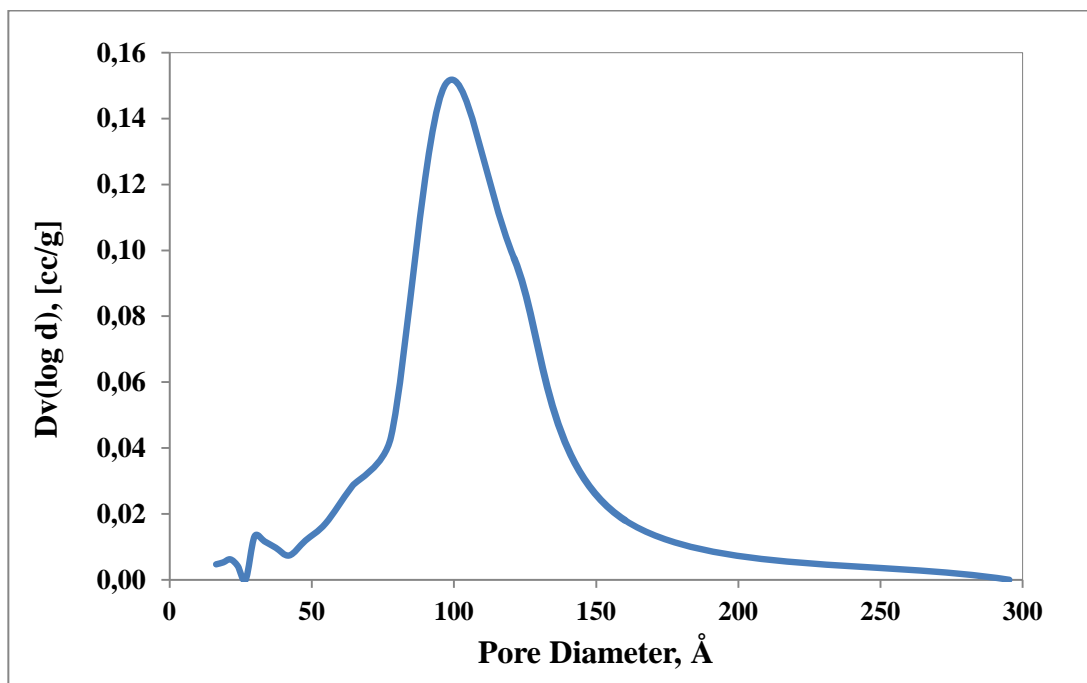


**Figure 34:** Pore Size Distribution of microporous SAPO-34

### 9.1.3. Scanning Electron Microscopy Analysis (SEM)

Scanning Electron Microscopy (SEM) images of Microporous SAPO-34 are given Figure 35. Cubic like rhombohedra crystals are observed. This type of crystal is similar to natural Chabasite (CHA). Crystals have average dimensions of 29.5 X 23.7 X 9.5  $\mu\text{m}$ .

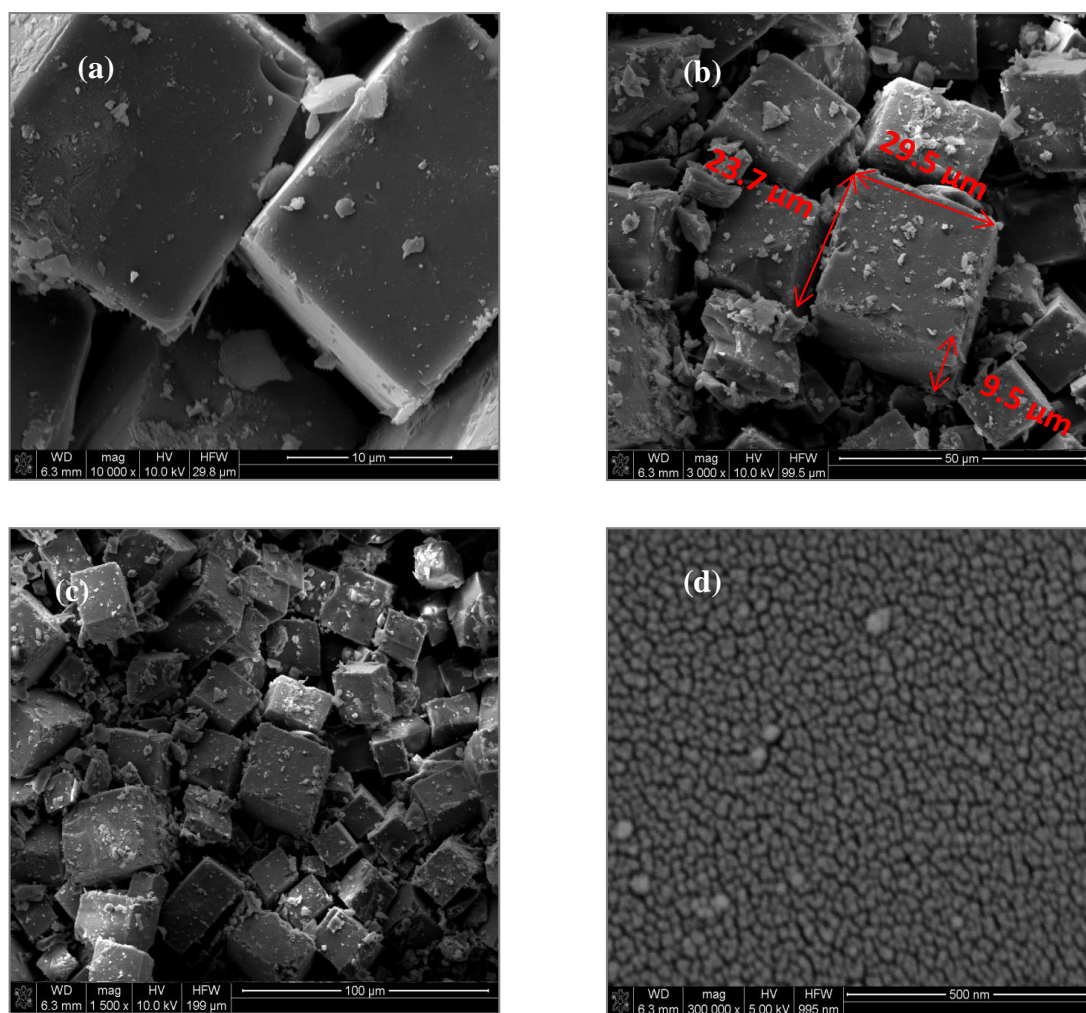


**Figure 35:** SEM images of Microporous SAPO-34, (a) with 10000 magnification, (b) with 3000 magnification, (c) with 1500 magnification, (d) with 300000 magnification

## 9.2. CHARACTERIZATION RESULTS OF MESOPOROUS SAPO-34-LIKE CATALYSTS

Mesoporous SAPO-34 was synthesized within two different solution pH values, in order to see the influence of solution pH on the characterization results of the synthesized materials. In the first route the synthesis solution pH was neutral (pH=7.4) and in the other procedure the solution pH was acidic with (pH=2.4). Characterization results of both catalysts are reported in the following sections.

### 9.2.1. X-Ray Diffraction (XRD) Result

Small angle X-ray diffraction results of Mesoporous SAPO-34 (neutral and acidic) are represented in Figure 36 and 37 respectively. The diffraction patterns in the small angle range ( $2\theta < 10^\circ$ ) confirm the presence of uniform mesopores in the material. The small angle XRD pattern of mesoporous SAPO-34 (neutral) has an intense peak at  $2\theta = 3.08^\circ$  (Figure 36). This means that, the synthesized catalyst is in the mesoporous range.

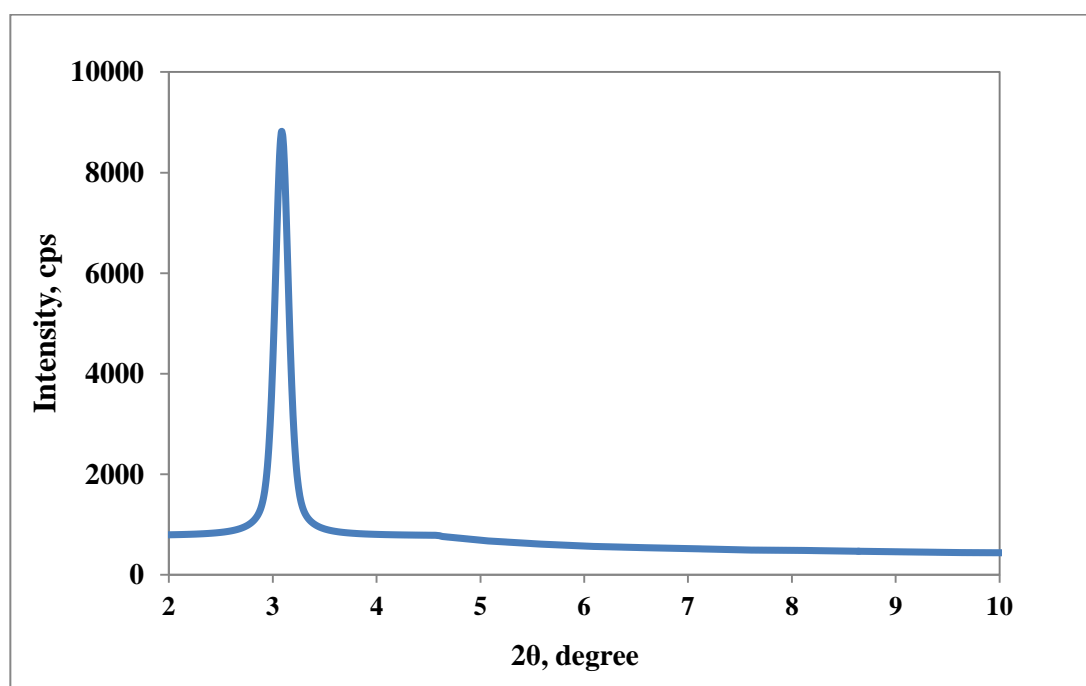


**Figure 36:** The small angle XRD pattern of Mesoporous SAPO-34, (neutral)

The small angle XRD pattern of Mesoporous SAPO-34 (acidic) (Figure 37) has a major peak at  $2\theta=1.03^\circ$ . As a result Mesoporous SAPO-34 (acidic) is also in mesoporous range.

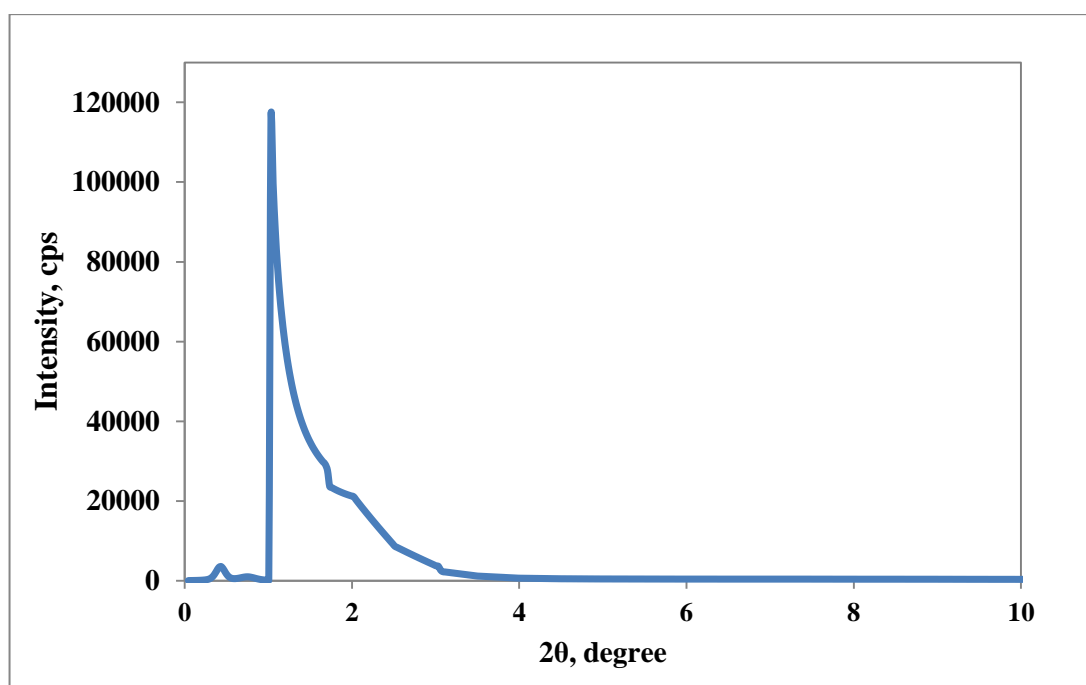


**Figure 37:** The small angle XRD pattern of Mesoporous SAPO-34, acidic

Wide angle XRD patterns of Mesoporous SAPO-34 (neutral and acidic) are presented in Figure 38. These XRD patterns are different from the characteristic XRD patterns of microporous SAPO-34 (Figure 7). The mesoporous structure might have influenced the characteristics.

Mesoporous SAPO-34 acidic, had a major peak at  $2\theta = 20.33^\circ$ , and minor peaks at  $21.50^\circ$ ,  $22.96^\circ$  and  $35.48^\circ$ , which correspond to Tridymite ( $\text{SiO}_2$ ) crystals. In the wide angle XRD pattern of Mesoporous SAPO-34 (neutral), no crystal peaks were observed. At  $2\theta \approx 20$  amorphous silica peak was observed.

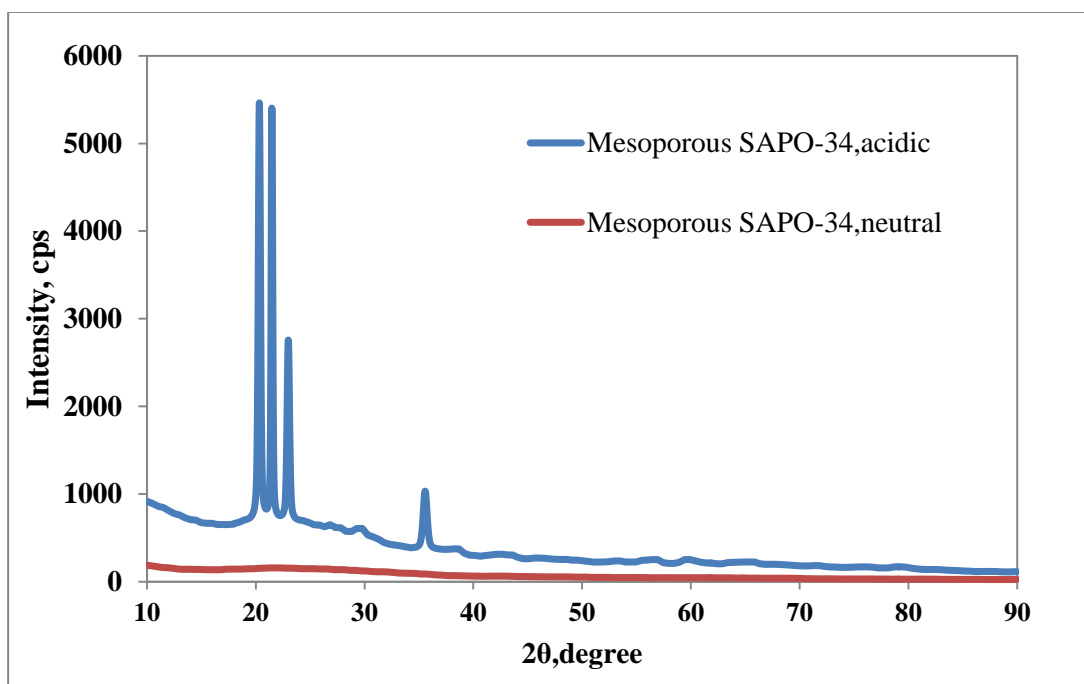


**Figure 38:** The wide angle XRD pattern of mesoporous SAPO-34, (neutral and acidic)

### 9.2.2. N<sub>2</sub> Physisorption (BET) Results

Nitrogen physisorption isotherms of mesoporous SAPO-34 (neutral and acidic) are given in Figure 39 and Figure 40 respectively. These isotherms resemble each other. They showed like Type IV isotherm, as described by the IUPAC classification, indicating mesoporous structure.

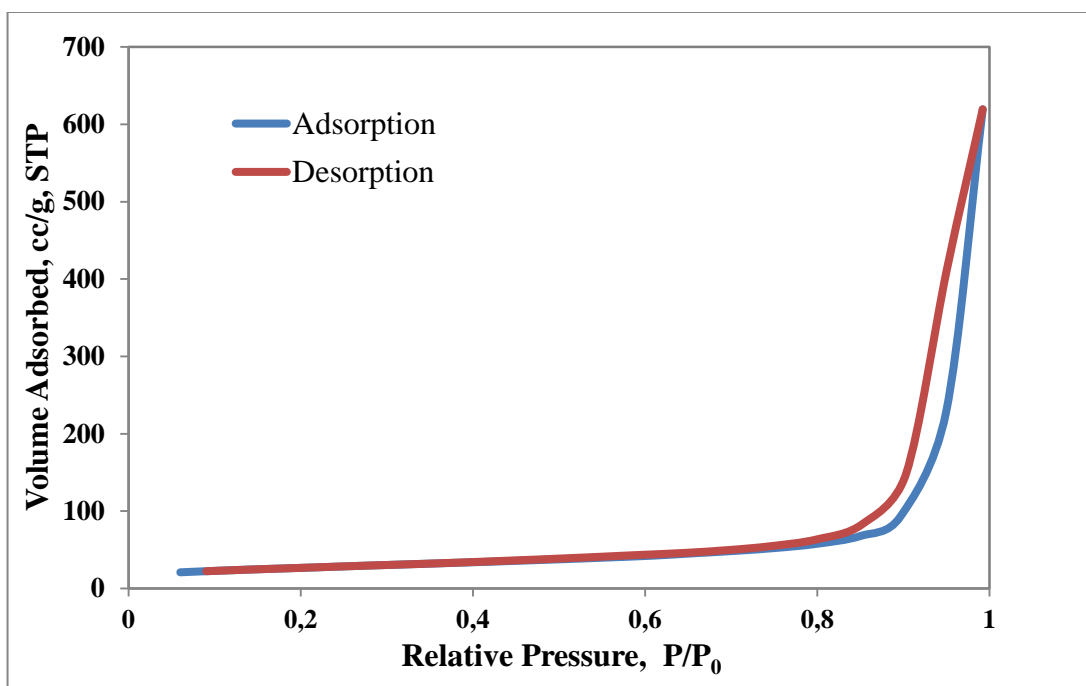


**Figure 39:** Nitrogen physisorption isotherm of mesoporous SAPO-34, (neutral)

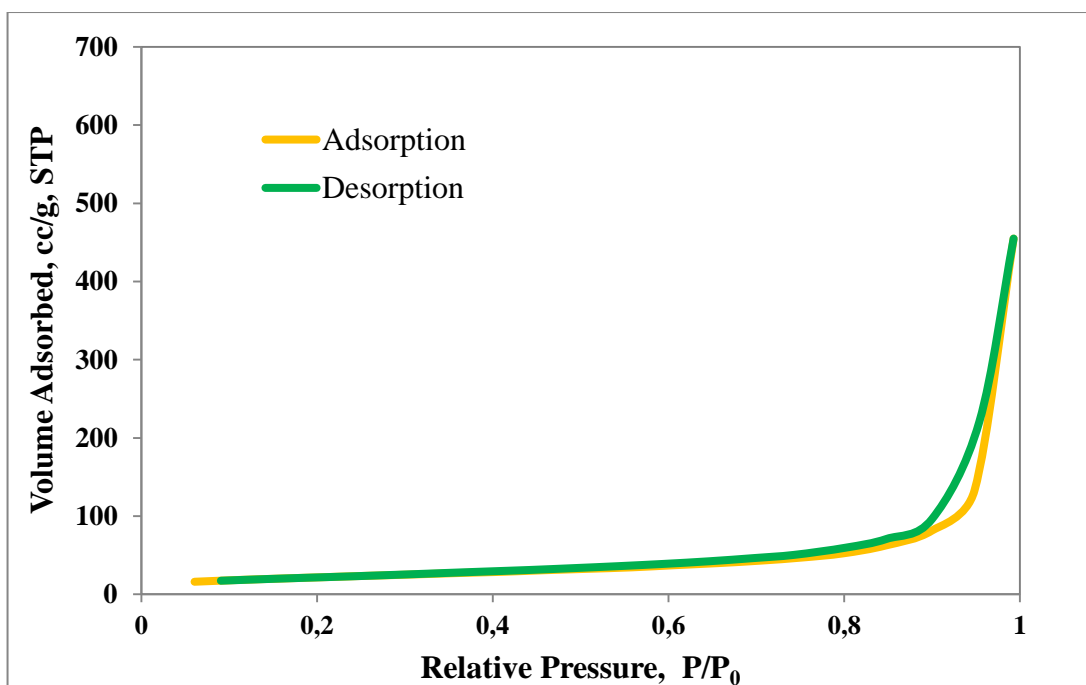


**Figure 40:** Nitrogen physisorption isotherm of mesoporous SAPO-34, acidic

BET surface area, pore volume, pore diameter and micropore volume of mesoporous SAPO-34 (neutral and acidic) are listed in Table 13. The surface areas of mesoporous SAPO-34, (neutral) and acidic were 94 and 78 m<sup>2</sup>/g, respectively. It is clearly seen from Table 13 synthesis of materials having pore sizes in the mesopore were successfully achieved.

**Table 13:** BET and BJH surface area, pore volume and size and micropore volume data of Mesoporous SAPO-34, (neutral and acidic)

<b>Catalyst</b>	<b>BET Surface Area,(m<sup>2</sup>/g)</b>	<b>BJH Surface Area, (m<sup>2</sup>/g)</b>	<b>BJH Desorption Pore Volume (cm<sup>3</sup>/g)</b>	<b>BJH Desorption Pore Diameter (nm)</b>	<b>DR Micropore Volume, ( cm<sup>3</sup>/g)</b>
<b>Mesoporous SAPO-34, (neutral)</b>	94.08	109.4	0.9738	31.2	0.047
<b>Mesoporous SAPO-34, (acidic)</b>	78.72	88.9	0.709	32.2	0.040

As shown in Figure 41 pore size distributions of Mesoporous SAPO-34 (neutral and acidic) are very broad. As a result, pores are not well ordered.

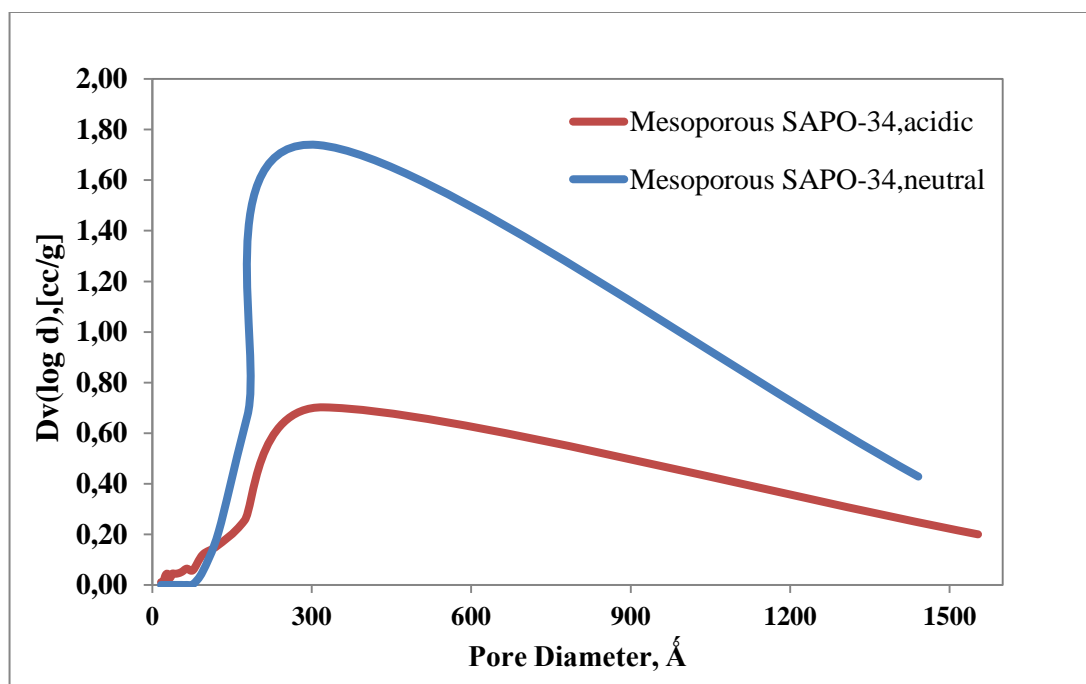


**Figure 41:** Pore Size Distribution of mesoporous SAPO-34, (neutral and acidic)

Both of the mesoporous SAPO-34 materials synthesized in the neutral and acidic media were in the mesoporous range. However, the pore volume of mesoporous SAPO-34 (neutral) ( $0.97 \text{ cm}^3/\text{g}$ ) was higher than Mesoporous SAPO-34 (acidic) ( $0.71 \text{ cm}^3/\text{g}$ ). High pore volume means that deactivation of the catalyst by plugging is more difficult. Therefore Mesoporous SAPO-34, (neutral) was selected as the best catalyst and tested in etherification of glycerol with i-butene.

### 9.2.3. Scanning Electron Microscopy Analysis (SEM)

Scanning Electron Microscopy (SEM) images of Mesoporous SAPO-34 (neutral and acidic) are given in Figure 42 and 43 respectively. Especially in case of 250 000 magnification, the pores are seen.

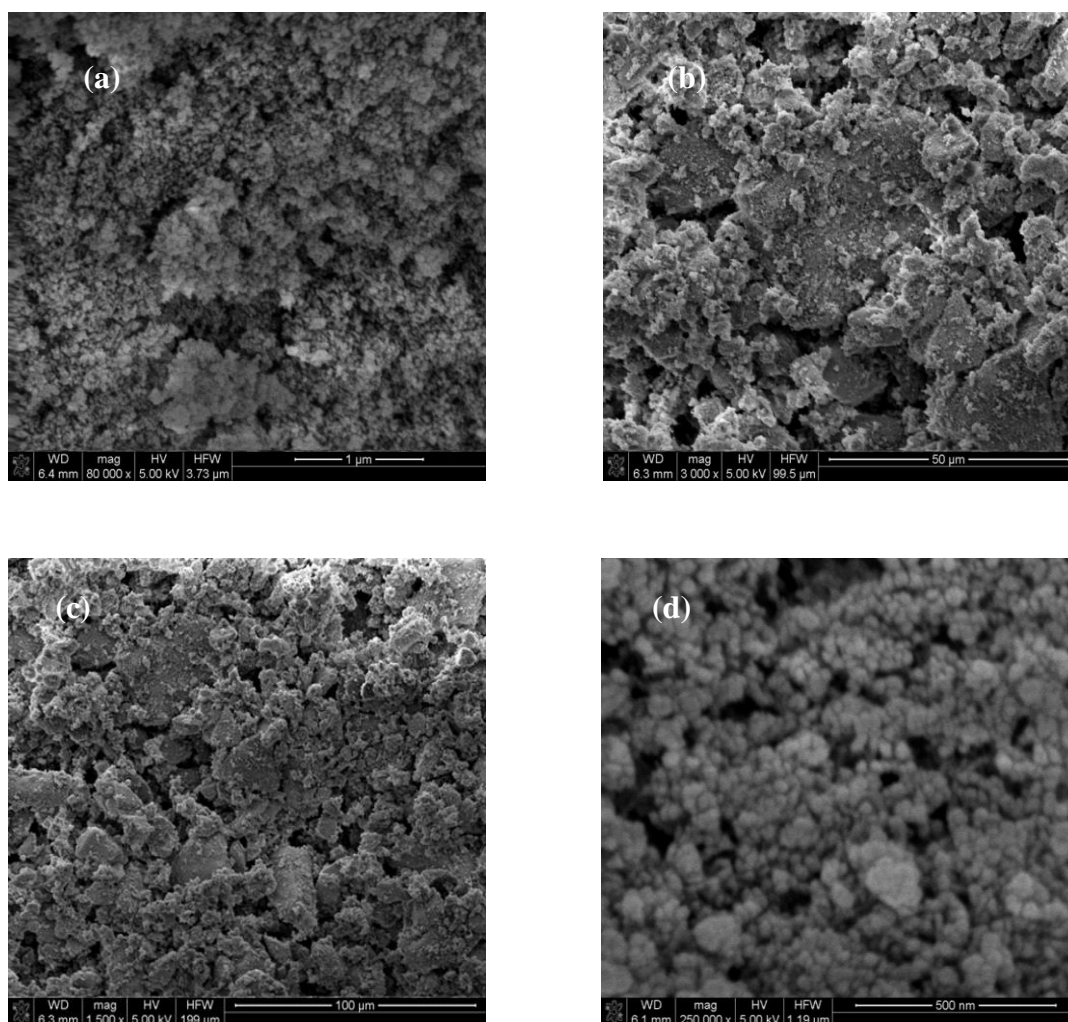


**Figure 42:** SEM images of Mesoporous SAPO-34, (neutral), (a) with 50000 magnification, (b) with 3000 magnification, (c) with 1500 magnification, (d) with 250000 magnification

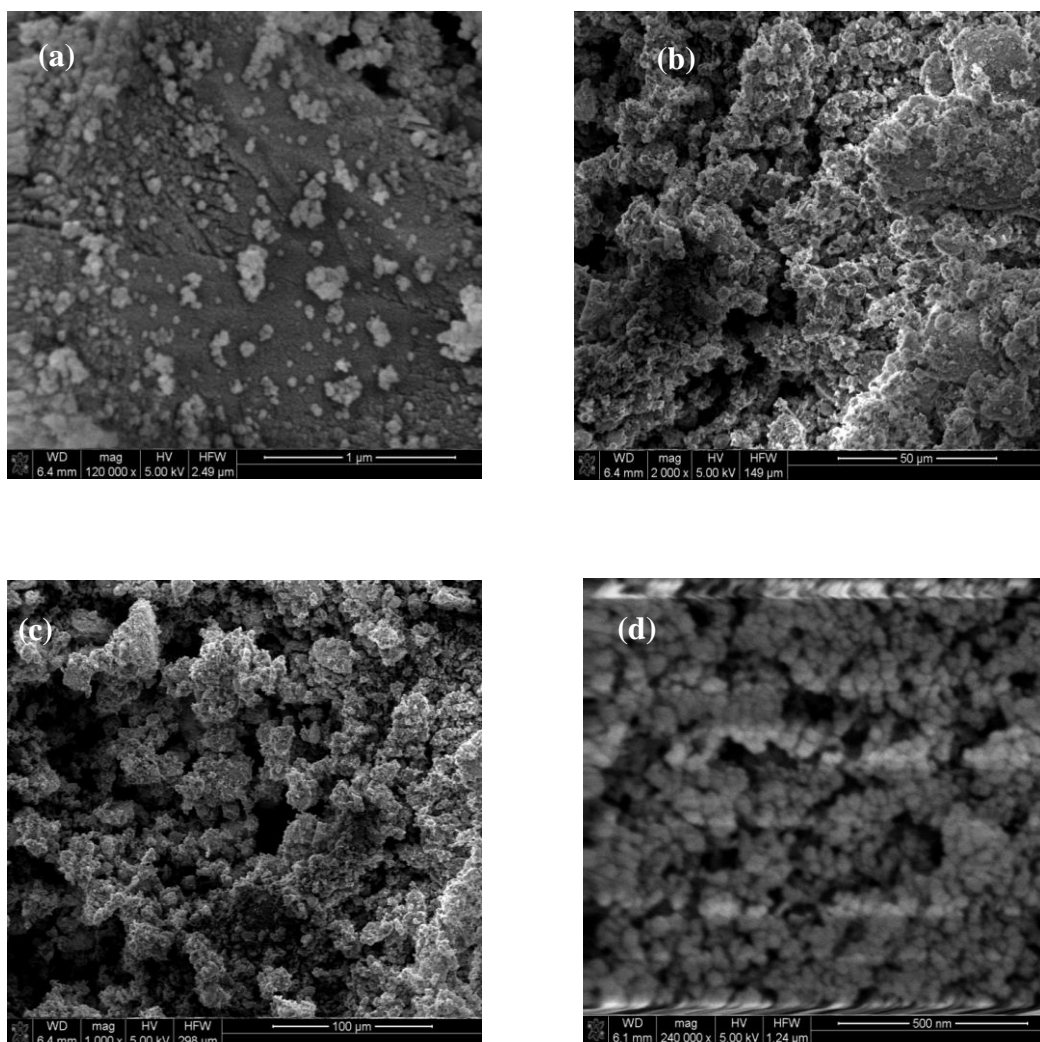


**Figure 43:** SEM images of Mesoporous SAPO-34, acidic, (a) with 120000 magnification, (b) with 2000 magnification, (c) with 1000 magnification, (d) with 240000 magnification

### 9.3. CHARACTERIZATION OF STA@MESOPOROUS SAPO-34, (NEUTRAL)

In order to increase the acidity of Mesoporous SAPO-34 (neutral) Silicotungstic acid (STA) was impregnated on Mesoporous SAPO-34 (neutral).

#### 9.3.1. N<sub>2</sub> Physisorption (BET) Results

Nitrogen physisorption isotherm of STA@Mesoporous SAPO-34 (neutral) is presented in Figure 44. The isotherm is like the one for Mesoporous SAPO-34 (neutral) (Figure 39).

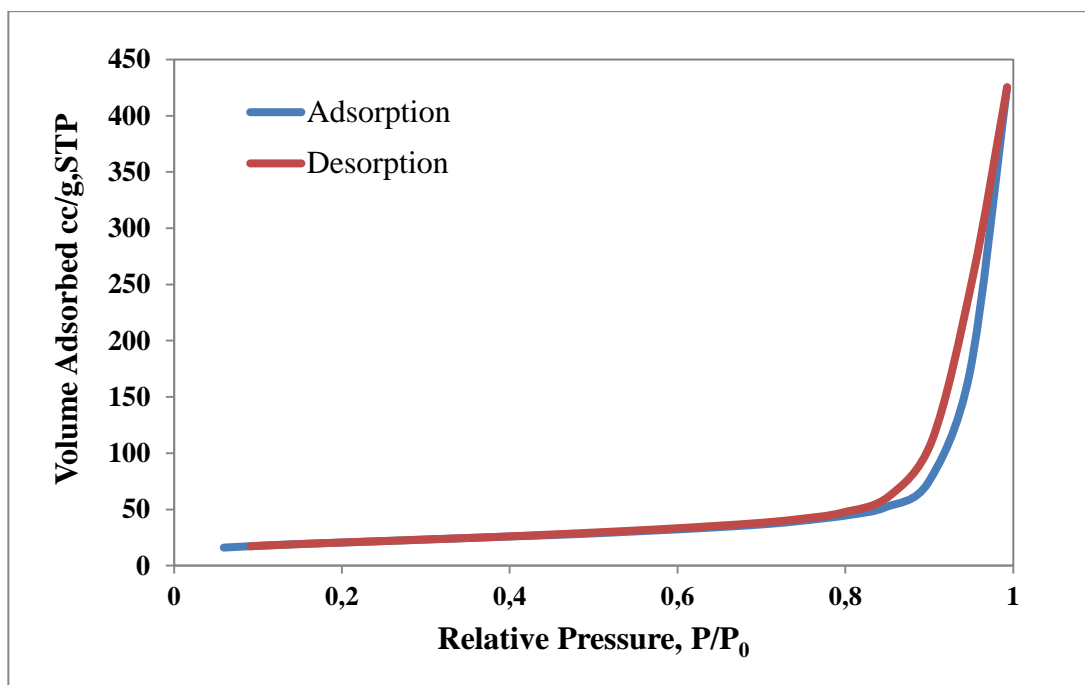


**Figure 44:** Nitrogen physisorption isotherm of STA@Mesoporous SAPO-34, (neutral)

Surface area, pore volume, pore size and micropore area data of Mesoporous SAPO-34 (neutral) and STA@Mesoporous SAPO-34(neutral) is given in Table 14. Compared with Mesoporous SAPO-34, (neutral) silicotungstic acid impregnation on Mesoporous SAPO-34 (neutral) caused in decrease of BET and BJH surface area and mesoporous volume. The decrease could be due to after STA impregnation the surface covered with STA and surface area decreases. The pore size distribution of STA@Mesoporous SAPO-34, (neutral) is presented in Figure 45 and it is seen that the pore size distribution is like Mesoporus SAPO-34, (neutral) (Figure 41). After Silicotungstic acid impregnation pore size distribution did not change.

**Table 14:** BET and BJH surface area, pore volume pore size and micropore volume data of Mesoporous SAPO-34 (neutral) and STA@Mesoporous SAPO-34, (neutral).

Catalyst	BET Surface Area, (m <sup>2</sup> /g)	BJH Surface Area, (m <sup>2</sup> /g)	BJH Desorption Pore Volume (cm <sup>3</sup> /g)	BJH Desorption Pore Diameter (nm)	DR Micropore Volume, ( cm <sup>3</sup> /g)
Mesoporous SAPO-34, (neutral)	94.08	109.4	0.9738	31.2	0.047
STA@Mesoporous SAPO-34, (neutral)	71.85	71.18	0.6592	31.77	0.036

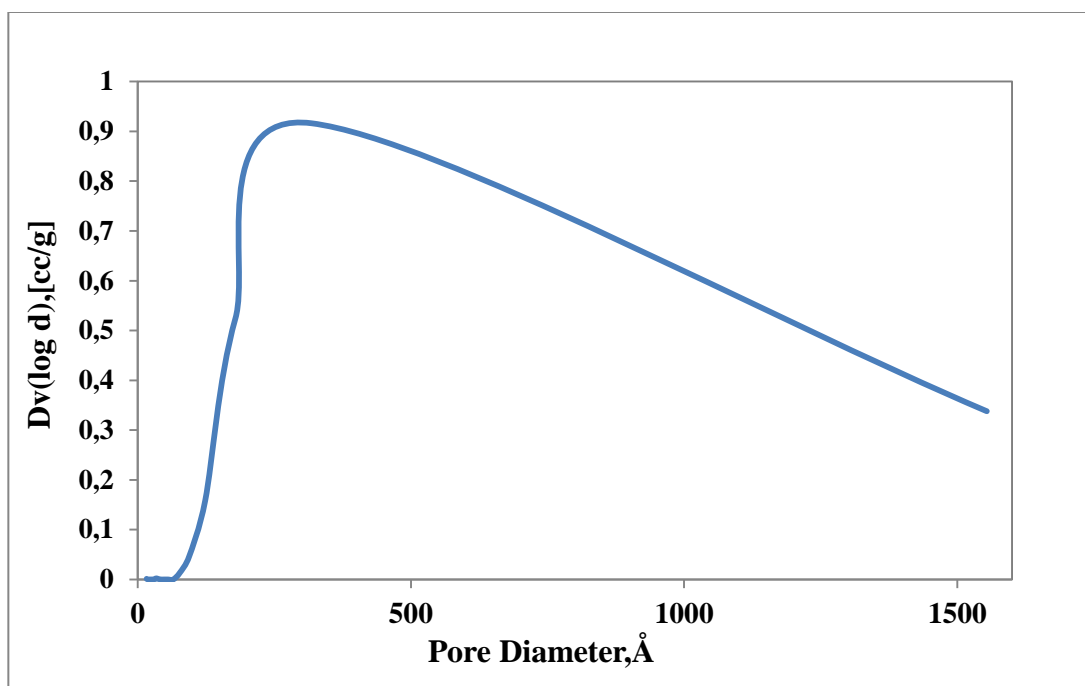


**Figure 45:** Pore Size Distribution of STA@ Mesoporous SAPO-34, (neutral)

### 9.3.2. Scanning Electron Microscopy Analysis (SEM)

Scanning Electron Microscopy (SEM) images of STA@Mesoporous SAPO-34, (neutral) are given in Figure 46. Especially in case of 250000 magnification pores are seen clearly.

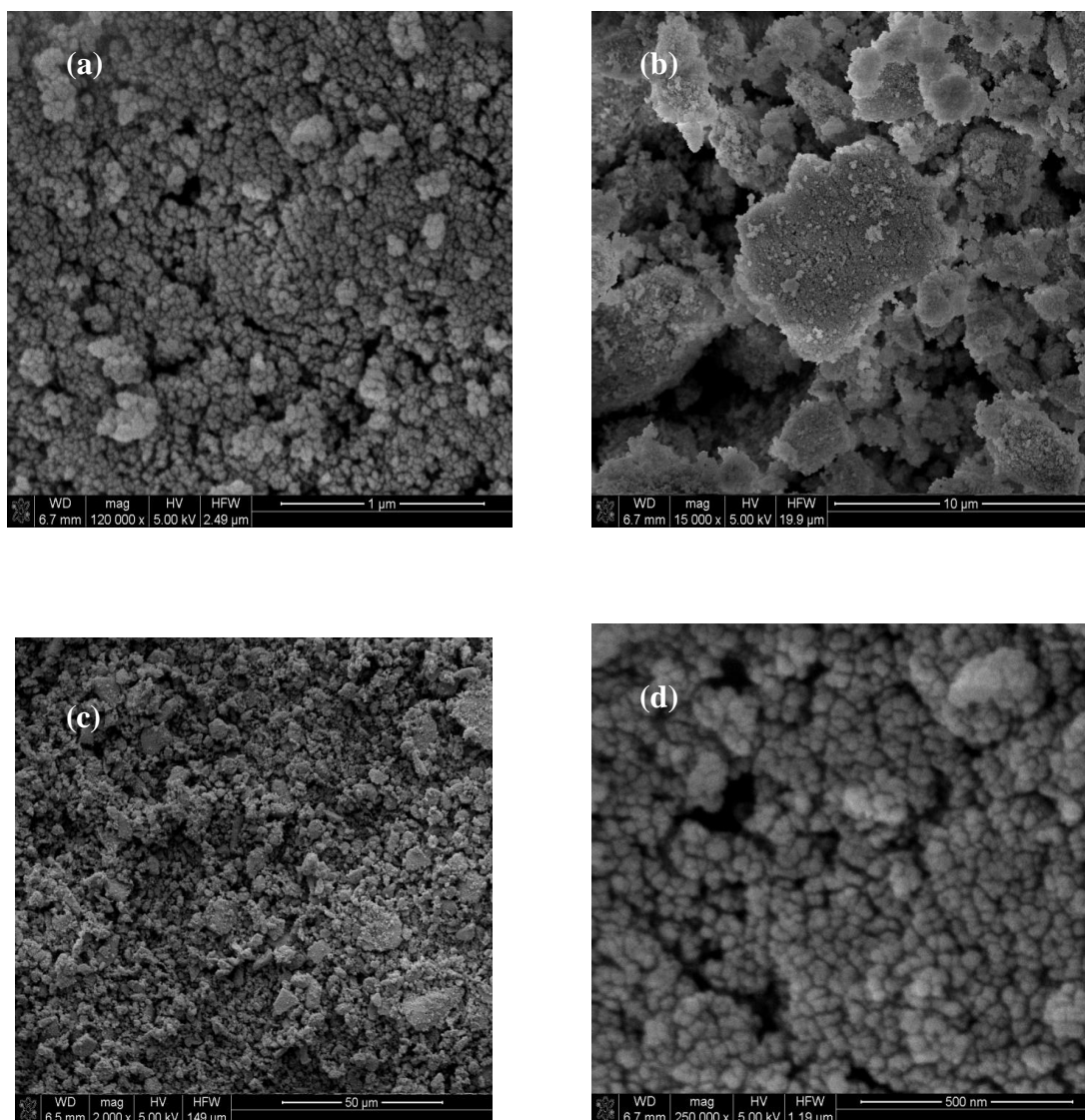


**Figure 46:** SEM images of STA@Mesoporous SAPO-34, (neutral), (a) with 120000 magnification, (b) with 15000 magnification, (c) with 2000 magnification, (d) with 250000 magnification

#### 9.4. DRIFTS ANALYSIS OF SYNTHESIS SAPO-34-LIKE CATALYSTS

Diffuse Reflectance Fourier Transform IR Spectroscopy (DRIFTS) analysis of pyridine adsorbed samples was performed to determine the relative strengths of the Brønsted and Lewis acid sites on the surface of synthesis catalysts in this study (Figure 47). Distinctive bands, which appear at 1540 and 1640  $\text{cm}^{-1}$  correspond to the Brønsted acid sites. However, for the Lewis acid sites, bands are expected at 1450 and 1598  $\text{cm}^{-1}$  [2].

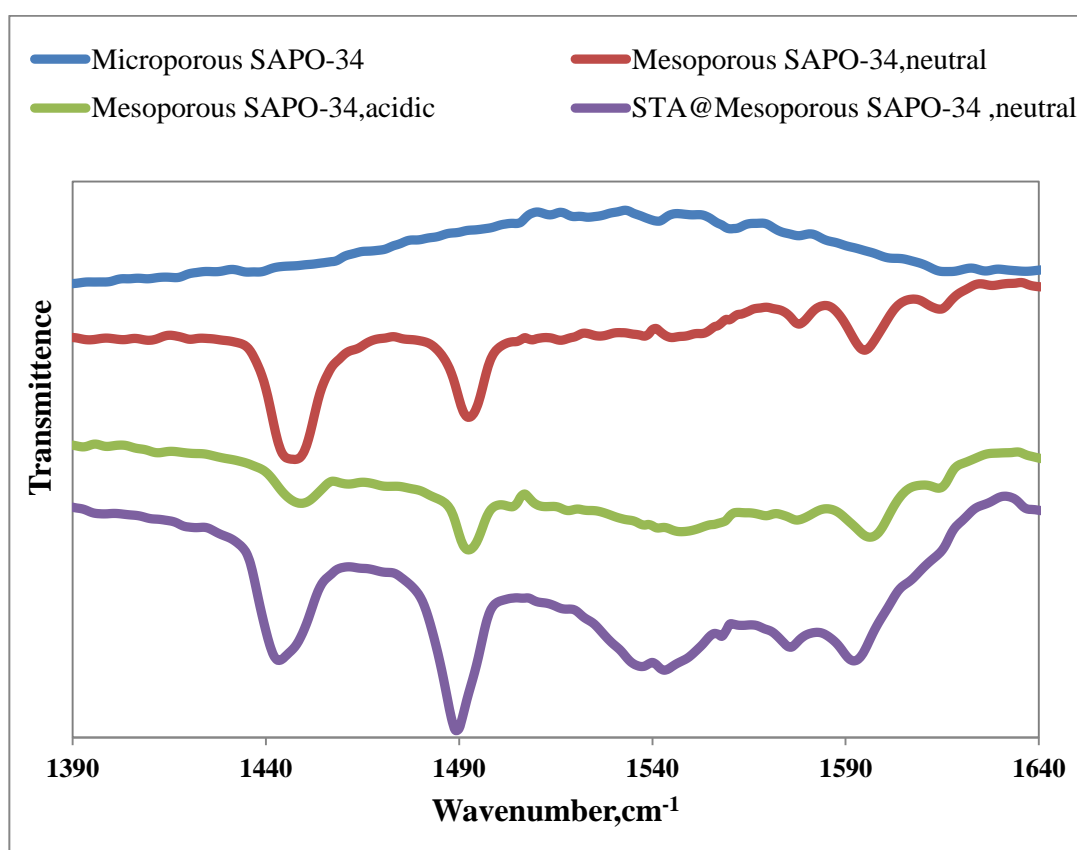


**Figure 47:** Drift spectrums of Microporous SAPO-34, Mesoporous SAPO-34, (neutral), Mesoporous SAPO-34, acidic and STA@Mesoporous SAPO-34, (neutral).

According to DRIFTS given in Figure 47, for Microporous SAPO-34, intensity of the bands corresponding to Lewis and Bronsted acid sites are quite weak. In the case of Mesoporous SAPO-34 (neutral and acidic) mainly Lewis acid sites are seen. Contribution of Brønsted and Lewis acid sites gives a band at  $1490\text{ cm}^{-1}$  which can be visibly seen for Mesoporous SAPO-34 (neutral and acidic). Because of low Bronsted acidity it can be considered that the band at  $1490\text{ cm}^{-1}$  was also mainly due to Lewis acid sites. DRIFTS analysis indicated somewhat higher intensity of Lewis acid sites for Mesoporous SAPO-34 (neutral). In the case of STA@Mesoporous SAPO-34, (neutral), intensities of the bands corresponding to Lewis, Bronsted and contribution of Lewis and Bronsted acid sites increased. Especially Bronsted acid sites are visibly seen. This means that impregnation of Silicotungstic acid increased the acid strength of Mesoporous SAPO-34, (neutral).

## 9.5. ACTIVITY RESULTS OF SYNTHESIS SAPO-34-LIKE CATALYSTS

Microporous SAPO-34, Mesoporous SAPO-34, (neutral) and Mesoporous SAPO-34, (acidic) were synthesized successfully during this study. Mesoporous SAPO-34, (neutral) with  $94.08\text{ m}^2/\text{g}$  surface area,  $0.97\text{ cm}^3/\text{g}$  pore volume and  $31\text{ nm}$  pore diameter was chosen as the best catalyst among others and tested in etherification reactions with *i*-butene. But mesoporous SAPO-34, (neutral) was not active in this reaction. Catalysts with high Brønsted acidity are preferred in etherification reactions due to smooth proton exchange capacity. However the Bronsted acidity of Mesoporous SAPO-34, (neutral) was quite low (Figure 47). In order to enhance the acidity Silicotungstic acid (STA) was impregnated on Mesoporous SAPO-34, (neutral). Hereby, mainly Bronsted acidity of the catalyst was increased (Figure 47). STA@Mesoporous SAPO-34, (neutral) was tested also in etherification of glycerol with *i*-butene. Reactions were performed in a temperature range of  $70\text{--}200^\circ\text{C}$ . Maximum glycerol conversion was recorded as  $1\%$  at  $200^\circ\text{C}$ . This conversion value was very low compared with commercial solid acid catalysts. Maximum operating temperature of the autoclave reactor which was used during all the etherification reactions in this study was  $200^\circ\text{C}$ . Therefore maximum reaction temperature was

chosen as 200°C. It is quite probable that further increase of the temperature might have increased glycerol conversion. The decrease in micropore volume after Silicotungstic acid (STA) impregnation could be explained as; Silicotungstic acid was located in microporous not on the catalyst surface. i-butene has a large structure and could not entire the microporous and therefore the catalyst was not active in this reaction. As a result it was seen that synthesized catalyst during this study could not bring a new dimension to commercial solid acid catalysts for etherification reactions.

## CHAPTER 10

### CONCLUSIONS

In the first part of this study etherification of glycerol with i-butene was studied. Activity of solid acid catalysts used in this study namely; Amberlyst-36, Dowex DR-2030 and Silicotungstic acid were compared in a temperature range of 70-120°C. Results showed that; Silicotungstic acid was the best catalyst at lower reaction temperatures (T=70 and 80°C) while Dowex DR-2030 was better at higher reaction temperatures (T=90 and 120°C) in etherification of glycerol with i-butene.

In the second part of this study etherification of glycerol with 2-Methyl-2-Butene (2M2B) was firstly studied in the literature. In order to determine the influence of catalyst type and catalyst amount on glycerol conversion, etherification of glycerol was studied over Amberlyst-36 and Dowex DR-2030 resins at 120°C. The catalytic activities of Amberlyst-36 and Dowex DR 2030 were quite similar and a significant increase was observed in conversion values, with an increase in catalyst amount. Effects of reaction temperature, reaction time and catalyst amount on glycerol conversion and product distributions were evaluated over Amberlyst-36 resin. Increasing reaction temperature and amount of catalyst loading was increased reaction rate. At 140°C with 1 g of catalyst, the reaction was very fast in the first hour and glycerol conversion value reached to 70%. Mono-, di- and tri-ethers were obtained in the study. Di-ether selectivity values of about 0.7 and tri-ether selectivities approaching to 0.1 obtained with 1.0 g catalyst at reaction times longer than 12 h at 120°C were highly promising.

In the third part of this study microporous, mesoporous and Silicotungstic acid impregnated SAPO-34 catalysts were synthesized successfully in order to bring a new dimension to commercial solid acid catalyst for etherification reactions. Activity of Mesoporous SAPO-34 and STA@Mesoporous SAPO-34 were tested in etherification of glycerol with i-butene. However it was seen that, these catalyst were not active in etherification of glycerol with i-butene.

As a result of this study it was concluded that, fuel oxygenates can be successfully produced through etherification of glycerol with iso-amylene (2M2B), as well as with i-butene. This is the first detailed study in the literature for the etherification of glycerol with 2M2B.

## REFERENCES

- [1] Tokay K. C., Dogu T., Dogu G., Dimethyl ether synthesis over alumina based catalysts, *Chemical Engineering Journal*, 184:278–285, 2012.
- [2] Ozbay N., Oktar N., Dogu G., Dogu T., Activity Comparison of Different Solid Acid Catalysts in Etherification of Glycerol with tert-Butyl Alcohol in Flow and Batch Reactors, *Topics in Catalysis*, 56:1790–1803, 2013.
- [3] Atabani A.E., Silitonga A.S., Badruddin I. A., Mahlia T. M. I., Masjuki H. H., Mekhilef S., A comprehensive review on biodiesel as an alternative energy resource and its characteristics, *Renewable and Sustainable Energy Reviews*, 16:2070–2093, 2012.
- [4] Varisli D., Dogu T., Dogu G., Petrochemicals from ethanol over a W–Si-based nanocomposite bidisperse solid acid catalyst, *Chemical Engineering Science*, 65:153–159, 2010.
- [5] Sensoz S., Demiral I., Gerçel H.F., Olive bagasse (*Olea europea* L.) pyrolysis., *Bioresource Technology*, 97:429–36, 2006.
- [6] Agarwal A. K., Biofuels (alcohols and biodiesel) applications as fuels for internal combustion engines, *Progress in Energy and Combustion Science*, 33:233–271, 2007.
- [7] Ma F., Hanna M. A., Biodiesel production: a review 1, *Bioresource Technology*, 70:1–15, 1999.
- [8] Srivastava A., Prasad R., Triglycerides-based diesel fuels, *Renewable and Sustainable Energy Review*, 4:111–133, 2000.
- [9] Li D., Zhen H., Xingcai L., Wu-gao Z., Jian-guang Y., Physico-chemical properties of ethanol–diesel blend fuel and its effect on performance and emissions of diesel engines, *Renewable Energy*, 30:967–976, 2005.
- [10] Canakci M., Combustion characteristics of a turbocharged DI compression ignition engine fueled with petroleum diesel fuels and biodiesel, *Bioresource Technology*, 98:1167–1175, 2007.

- [11] Subramanian K.A., Singal S.K., Saxena M., Singhal S., Utilization of liquid biofuels in automotive diesel engines: An Indian perspective, *Biomass and Bioenergy*, 29:65–72,2005.
- [12] Xing-cai L., Jian-guang Y., Wu-gao Z., Zhen H., Effect of cetane number improver on heat release rate and emissions of high speed diesel engine fueled with ethanol–diesel blend fuel, *Fuel*, 83:2013–2020,2004.
- [13] Zakaria Z.Y., Amin N. A. S., Linnekoski J., A perspective on catalytic conversion of glycerol to olefins, *Biomass and Bioenergy*, 55:370–385,2013.
- [14] Ozbay N., Oktar N., Dogu G., Dogu T., Conversion of Biodiesel By-Product Glycerol to Fuel Ethers over Different Solid Acid Catalysts ,*International Journal of Chemical Reactor Engineering*,8:A-18, 2010.
- [15] Ozbay N., Oktar N., Dogu G., Dogu T, Effects of Sorption Enhancement and Isobutene Formation on Etherification of Glycerol with tert-Butyl Alcohol in a Flow Reactor, *Industrial & Engineering Chemistry Research*, 51:8788–8795 ,2012.
- [16] Ahmed S., et al.,*Renewables 2012 Global Status Report*, 2012.
- [17] Othmer K., *Encyclopedia of Chemical Technology*, Mc Graw Hill, New York,1978.
- [18] Izquierdo J. F., Montiel M., Palés I., Outón P. R., Galán M., Jutglar L., Villarrubia M., Izquierdo M., Hermo M. P., Ariza X., Fuel additives from glycerol etherification with light olefins: State of the art, *Renewable and Sustainable Energy Reviews*,16:6717–6724,2012.
- [19] Tsukuda E., Sato S., Takahashi R., Sodesawa T., Production of acrolein from glycerol over silica-supported heteropoly acids, *Catalysis Communications*, 8:1349–1353, 2007.
- [20] Chai S.-H., Wang H.-P., Liang Y., Xu B.-Q.,Sustainable production of acrolein: Preparation and characterization of zirconia-supported 12-tungstophosphoric acid catalyst for gas-phase dehydration of glycerol, *Applied Catalysis A:General*, 353:213–222,2009.
- [21] Corma A., Huber G.W., Sauvanaud L., Oconnor P., Biomass to chemicals: Catalytic conversion of glycerol/water mixtures into acrolein, reaction network, *Journal of Catalysis*, 257:163–171, 2008.

- [22] Chai S., Wang H., Liang Y., Xu B., Sustainable production of acrolein: Gas-phase dehydration of glycerol over Nb<sub>2</sub>O<sub>5</sub> catalyst, *Journal of Catalysis*, 250:342–349,2007.
- [23] Pompeo F., Santori G.,Nichio N. N., Hydrogen and/or syngas from steam reforming of glycerol. Study of platinum catalysts, *International Journal of Hydrogen Energy*, 35:8912–8920, 2010.
- [24] Wen G., Xu Y., Ma H., Xu Z.,Tian Z., Production of hydrogen by aqueous-phase reforming of glycerol, *International Journal of Hydrogen Energy*,33:6657–6666, 2008.
- [25] Kunkes E. L., Soares R. R., Simonetti D. A., Dumesic J. A.,An integrated catalytic approach for the production of hydrogen by glycerol reforming coupled with water-gas shift, *Applied Catalysis B: Environmental*, 90:693–698, 2009.
- [26] Dou B., Dupont V., Rickett G., Blakeman N., Williams P. T., Chen H., Ding Y., Ghadiri M.,Hydrogen production by sorption-enhanced steam reforming of glycerol., *Bioresource Technology*,100:3540–3547, 2009.
- [27] Byrd A.J., Pant K., Gupta R., Hydrogen production from glycerol by reforming in supercritical water over Ru/Al<sub>2</sub>O<sub>3</sub> catalyst, *Fuel*, 87:2956–2960, 2008.
- [28] Barbirato F., Himmi E. H., Conte T., Bories A., “1,3-propanediol production by fermentation: An interesting way to valorize glycerin from the ester and ethanol industries, *Industrial Crops and Products* ,7:281–289,1998.
- [29] Zhao Y.-N., Chen G.,Yao S.-J., Microbial production of 1,3-propanediol from glycerol by encapsulated *Klebsiella pneumoniae*, *Biochemical Engineering Journal* ,32:93–99, 2006.
- [30] González M. D., Cesteros Y., Salagre P., Establishing the role of Brønsted acidity and porosity for the catalytic etherification of glycerol with tert-butanol by modifying zeolites, *Applied Catalysis A:General*,450:178–188, 2013.
- [31] Klepáčova K., Mravec D., Hájeková E., Bajus M., Etherification of glycerol, *Petroleum and Coal*, 45:54–57,2003.
- [32] Frusteri F., Arena F., Bonura G., Cannilla C., Spadaro L., Di Blasi O.,Catalytic etherification of glycerol by tert-butyl alcohol to produce oxygenated additives for diesel fuel, *Applied Catalysis A:General*, 367:77–83,2009.

- [33] Frusteri F., Frusteri L., Cannilla C., Bonura G., Catalytic etherification of glycerol to produce biofuels over novel spherical silica supported Hyflon® catalysts, *Bioresource Technology*, 118:350–358, 2012.
- [34] Melero J. A., Vicente G., Morales G., Paniagua M., Moreno J. M., Roldán R., Ezquerro A., Pérez C., Acid-catalyzed etherification of bio-glycerol and i-butene over sulfonic mesostructured silicas, *Applied Catalysis A:General*, 346:44–51, 2008.
- [35] Xiao L., Mao J., Zhou J., Guo X., Zhang S., Enhanced performance of HY zeolites by acid wash for glycerol etherification with isobutene, *Applied Catalysis A:General*, 393:88–95, 2011.
- [36] Karinen R. S., Krause A. O. I., New biocomponents from glycerol, *Applied Catalysis A: General*, 306:128–133, 2006.
- [37] Klepáčová K., Mravec D., Kaszonyi A., Bajus M., Etherification of glycerol and ethylene glycol by i-butene, *Applied Catalysis A:General*, 328:1–13, 2007.
- [38] Lee H. J., Seung D., Jung K. S., Kim H., Filimonov I. N., Etherification of glycerol by i-butene: Tuning the product composition, *Applied Catalysis A:General*, 390:235–244, 2010.
- [39] Oktar N., Murtezaoglu K., Dogu, G., Gonderten I., Dogu, T., Etherification rates of 2-methyl-2-butene and 2-methyl-1-butene with ethanol for environmentally clean gasoline production, *Journal of Chemical Technology and Biotechnology*, 161:155–161, 1999.
- [40] Oye G., Sjoblom J., Stocker M., Synthesis, characterization and potential applications of new materials in the mesoporous range.,” *Advances in Colloid and Interface Science*, 89–90:439–466, 2001.
- [41] Corma A., From Microporous to Mesoporous Molecular Sieve Materials and Their Use in Catalysis, *Chemical Review*, 97:2373–2420, 1997.
- [42] Jhung S. H., Chang J.-S., Hwang J. S., Park S.-E., Selective formation of SAPO-5 and SAPO-34 molecular sieves with microwave irradiation and hydrothermal heating, *Microporous and Mesoporous Materials*, 64:33–39, 2003.
- [43] Lok, B.M., Messina, C.A., Patton, R.L., Gajek, R.T., Cannan, T.R., Flanigen, E.M., Silicoaluminophosphate Molecular Sieves: Another New Class of, Microporous Crystalline Inorganic Solids, *J.Am.Chemical Soc.*, 106:6092-6093, 1984.

- [44] Izadbakhsh A., Farhadi F., Khorasheh F., Sahebdehfar S., Asadi M., Yan Z. F., Key parameters in hydrothermal synthesis and characterization of low silicon content SAPO-34 molecular sieve, *Microporous and Mesoporous Materials*, 126:1–7,2009.
- [45] Liu G., Tian P., Zhang Y., Li J., Xu L., Meng S., Liu Z., Synthesis of SAPO-34 templated by diethylamine: Crystallization process and Si distribution in the crystals, *Microporous and Mesoporous Materials*,114:416–423,2008.
- [46] Wilson S.T., Synthesis of  $\text{AlPO}_4$  – based molecular sieves, *Studies in Surface Science and Catalysis*, 58: 137-151, 1991.
- [47] Demir H., Dimethyl ether (DME) Synthesis Using Mesoporous SAPO-34 like Catalytic Materials, M.Sc.Thesis, Middle East Technical University, 2011.
- [48] Kulprathipanja S., *Zeolites in Industrial Separation and Catalysis*, Wiley, New York, Weinheim, 2010.
- [49] Mccusker L. B., Olson D. H., *Atlas of Zeolite Framework Types*, Elsevier,2007.
- [50] Liu G., Tian P., Li J., Zhang D., Zhou F., Liu Z., Synthesis, characterization and catalytic properties of SAPO-34 synthesized using diethylamine as a template, *Microporous and Mesoporous Materials*, 111:143–149,2008.
- [51] Liu G., Tian P., Liu Z., Synthesis of SAPO-34 Molecular Sieves Templated with Diethylamine and Their Properties Compared with Other Templates, *Chinese Journal of Catalysis*, 33:174–182, 2012.
- [52] Xu L., Du A., Wei Y., Wang Y., Yu Z., He Y., Zhang X.,Liu Z., Synthesis of SAPO-34 with only Si(4Al) species: Effect of Si contents on Si incorporation mechanism and Si coordination environment of SAPO-34, *Microporous and Mesoporous Materials*,115:332–337,2008.
- [53] Dubois D. R., Obrzut D. L., Liu J., Thundimadathil J., Adekkanattu P. M., Guin J. A., Punnoose A., Seehra M. S., Conversion of methanol to olefins over cobalt-, manganese- and nickel-incorporated SAPO-34 molecular sieves, *Fuel Processing Technology*, 83:203–218, 2003.
- [54] Lok, B.M., Messina, C.A., Patton, R.L., Gajek, R.T., Cannan, T.R., Flanigen, E.M.,Crystalline Silicoaluminophosphates, US Patent 4,440,871, 1984
- [55] Yang S.-T., Kim J.-Y., Chae H.-J., Kim M., Jeong S.-Y., Ahn W.-S., Microwave synthesis of mesoporous SAPO-34 with a hierarchical pore structure, *Material Research Bulletin*, 47:3888–3892,2012.

- [56] Liu Y., Wang L., Zhang J., Chen L., Xu H., A layered mesoporous SAPO-34 prepared by using as-synthesized SBA-15 as silica source, *Microporous and Mesoporous Materials*, 145:150–156, 2011.
- [57] Ozbay N., Formulation of New High Quality Fuels By Etherification of Glycerol which is a By-product in Biodiesel Production, M.Sc.Thesis, Gazi University, 2008
- [58] Ozbay N., Synthesis of Glycerol Tertiary Ethers and Investigation of Reaction Kinetics, Ph.D.Thesis, Gazi University, 2013.
- [59] [http://www.chem.ucla.edu/harding/notes/notes\\_14C\\_MS.pdf](http://www.chem.ucla.edu/harding/notes/notes_14C_MS.pdf), (last accessed on, July, 2014)
- [60] <http://www.chem.queensu.ca/Facilities/ms/MSInstrumentdemoCHEM39X.pdf>, (last accessed on, July, 2014)
- [61] Varisli D., Dogu T., Dogu G., Silicotungstic Acid Impregnated MCM-41-like Mesoporous Solid Acid Catalysts for Dehydration of Ethanol, *Industrial & Engineering Chemistry Research*, 47: 4071–4076, 2008.
- [62] Varisli D., Dogu T., Dogu G., Novel Mesoporous Nanocomposite WO<sub>x</sub>-Silicate Acidic Catalysts: Ethylene and Diethylether from Ethanol, *Ind. Eng. Chem. Res.*, 48 : 9394–9401, 2009.
- [63] Jamróz M. E., Jarosz M., Witowska-Jarosz J., Bednarek E., Tecza W., Jamróz M. H., Dobrowolski J. C., Kijeński J., Mono-, di-, and tri-tert-butyl ethers of glycerol. A molecular spectroscopic study., *Spectrochimica Acta Part A*, 67:980–988, 2007.

## APPENDIX A

### XRD DATA AND PATTERNS

#### A1. XRD DATA OF SAPO-34

**Table 15:** Generalized X-ray diffraction data of SAPO-34 [51]

$2\theta$	$d(\text{\AA})$	$100 \times I/I_0$	$2\theta$	$d(\text{\AA})$	$100 \times I/I_0$
9.45-9.65	9.36-9.17	81-100	31.05-31.4	2.880-2.849	15-28
12.8-13.05	6.92-6.78	8-20	32.2-32.4	2.780-2.763	1-5
13.95-14.2	6.35-6.24	8-23	33.4-33.85	2.683-2.648	0-6
16.0-16.2	5.54-5.47	25-54	34.35-34.65	2.611-2.589	4-15
17.85-18.15	4.97-4.89	11-76	36.0-36.5	2.495-2.462	2-11
19.0	4.67	0-2	38.8-38.9	2.321-2.315	0-2
20.55-20.9	4.32-4.25	44-100	39.6-39.7	2.276-2.270	2-4
22.05-22.5	4.03-3.95	0-5	43.1-43.5	2.099-2.080	3-6
23.0-23.15	3.87-3.84	2-10	47.4-47.7	1.918-1.907	2-6
24.95-25.4	3.57-3.51	12-87	48.8-49.2	1.866-1.852	4-7
25.8-26.0	3.45-3.43	14-26	49.9-50.45	1.828-1.809	0-2
27.5-27.7	3.243-3.220	1-4	50.65-51.3	1.802-1.781	1-8
28.05-28.4	3.181-3.143	1-12	53.0-53.25	1.728-1.720	2-7
29.2-29.6	3.058-3.018	3-9	54.25-54.7	1.691-1.678	0-4
30.5-30.7	2.931-2.912	19-75	55.7-55.9	1.650-1.645	2-5

## A2. XRD PATTERN OF SiO<sub>2</sub> and AlPO<sub>4</sub>

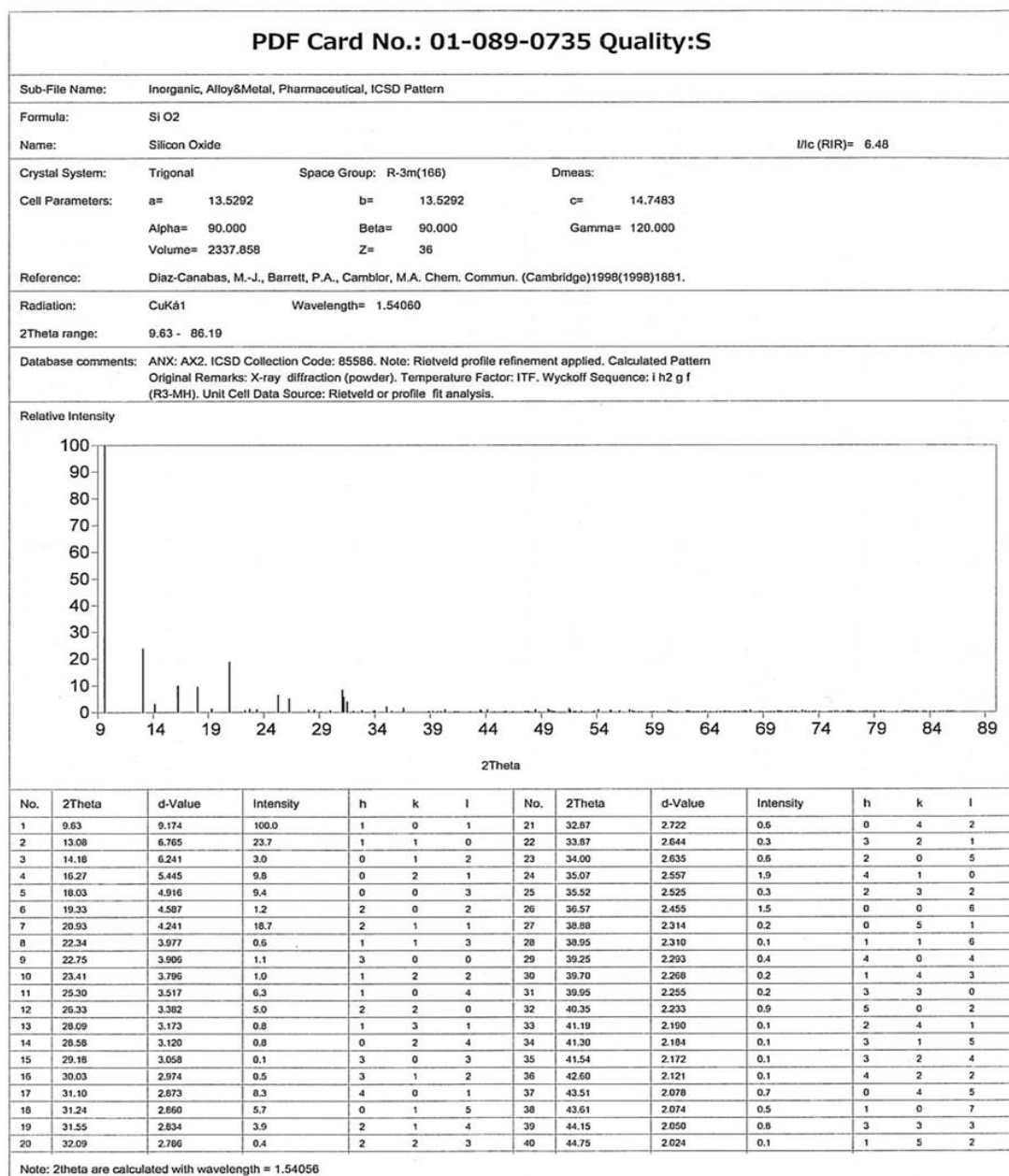


**Figure 48:** XRD pattern of SiO<sub>2</sub>

**PDF Card No.: 01-073-5966 Quality:B**

Sub-File Name:	Inorganic, ICSD Pattern												
Formula:	Al ( P O4 )												
Name:	Aluminum phosphate(V)			I/c (RIR)= 6.32									
Crystal System:	Trigonal	Space Group:	R-3(148)	Dmeas:									
Cell Parameters:	a= 13.8837	b= 13.8837	c= 14.9696										
	Alpha= 90.000	Beta= 90.000	Gamma= 120.000										
	Volume= 2498.914	Z= 18											
Reference:	Poulet, G., Sautet, P., Tuel, A. J. Phys. Chem. B106(2002)8599.												
Radiation:	CuKá1 Wavelength= 1.54060												
2Theta range:	9.43 - 72.05												
Database comments:	ANX: ABX4, ICSD Collection Code: 95431 . Hyperthetical Structure: Structure calculated theoretically. Calculated Pattern Original Remarks: Hexagonal setting: 13.884, 16.969. Test from ICSD: At least one temperature factor missing in the paper. Minor Warning: Minor test comments from ICSD exist. Wyckoff Sequence: f6 (R3-R). Unit Cell Data Source: Powder Diffraction.												
<p>Relative Intensity</p> <p align="center">2Theta</p>													
No.	2Theta	d-Value	Intensity	h	k	l	No.	2Theta	d-Value	Intensity	h	k	l
1	9.43	9.374	100.0	1	0	1	21	32.05	2.789	0.6	0	4	2
2	12.74	6.942	23.7	1	1	0	22	32.99	2.713	0.3	3	2	1
3	13.93	6.354	2.6	0	1	2	23	33.41	2.680	0.6	2	0	5
4	15.87	5.579	9.9	0	2	1	24	34.14	2.624	2.6	4	1	0
5	17.76	4.950	11.0	0	0	3	25	34.63	2.588	0.4	3	2	-2
6	18.92	4.687	1.2	2	0	2	26	35.89	2.500	1.7	2	1	-5
7	20.41	4.349	21.3	1	2	-1	27	36.04	2.450	1.0	3	1	-4
8	21.92	4.052	1.1	1	1	-3	28	37.66	2.374	0.3	0	5	1
9	22.16	4.008	0.9	3	0	0	29	38.38	2.344	0.6	4	0	4
10	22.87	3.885	1.8	2	1	-2	30	38.74	2.322	0.2	4	1	-3
11	24.90	3.573	7.0	1	0	4	31	38.89	2.314	0.2	3	3	0
12	25.64	3.471	5.6	2	2	0	32	39.32	2.289	1.1	5	0	2
13	27.38	3.255	0.9	3	1	-1	33	40.10	2.247	0.1	4	2	-1
14	28.05	3.177	0.9	0	2	4	34	40.46	2.228	0.1	1	3	-5
15	28.54	3.125	0.1	3	0	3	35	40.60	2.220	0.1	2	3	-4
16	29.30	3.046	0.6	1	3	-2	36	41.50	2.174	0.2	2	4	-2
17	30.30	2.947	9.1	4	0	1	37	42.25	2.137	0.1	1	5	-1
18	30.75	2.905	2.6	0	1	5	38	42.58	2.121	0.7	0	3	6
19	30.93	2.889	4.7	1	2	-4	39	42.92	2.105	0.4	1	0	7
20	31.37	2.849	0.7	2	2	-3	40	43.05	2.099	1.2	3	3	-3

Note: 2theta are calculated with wavelength = 1.54056

2013-Apr-01 16:34:47 Page-1/2

**Figure 49:** XRD pattern of AlPO<sub>4</sub>



## APPENDIX B

### CALIBRATION FACTORS OF COMPONENTS IN ETHERIFICATION OF GLYCEROL WITH 2M2B

Before starting etherification reactions of glycerol with 2M2B, the calibration factors of, 2M2B, Ethanol, glycerol, Monoether (ME), Diether (DE), Triether(TE) and dimer were calculated. In the following section calculation of calibration factors is given in detail.

#### B1. CALIBRATION FACTOR OF GLYCEROL FROM GLYCEROL AND ETHANOL MIXTURE (G:ETOH=1/8)

Glycerol and Ethanol mixture was prepared in G:EtOH=1/8 molar ratio and Calibration factor for glycerol is calculated using Equation [A1] ;

$$\frac{x_A}{x_B} = \frac{A_A \beta_A}{A_B \beta_B} \quad [B1]$$

**A=Glycerol, B= Ethanol;**

$A_i$  = Area of component, i

$X_i$  = Molar ratio of component, i

$\beta_i$  = calibration factor of component, i

In order to calculate the calibration factor of glycerol calibration factor of ethanol was taken as unity and the calibration factor of glycerol was determined relative to ethanol. Sample calculation is given below and in Table 16 area obtained from gas chromatography and calculated calibration values are represented.

➤ **Sample Calculation**

$$A_A = 20001.6$$

$$A_B = 262742.3$$

$$\beta_B = 1$$

From [B1],

$$\frac{X_A}{X_B} = \frac{A_A \beta_A}{A_B \beta_B} = \frac{20001,6 * \beta_A}{262742,3 * 1} = \frac{1}{8} = \beta_A = 1.64$$

**Table 16:** Area obtained from gas chromatography and calculated calibration factors of glycerol

<b>A<sub>A</sub> (Gliserol)</b>	<b>A<sub>B</sub> (Etanol)</b>	<b>β<sub>A</sub></b>
20001.6	262742.3	1.64
12415.4	110209.0	1.11
16823.5	139091	1.03
17160.2	235940.1	1.72
14064.0	122882.0	1.09
19243.9	243224.9	1.58
9730.5	88516.7	1.14
18758.2	257967.7	1.72

## **B2. CALIBRATION FACTOR OF GLYCEROL AND 2M2B FROM GLYCEROL, ETHANOL AND 2M2B TERNARY MIXTURE**

Due to insolubility of glycerol in 2M2B ethanol was used as solvent. As a result a ternary mixture of glycerol, ethanol and 2M2B was prepared in two different molar ratios (G:2M2B:EtOH= 1:4:8 and 0.5:2:8) and calibration factors of glycerol and 2M2B were calculated.

### **B2.1. Calibration factor of glycerol and 2M2B from glycerol, ethanol and 2M2B ternary mixture (G:EtOH:2M2B=1:8:4 )**

Glycerol, ethanol and 2M2B mixture was prepared in **G:EtOH:2M2B; 1:8:4** molar ratio and Calibration factor for glycerol and 2M2B was calculated using Equation [B1] and [B2].

$$\frac{x_A}{x_B} = \frac{A_A \beta_A}{A_B \beta_B} \quad [B1]$$

$$\frac{x_C}{x_B} = \frac{A_C \beta_C}{A_B \beta_B} \quad [B2]$$

**A=Glycerol, B=Ethanol, C=2M2B;**

$A_i$  = Area of component, i

$X_i$  = Molar ratio of component, i

$\beta_i$  = calibration factor of component, i

In order to calculate the calibration factor of glycerol and 2M2B calibration factor of ethanol was taken as unity and the calibration factor of glycerol and 2M2B was determined relative to ethanol. Sample calculation is given below and in Table 17, area obtained from gas chromatography and calculated calibration values are represented.

➤ Sample Calculation

$$A_A = 5974.7$$

$$A_B = 62054.8$$

$$A_C = 103859.1$$

$$\beta_B = 1$$

From [B1],

$$\frac{X_A}{X_B} = \frac{A_A \beta_A}{A_B \beta_B} = \frac{5974,7 * \beta_A}{62054,8 * 1} = \frac{1}{8} = \beta_A = 1.31$$

From [B2],

$$\frac{X_C}{X_B} = \frac{A_C \beta_C}{A_B \beta_B} = \frac{103859,1 * \beta_C}{62054,8 * 1} = \frac{4}{8} = \beta_C = 0.3$$

**Table 17:** Area obtained from gas chromatography and calculated calibration factors of glycerol and 2M2B

<b>A<sub>A</sub> (Gliserol)</b>	<b>A<sub>B</sub> (Etanol)</b>	<b>A<sub>C</sub> (2M2B)</b>	<b>β<sub>A</sub></b>	<b>β<sub>C</sub></b>
5974.7	62054.8	103859.1	1.31	0.3
6218.8	68502.4	115581.4	1.38	0.3
6503.8	77808.6	134926.4	1.49	0.29

**B2.2. Calibration factor of glycerol and 2M2B from glycerol, ethanol and 2M2B ternary mixture (G:EtOH:2M2B; 0.5:8:2 )**

Glycerol, ethanol and 2M2B mixture was prepared in **G:EtOH:2M2B; 0.5:8:2** molar ratio and Calibration factor for glycerol and 2M2B was calculated as described above in Section B2.1. In Table 18 area obtained from gas chromatography and calculated calibration values are represented.

**Table 18:** Area obtained from gas chromatography and calculated calibration factors of glycerol and 2M2B

<b>A<sub>A</sub> (Gliserol)</b>	<b>A<sub>B</sub> (Etanol)</b>	<b>A<sub>C</sub> (2M2B)</b>	<b>β<sub>A</sub></b>	<b>β<sub>C</sub></b>
2073.5	44004.5	33768.7	1.3	0.32
3459.1	65468.2	52806.1	1.2	0.31
3143.8	70404.3	56672.9	1.4	0.31
5059.8	139102	117111.8	1.72	0.3

In order to determine the calibration factors of glycerol and 2M2B, average of calculated calibration factors from sections B1, B2, B2.1 and B2.2 were taken. Hereby calibration factor of glycerol and 2M2B were **β<sub>G</sub> = 1.4** and **β<sub>2M2B</sub> = 0.31** respectively.

### B3.CALIBRATION FACTORS OF REACTION PRODUCTS

Because of etherification of glycerol with 2M2B was not studied in the literature, the commercial solutions of products were not found. Therefore the calibration factors from [54] in Table 19 were taken as reference and normalized for etherification of glycerol with 2M2B.

**Table 19:** Calibration factors of components [63].

Component	Calibration Factor,( $\beta$ )
i-butene	1
TTBG	1.05
DTBG	1.29
MTBG	1.54
G	3.2

Calibration factor of Monoether (ME)

$$\beta_{ME} = 1.54 \frac{1.4}{3.2} = 0.67$$

Calibration factor of Diether (DE)

$$\beta_{DE} = 1.29 \frac{1.4}{3.2} = 0.56$$

Calibration factor of Triether (TE)

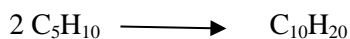
$$\beta_{TE} = 1.05 \frac{1.4}{3.2} = 0.46$$

### B4. CALIBRATION FACTOR OF DIMER

Experiments performed by using only 2M2B as the reactant (without glycerol) had indicated formation of some undesired side reactions, such as its oligomerization

(mainly dimerization). Therefore calibration factor of 2M2B dimer is calculated. Area obtained from gas chromatography for reaction of 2M2B (without glycerol) with A-36 at T=140°C is given in Table 20. Details for calculation are given below.

Dimerization reaction;



Conversion of 2M2B:

$$X_{2M2B} = \frac{A_0 \times \beta_{2M2B} - A_1 \times \beta_{2M2B}}{A_0 \times \beta_{2M2B}} = \frac{A_0 - A_1}{A_0} \quad [\text{B3}]$$

$$N_{0(2M2B)} * X_{2M2B} = 2 * N_{Dimer} \quad [\text{B4}]$$

$$N_{Dimer} = \frac{N_{0(2M2B)} * X_{2M2B}}{2}$$

$$\frac{N_{Dimer}}{N_{0(2M2B)} * (1 - X_{2M2B})} = \frac{A_{Dimer} * \beta_{Dimer}}{A_1 * \beta_{2M2B}} \quad [\text{B5}]$$

$N_{0(2M2B)}$  = Amount of 2M2B reacting, (mol)

$N_{Dimer}$  = Amount of Dimer produced, (mol)

$\beta_{Dimer}$  = Calibration factor of Dimer

$\beta_{2M2B}$  = Calibration factor of 2M2B

$A_0 = A_{avg}$  = Area of pure 2M2B

$A_1 = A_{avg}$  = Area of 2M2B from reaction of 2M2B (without glycerol) with A-36 at T=140°C

$A_{dimer}$  = Area of 2M2B dimers produced from reaction of 2M2B (without glycerol) with A-36 at T=140°C

**Table 20:** Area obtained from gas chromatography for reaction of 2M2B (without glycerol) with A-36 at T=140°C

$A_0$	$A_1$	$A_{Dimer}$
250862.7	109517.8	26158
248665.5	113664.9	27243
280072.9	127498.3	29871
259959.5	125341.6	29852
<b><math>A_0 = A_{avg} = 259889</math></b>	<b><math>A_1 = A_{avg} = 119005</math></b>	<b><math>A_{Dimer} = A_{avg} = 28281</math></b>

From [B3],

$$X_{2M2B} = \frac{259889 - 119005}{259889} = 0.54$$

- 28 ml 2M2B was used in reaction of 2M2B (without glycerol) with A-36 at T=140 °C

$$N_{0(2M2B)} = \frac{\rho_{2M2B} * V_{2M2B}}{M a_{2M2B}} = \frac{0,662 * 28}{70,13} = 0.26$$

From [B4],

$$N_{Dimer} = \frac{0,26 * 0,54}{2} = 0.07$$

From [B5],

$$\frac{0,07}{0,26 * (1 - 0,54)} = \frac{28281 * \beta_{Dimer}}{119005 * 0,31}$$

$$\beta_{Dimer} = 0.76$$

## APPENDIX C

### CONVERSION AND SELECTIVITY CALCULATIONS OF ETHERIFICATION OF GLYCEROL WITH *i*-BUTENE

Sample calculations for conversion and selectivity of etherification of glycerol with *i*-butene are presented in this section.

#### Glycerol Conversion :

$$X_G = \frac{X_{MTBG1} + X_{MTBG2} + X_{DTBG1} + X_{DTBG2} + X_{TTBG}}{X_G + X_{MTBG1} + X_{MTBG2} + X_{DTBG1} + X_{DTBG2} + X_{TTBG}} \quad [7.1.]$$

If Equation 7.1. is written in terms of area and calibration factors;

$$X_G = \frac{A_{MTBG1}\beta_{MTBG} + A_{MTBG2}\beta_{MTBG2} + A_{DTBG1}\beta_{DTBG} + A_{DTBG2}\beta_{DTBG2} + A_{TTBG}\beta_{TTBG}}{A_G\beta_G + A_{MTBG1}\beta_{MTBG} + A_{MTBG2}\beta_{MTBG2} + A_{DTBG1}\beta_{DTBG} + A_{DTBG2}\beta_{DTBG2} + A_{TTBG}\beta_{TTBG}} \quad [C1]$$

#### Monoether Selectivity:

$$S_{MTBG/G} = \frac{X_{MTBG1} + X_{MTBG2}}{X_{MTBG1} + X_{MTBG2} + X_{DTBG1} + X_{DTBG2} + X_{TTBG}} \quad [7.2]$$

If Equation 7.2. is written in terms of area and calibration factors;

$$S_{\text{MTBG/G}} = \frac{A_{\text{MTBG1}}\beta_{\text{MTBG1}} + A_{\text{MTBG2}}\beta_{\text{MTBG2}}}{A_{\text{MTBG1}}\beta_{\text{MTBG1}} + A_{\text{MTBG2}}\beta_{\text{MTBG2}} + A_{\text{DTBG1}}\beta_{\text{DTBG1}} + A_{\text{DTBG2}}\beta_{\text{DTBG2}} + A_{\text{TTBG}}\beta_{\text{TTBG}}} \quad [\text{C2}]$$

**Diether selectivity;**

$$S_{\text{DTBG/G}} = \frac{X_{\text{DTBG1}} + X_{\text{DTBG2}}}{X_{\text{MTBG1}} + X_{\text{MTBG2}} + X_{\text{DTBG1}} + X_{\text{DTBG2}} + X_{\text{TTBG}}} \quad [\text{7.3.}]$$

If Equation 7.3. is written in terms of area and calibration factors;

$$S_{\text{DTBG/G}} = \frac{A_{\text{DTBG1}}\beta_{\text{DTBG1}} + A_{\text{DTBG2}}\beta_{\text{DTBG2}}}{A_{\text{MTBG1}}\beta_{\text{MTBG1}} + A_{\text{MTBG2}}\beta_{\text{MTBG2}} + A_{\text{DTBG1}}\beta_{\text{DTBG1}} + A_{\text{DTBG2}}\beta_{\text{DTBG2}} + A_{\text{TTBG}}\beta_{\text{TTBG}}} \quad [\text{C3}]$$

**Triether Selectivity;**

$$S_{\text{TTBG/G}} = \frac{X_{\text{TTBG}}}{X_{\text{MTBG1}} + X_{\text{MTBG2}} + X_{\text{DTBG1}} + X_{\text{DTBG2}} + X_{\text{TTBG}}} \quad [\text{7.4}]$$

If Equation 7.4. is written in terms of area and calibration factors;

$$S_{\text{TTBG/G}} = \frac{A_{\text{TTBG}}\beta_{\text{TTBG}}}{A_{\text{MTBG1}}\beta_{\text{MTBG1}} + A_{\text{MTBG2}}\beta_{\text{MTBG2}} + A_{\text{DTBG1}}\beta_{\text{DTBG1}} + A_{\text{DTBG2}}\beta_{\text{DTBG2}} + A_{\text{TTBG}}\beta_{\text{TTBG}}} \quad [\text{C4}]$$

**Di-i-butene Selectivity;**

$$S_{\text{DIB/IB}} = \frac{2 * X_{\text{DIB}}}{X_{\text{MTBG1}} + X_{\text{MTBG2}} + 2 * X_{\text{DTBG1}} + 2 * X_{\text{DTBG2}} + 3 * X_{\text{TTBG}} + X_{\text{TBA}} + 2 * X_{\text{DIB}}} \quad [\text{7.5}]$$

If Equation 7.5. is written in terms of area and calibration factors;

$$S_{DIB/IB} = \frac{2 * A_{DIB} \beta_{DIB}}{A_{MTBG} \beta_{MTBG} + A_{MTBG} \beta_{MTBG} + 2 * A_{DTBG} \beta_{DTBG} + 2 * A_{DTBG} \beta_{DTBG} + 3 * A_{TTBG} \beta_{TTBG} + A_{TBA} \beta_{TBA} + 2 * A_{DIB} \beta_{DIB}} \quad [C5]$$

Where;

$A_i$  = Area of component, i

$X_i$  = Molar ratio of component, i

$\beta_i$  = calibration factor of component, i

### **Sample Calculation;**

#### **Conversion of glycerol at 70 °C over Amberlyst-36**

$$X_G = \frac{0.434 * 7677 + 0.364 * 95.4 + 0.296 * 0}{1 * 4648 + 0.434 * 7677 + 0.364 * 95.4 + 0.296 * 0} = 0.42$$

#### **Monoether Selectivity at 70 °C over Amberlyst-36**

$$S_{MTBG/G} = \frac{7677 * 0.434}{7677 * 0.434 + 95.40 * 0.364 + 0 * 0.296} = 0.99$$

#### **Diether Selectivity at 70 °C over Amberlyst-36**

$$S_{DTBG/G} = \frac{95.40 * 0.364}{7677 * 0.434 + 95.40 * 0.364 + 0 * 0.296} = 0.01$$

#### **Triether Selectivity at 70 °C over Amberlyst-36**

$$S_{TTBG/G} = \frac{0 * 0.296}{7677 * 0.434 + 95.40 * 0.364 + 0 * 0.296} = 0.00$$

In Table 21, 22, and 23 average peak areas of each component in etherification of glycerol with i-butene over Amberlyst-36, Dowex DR-2030 and STA catalysts are given (obtained from GC analysis) respectively. Besides calculated glycerol conversion and product selectivity values are represented.

**Table 21:** Calculated glycerol conversion and product selectivity values at different reaction temperatures over A-36.

<b>A-36, <math>m_{\text{cat}}=0.3</math> g, Reaction time 6 h</b>											
T (°C)	A <sub>IB</sub>	A <sub>DIB</sub>	A <sub>TTBG</sub>	A <sub>DTBG</sub>	A <sub>MTBG</sub>	A <sub>G</sub>	X <sub>G</sub>	S <sub>MTBG/G</sub>	S <sub>DTBG/G</sub>	S <sub>TTBG/G</sub>	S <sub>DIB/IB</sub>
70	15973.12	44.00	0.00	95.40	7677.00	4648.00	0.42	0.99	0.01	0.00	0.00
80	18616.53	32.00	16.67	1796.00	18370.33	3423.00	0.72	0.92	0.08	0.00	0.00
90	8880.83	88.00	77.00	2584.33	6250.33	0.00	1.00	0.74	0.26	0.01	0.00
120	27180.80	13813.67	312.67	8281.33	19611.33	4372.00	0.73	0.73	0.26	0.01	0.15

**Table 22:** Calculated glycerol conversion and product selectivity values at different reaction temperatures over Dowex DR-2030.

<b>Dowex DR-2030, <math>m_{\text{cat}}=0.3</math> g, Reaction time 6 h</b>											
T (°C)	A <sub>IB</sub>	A <sub>DIB</sub>	A <sub>TTBG</sub>	A <sub>DTBG</sub>	A <sub>MTBG</sub>	A <sub>G</sub>	X <sub>G</sub>	S <sub>MTBG/G</sub>	S <sub>DTBG/G</sub>	S <sub>TTBG/G</sub>	S <sub>DIB/IB</sub>
70	5697	113.5	14	327.5	12933.5	3715	0.61	0.98	0.02	0.00	0.00
80	9665.5	771.5	1175.5	18401.5	15710	319	0.98	0.49	0.48	0.03	0.00
90	8601.5	20229.5	4149	21272	8611	0	1	0.29	0.61	0.10	0.16
120	16955.1	15261.5	313.5	5844	10123	535	0.93	0.66	0.32	0.01	0.24

**Table 23:** Calculated glycerol conversion and product selectivity values at different reaction temperatures over STA

<b>STA, m<sub>cat</sub>=0.3 g, Reaction time 6 h</b>											
<b>T (°C)</b>	<b>A<sub>IB</sub></b>	<b>A<sub>DIB</sub></b>	<b>A<sub>TTBG</sub></b>	<b>A<sub>DTBG</sub></b>	<b>A<sub>MTBG</sub></b>	<b>A<sub>G</sub></b>	<b>X<sub>G</sub></b>	<b>S<sub>MTBG/G</sub></b>	<b>S<sub>DTBG/G</sub></b>	<b>S<sub>TTBG/G</sub></b>	<b>S<sub>DIB/IB</sub></b>
70	42007.7	9	0	1182	26452	3152	0.79	0.96	0.036	0	0
80	40107.4	39092	7738.5	30512	8762.5	396	0.98	0.22	0.65	0.13	0.21
90	46722.3	51932	5344.5	30153	13319	359	0.98	0.32	0.60	0.09	0.26
120	55931.5	30223.5	421.5	5017	4413	3802.5	0.50	0.50	0.47	0.03	0.49



## APPENDIX D

### GC/MS ANALYSIS RESULTS

#### D1. MASS SPECTRUM OF GLYCEROL, 2M2B AND ETHANOL

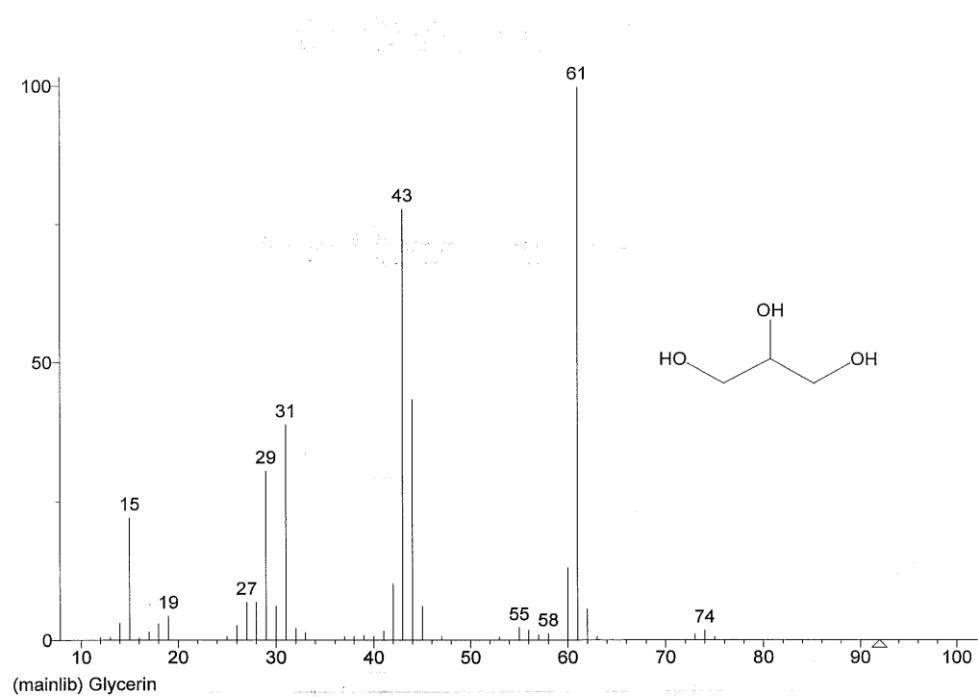


**Figure 50:** Mass Spectrum of Glycerol

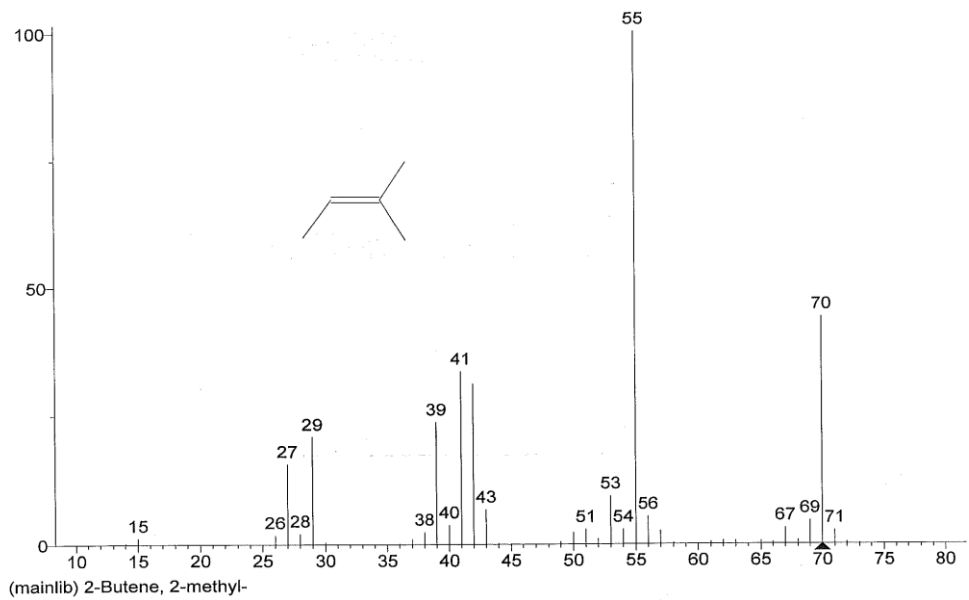


**Figure 51:** Mass spectrum of 2M2B

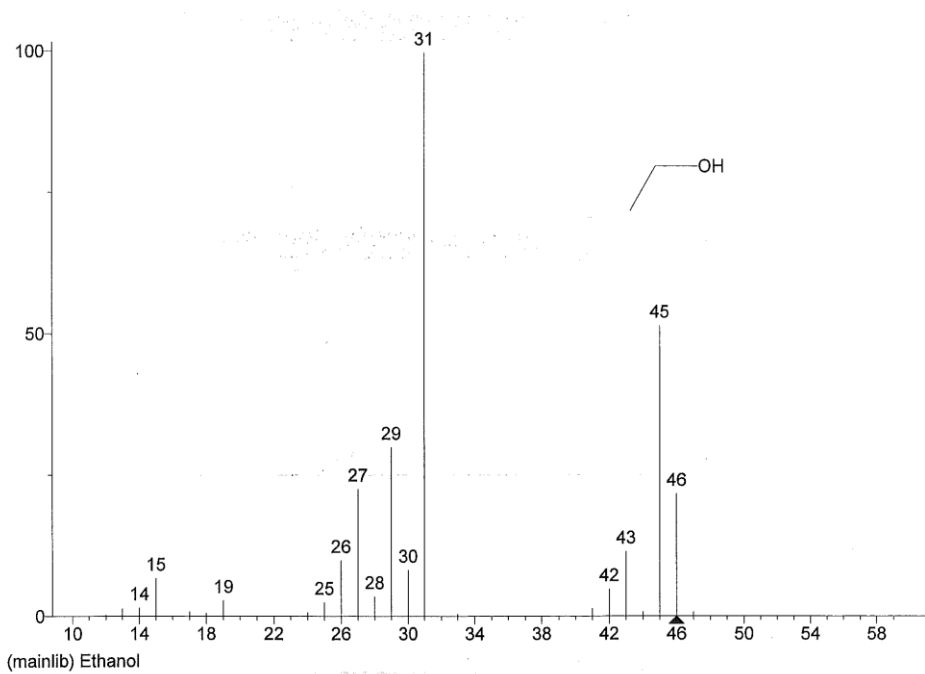


**Figure 52:** Mass spectrum of Ethanol

## D2. GC/MS ANALYSIS RESULTS AND RETENTION TIMES

➤ Pure 2M2B

Abundance

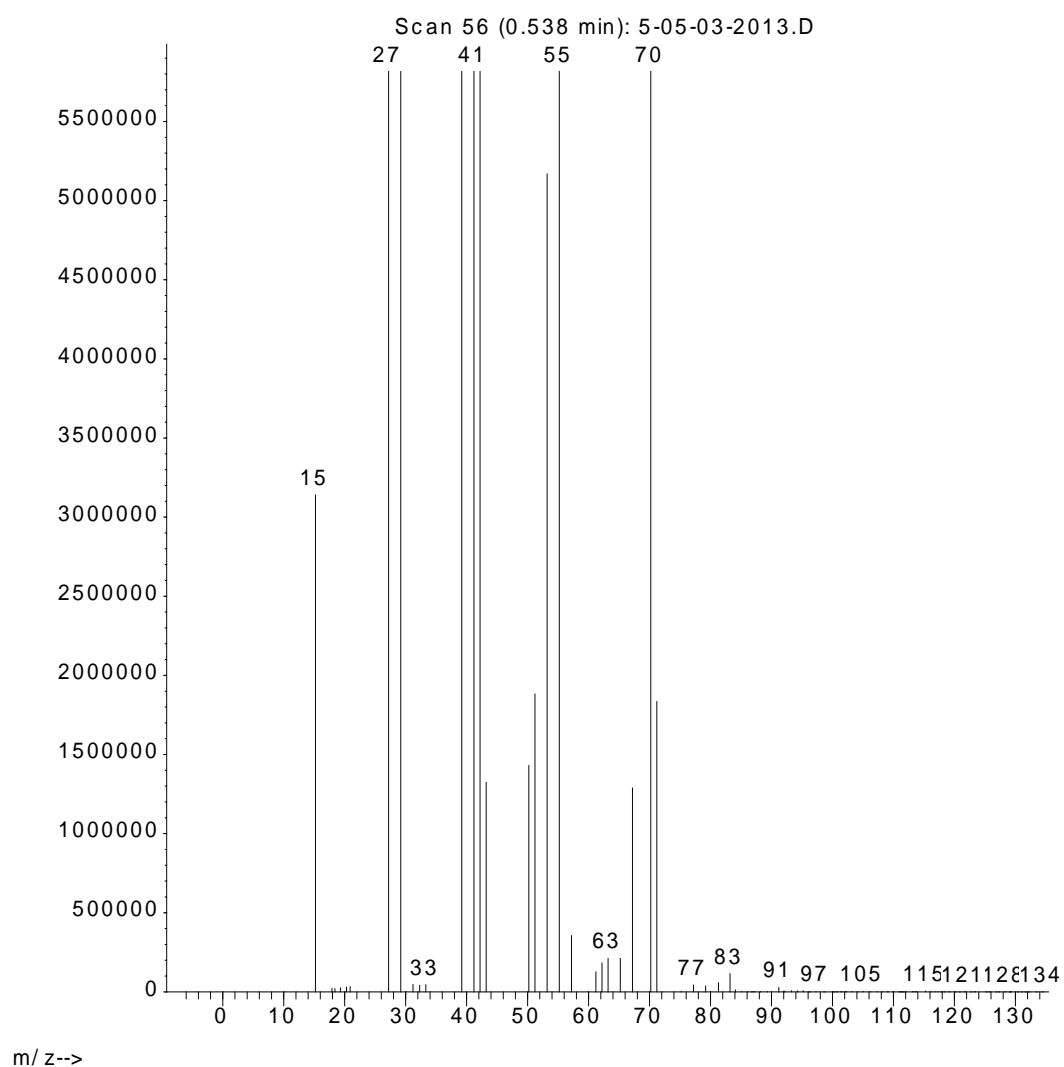


**Figure 53:** GC/MS analysis result of 2M2B to obtain retention time

➤ *Glycerol and Ethanol binary mixture with a molar ratio of (G/EtOH=1/8)*

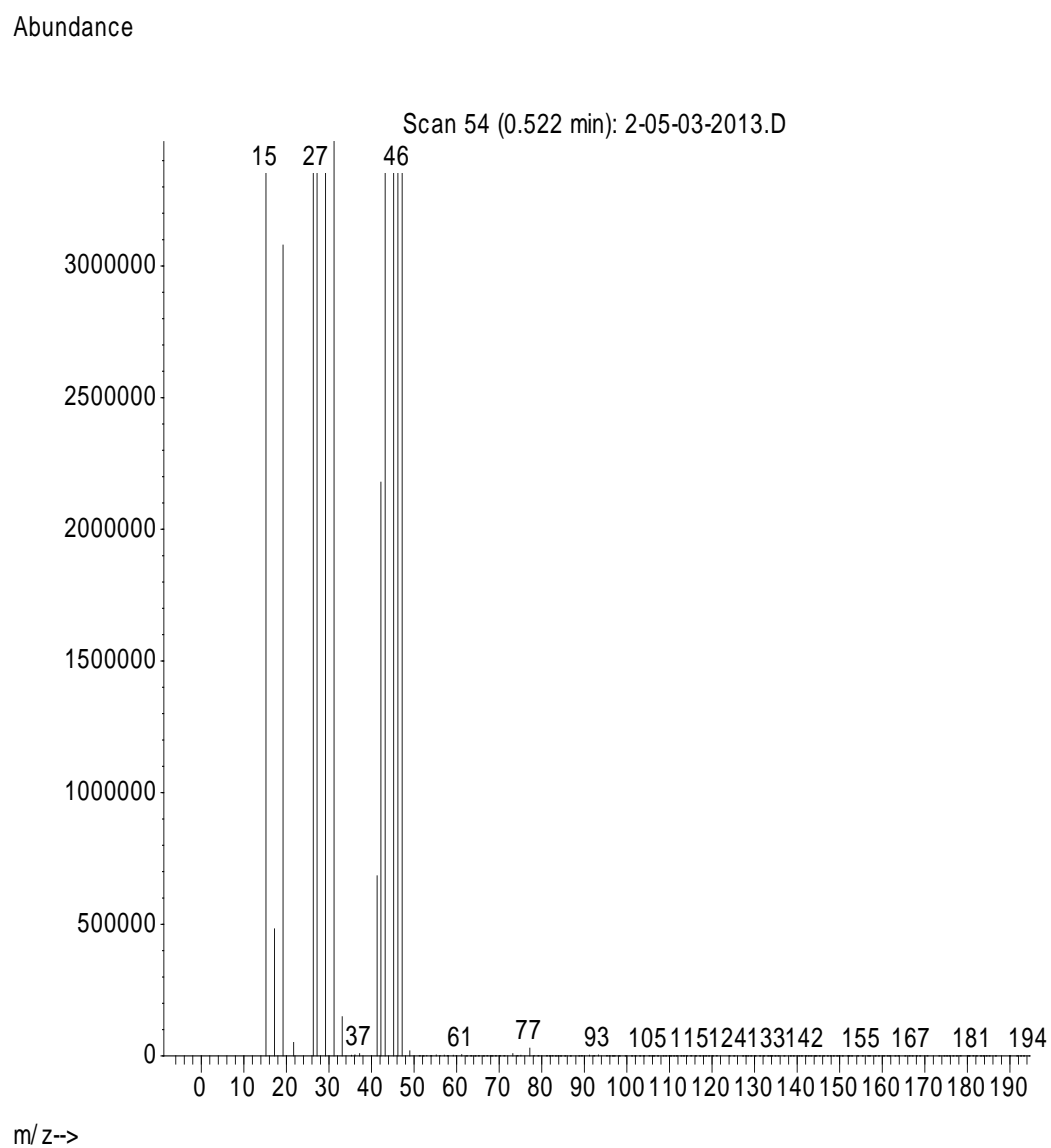


**Figure 54:** GC/MS analysis result of ethanol to obtain retention time

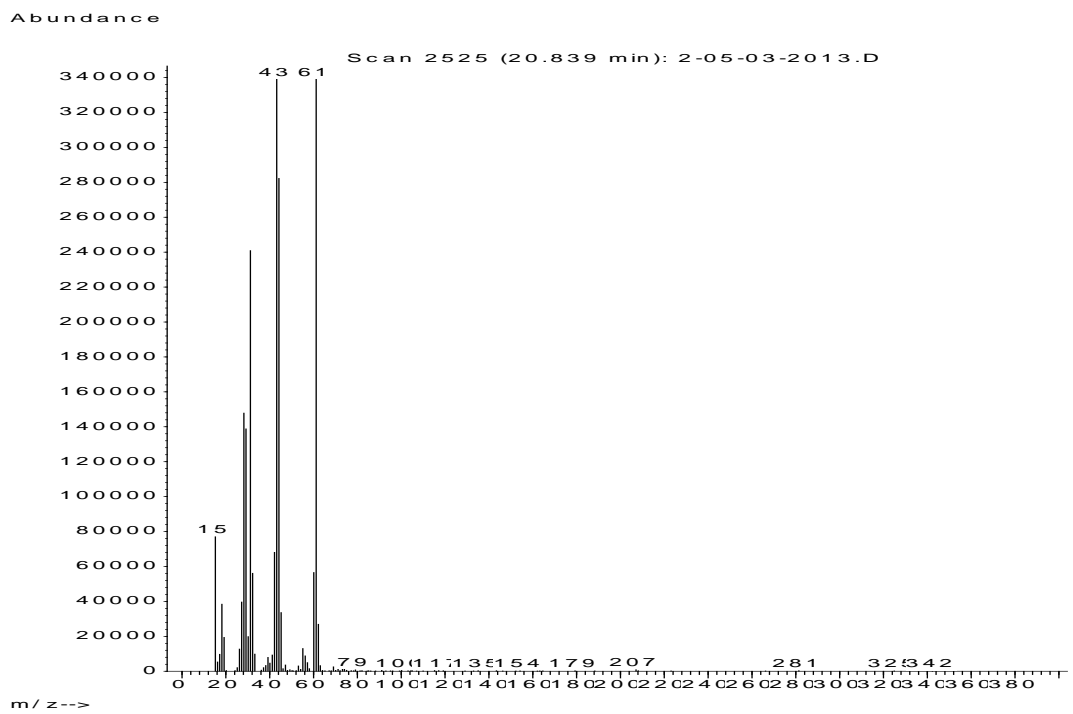
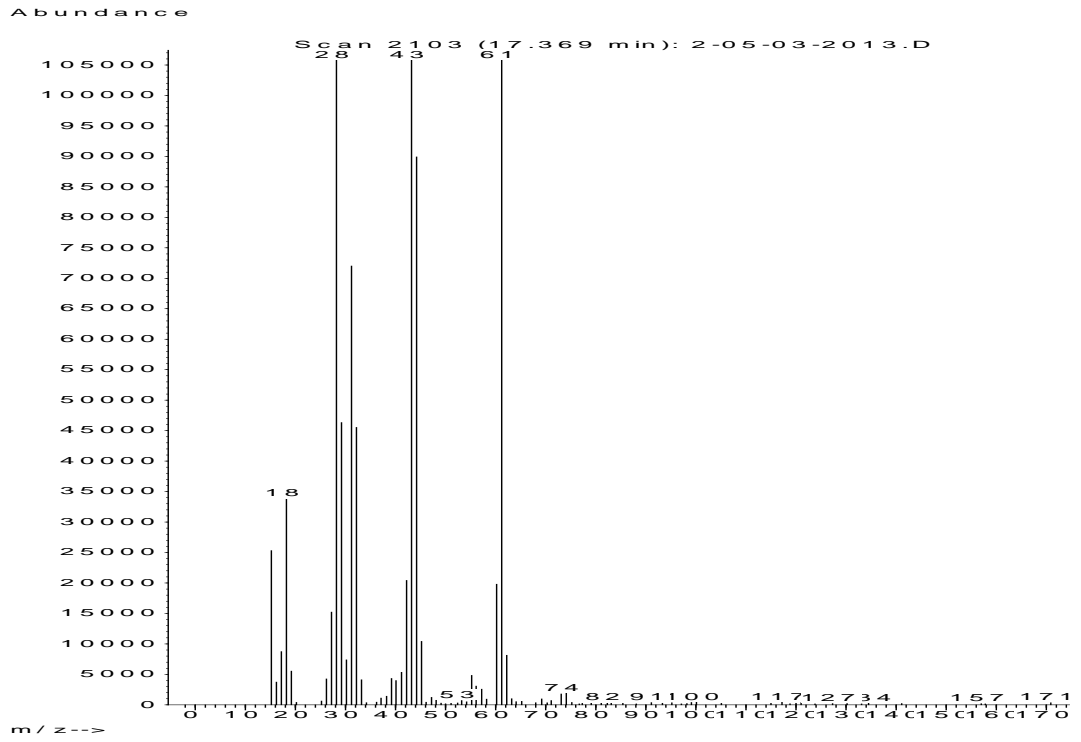


**Figure 55:** GC/MS analysis of Glycerol to obtain retention times

### D3. GC/MS ANALYSIS RESULTS FOR ETHERIFICATION OF 2M2B (WITHOUT GLYCEROL) OVER A-36

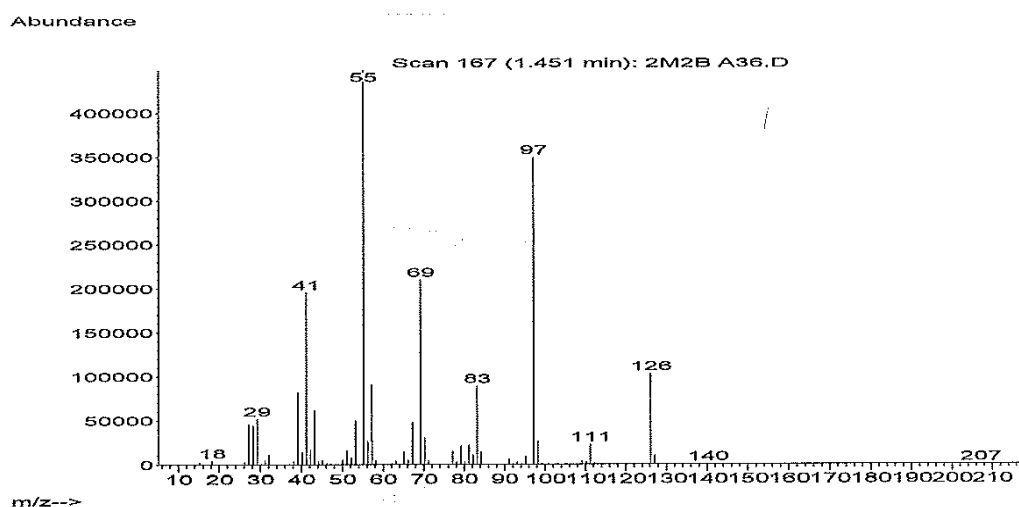
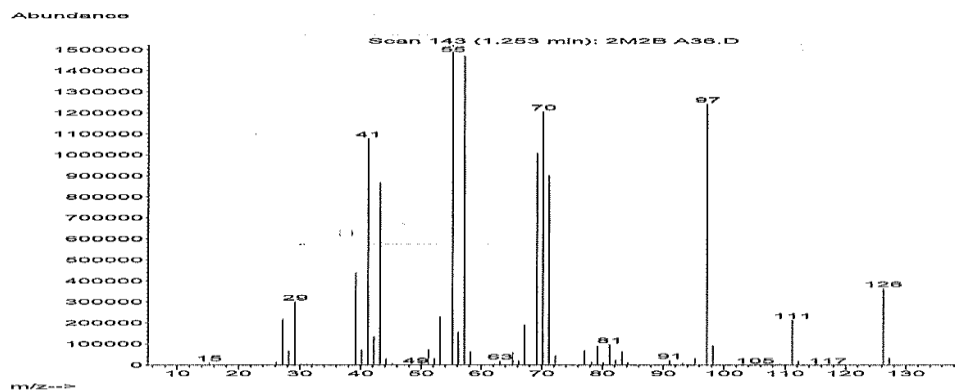
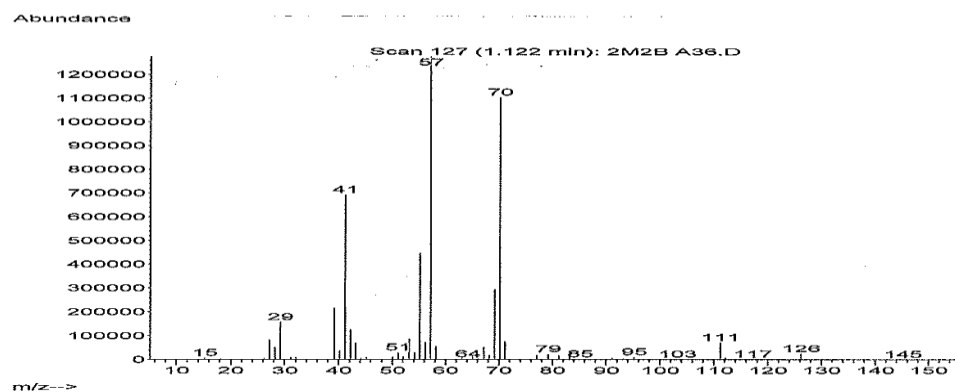


Figure 56: GC/MS analysis results for etherification of 2M2B (without glycerol) over A-36

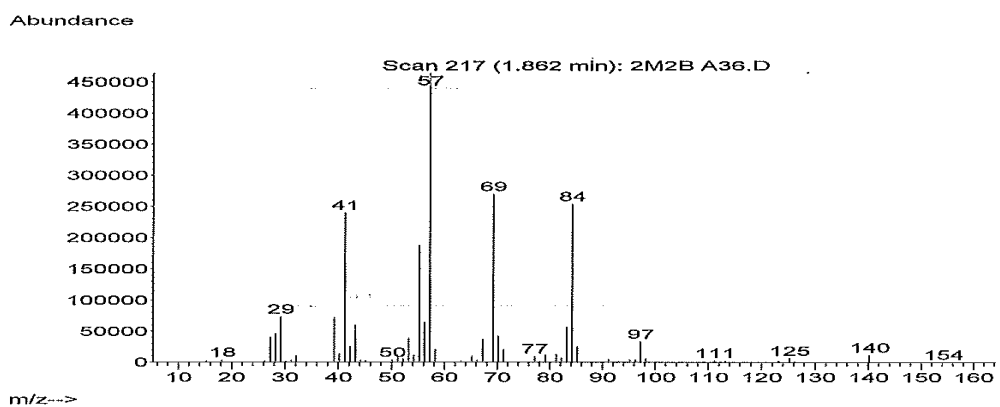
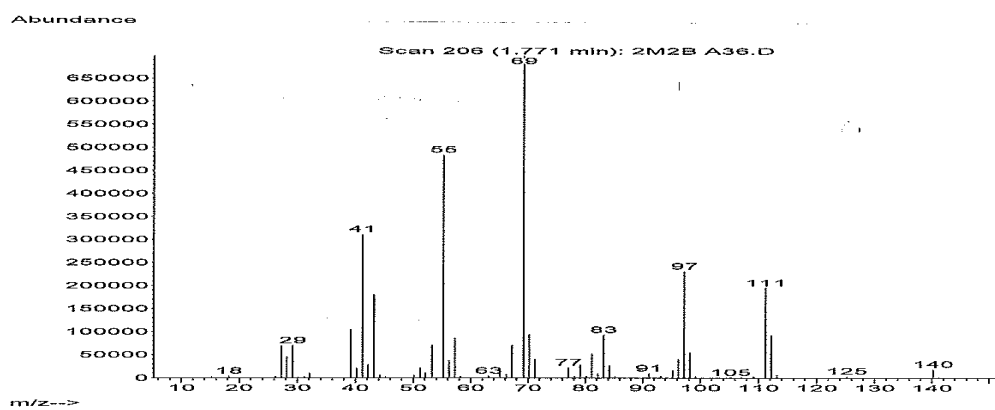
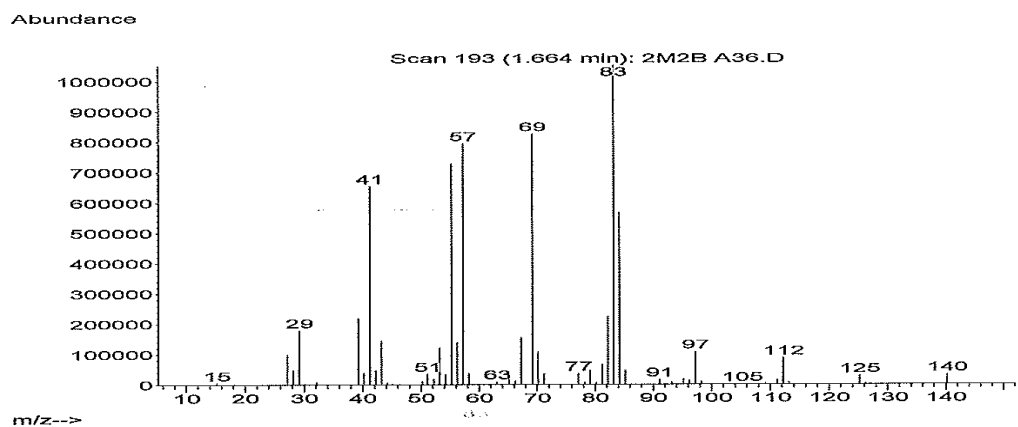


Figure 56: (continued)

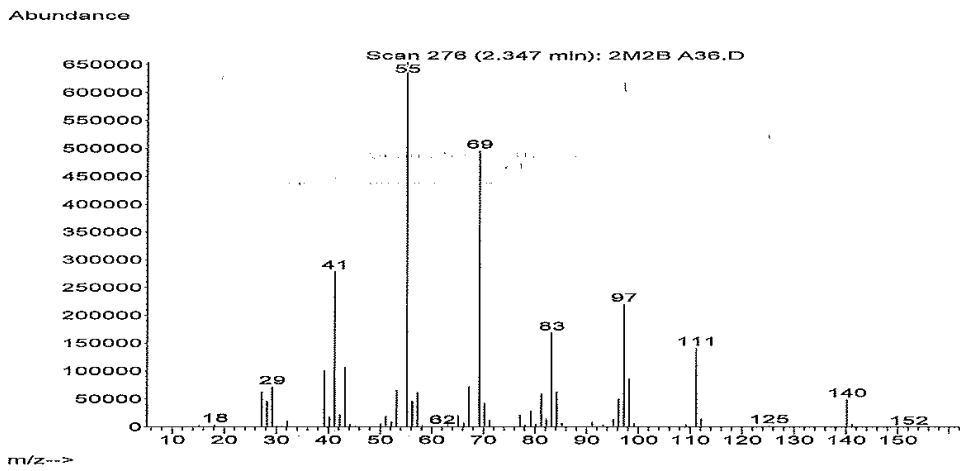
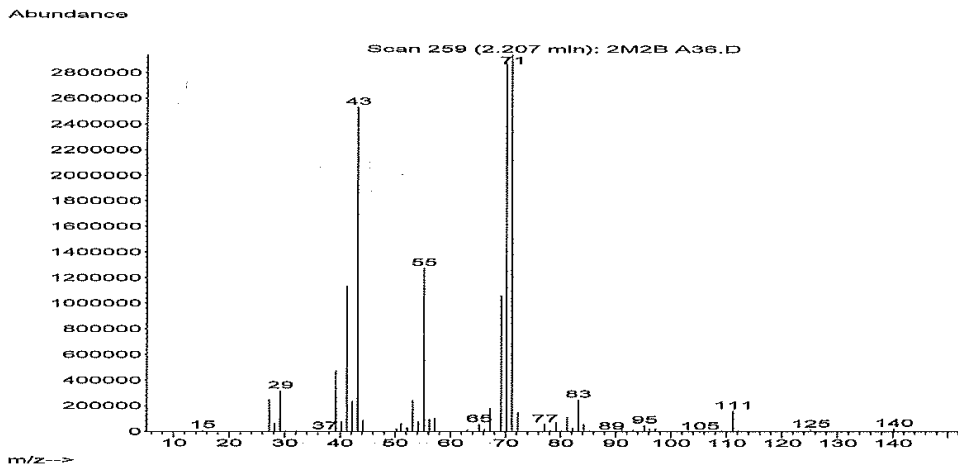
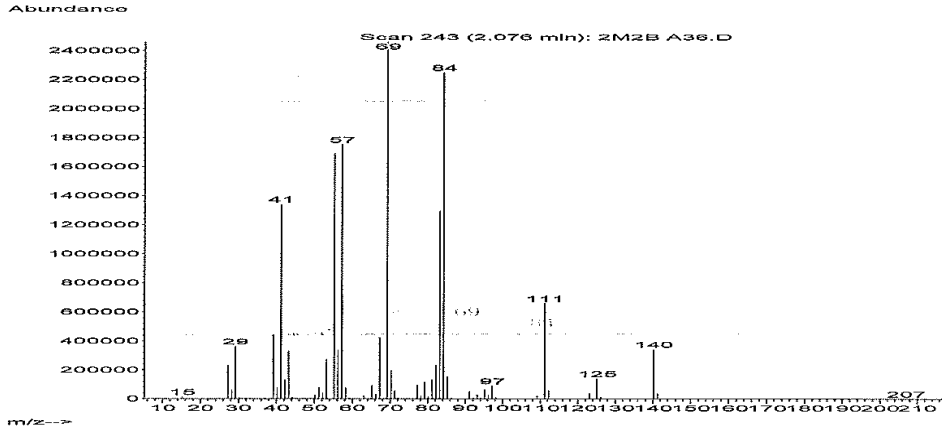


Figure 56: (continued)

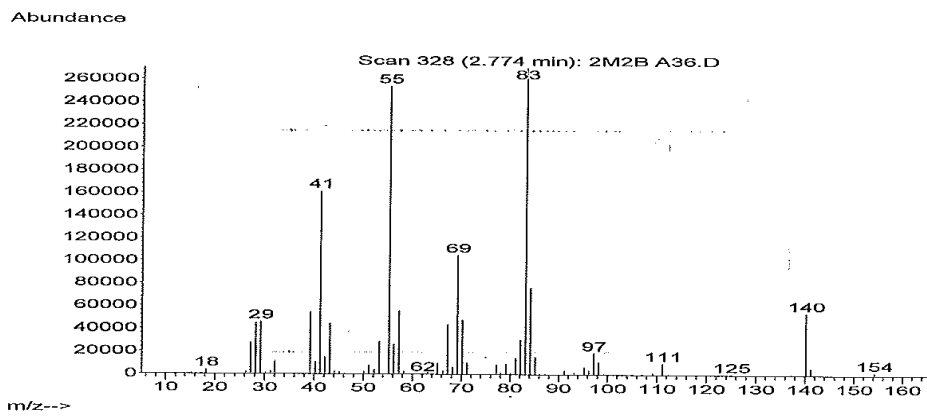
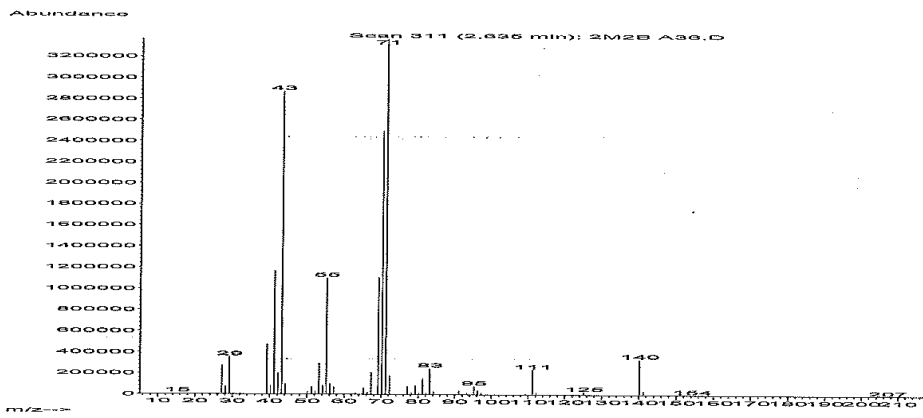
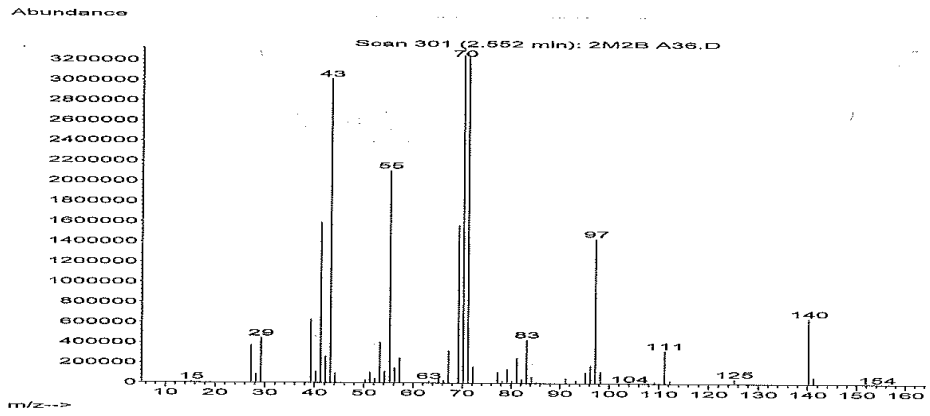


Figure 56: (continued)

### D3.1. Matched molecules from the library of GC/MS (Wiley and Nist) for etherification of 2M2B (without glycerol) over A-36

Library Search Report

Data Path : D:\BURAK TAVSANLI\BURCIN METHOD\  
 Data File : 2M2B A36.D  
 Acq On : 16 Apr 2013, 13:42  
 Operator : BURAK  
 Sample : 2M2B A36  
 Misc :  
 ALS Vial : 1 Sample Multiplier: 1

Search Libraries: C:\Database\NIST02.L Minimum Quality: 0  
 C:\Database\wiley7n.l Minimum Quality: 0  
 C:\Database\Wiley7Nist05.L

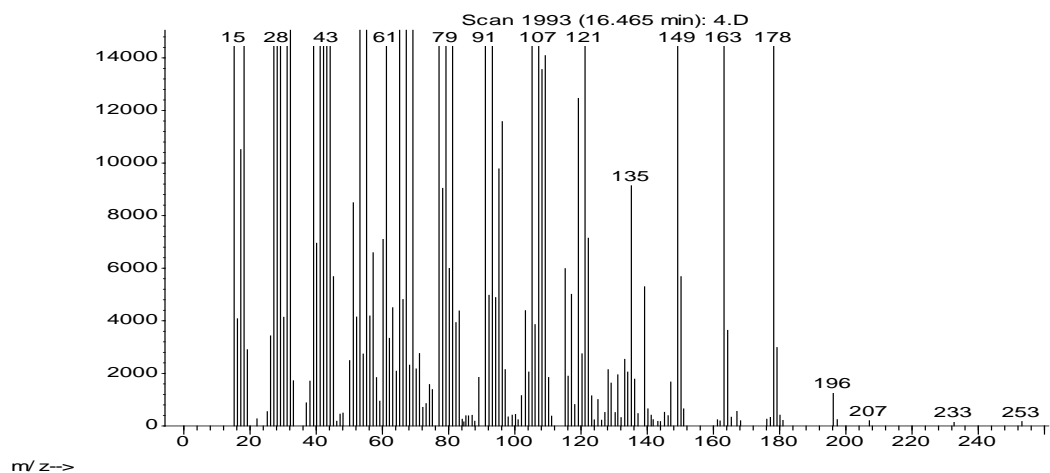
Unknown Spectrum: Apex  
 Integration Events: Chemstation Integrator - autoint1.e

Pk#	RT	Area%	Library/ID	Ref#	CAS#	Qual
1	0.53	8.10	C:\Database\NIST02.L			
6	1.12	1.96	C:\Database\NIST02.L			
			2-Hexene, 3,5,5-trimethyl-	11204	026456-76-8	53
			6,6-Dimethyl-cyclohex-2-en-1-ol	11082	038313-10-9	50
			Azetidene, 1,1'-methylenebis-	10874	038455-24-2	42
7	1.25	5.88	C:\Database\NIST02.L			
			3,5-Dimethyl-3-heptene	11182	059643-68-4	50
			3,5-Dimethyl-3-heptene	11184	059643-68-4	50
			Cyclohexane, 1-ethyl-4-methyl-, tr	11262	006236-88-0	45
			ans-			
8	1.45	1.45	C:\Database\NIST02.L			
			3,5-Dimethyl-3-heptene	11184	059643-68-4	93
			3,5-Dimethyl-3-heptene	11182	059643-68-4	81
			Cyclohexane, 1-ethyl-4-methyl-, ci	11258	004926-78-7	74
			S-			
9	1.66	2.48	C:\Database\NIST02.L			
			2,4,6-Trimethyl-3-heptene	17339	1000113-56-9	58
			1-Pentene, 2,3,3-trimethyl-	6579	000560-23-6	43
			3-Hexene, 3,4-dimethyl-	6534	030951-95-2	38
10	1.77	1.21	C:\Database\NIST02.L			
			Cyclohexane, 1-ethyl-1,4-dimethyl-	17407	062238-32-8	59
			, trans-			
			3-Methyl-3-hexene	3253	003404-65-7	52
			2,5-Dimethyl-3-hexene	6516	1000118-16-2	52
11	1.86	1.42	C:\Database\NIST02.L			
			3-Ethyl-2-methyl-1-heptene	17343	019780-60-0	64
			2-Pentene, 3-methyl-	1450	000922-61-2	53
			Cyclopentanone, 2-(1-methylpropyl)	18067	006376-92-7	53

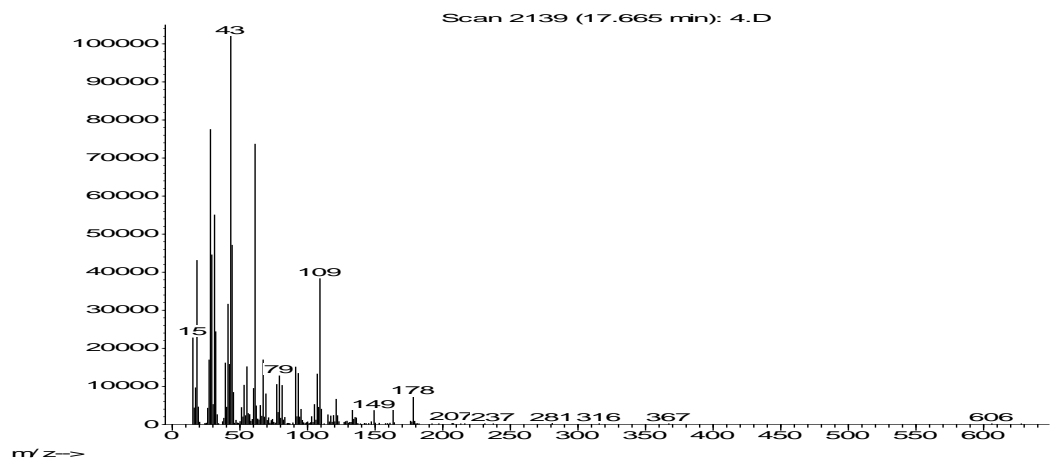
12	2.08	11.76	C:\Database\NIST02.L		
			Pentane, 3-methylene-	1469	000760-21-4 50
			1-Butene, 2,3-dimethyl-	1473	000563-78-0 50
			Cyclopropane, 1,1,2-trimethyl-	1497	004127-45-1 50
13	2.21	12.38	C:\Database\NIST02.L		
			Decane, 3,3,4-trimethyl-	45618	049622-18-6 72
			1-Butanol, 3-methyl-, carbonate (2:1)	57145	002050-95-5 64
			Butanoic acid, 3-methylbutyl ester	28824	000106-27-4 64
14	2.35	1.68	C:\Database\NIST02.L		
			2-Methyl-3-ethyl-2-heptene	17341	019780-61-1 80
			Cyclohexane, 1,2,3-trimethyl-	11217	001678-97-3 78
			3,4-Diethyl-2-hexene	17307	1000113-54-8 55
15	2.55	24.61	C:\Database\NIST02.L		
			Butane, 1,1'-oxybis[3-methyl-	28270	000544-01-4 50
			3,4-Diethyl hexane	18437	019398-77-7 47
			Pentane, 3-ethyl-	3895	000617-78-7 47
16	2.63	8.65	C:\Database\NIST02.L		
			Pentane, 2,3,4-trimethyl-	7463	000565-75-3 72
			Decane, 3,3,4-trimethyl-	45618	049622-18-6 72
			Pentane, 2,3,4-trimethyl-	7464	000565-75-3 72
17	2.77	0.84	C:\Database\NIST02.L		
			2,3-Dimethyl-2-octene	17311	019781-18-1 87
			2-Hydroxy-2-methyl-but-3-enyl 2-methyl-2(Z)-butenoate	45105	080758-67-4 59
			Cyclopropane, 1,1,2-trimethyl-3-(2-methylpropyl)-	17415	041977-43-9 59

#### D4. GC/MS analysis results for etherification of glycerol with 2M2B over A-36

Abundance



Abundance



Abundance

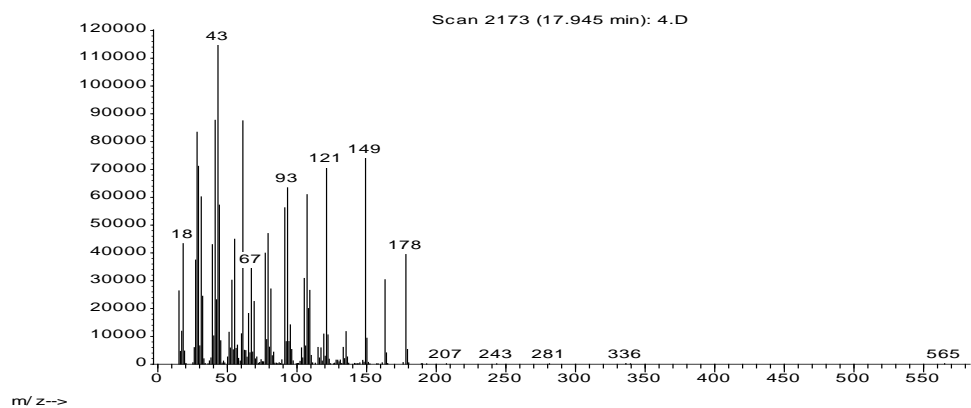


Figure 57: GC/MS analysis results for etherification of glycerol with 2M2B over A-

36

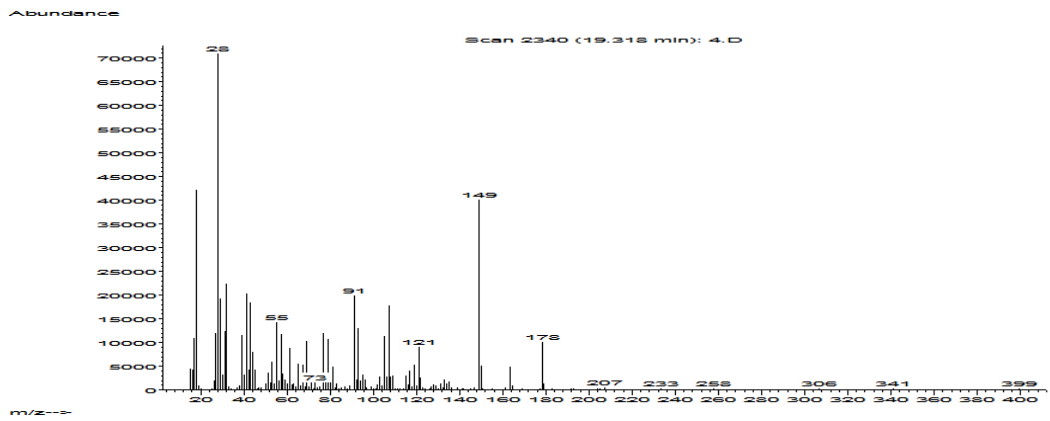
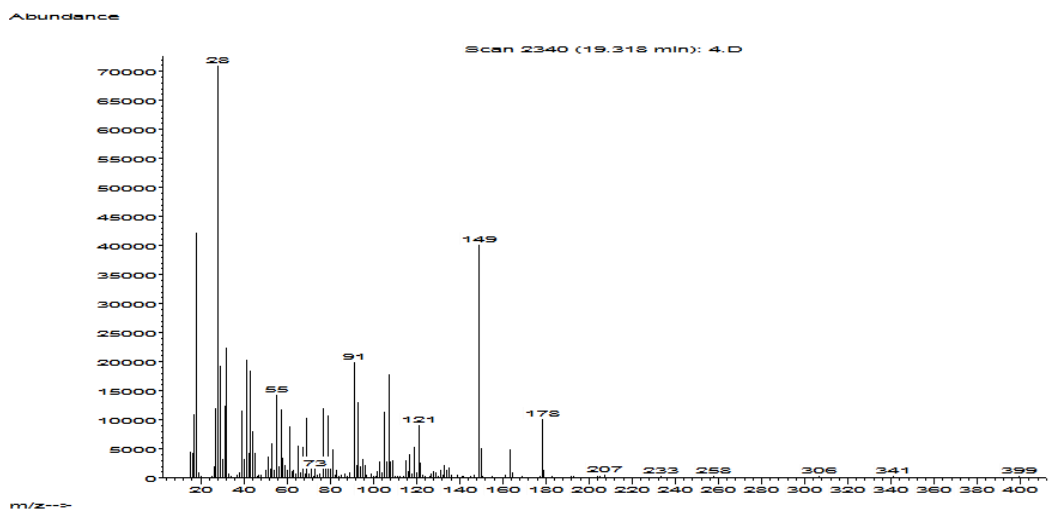
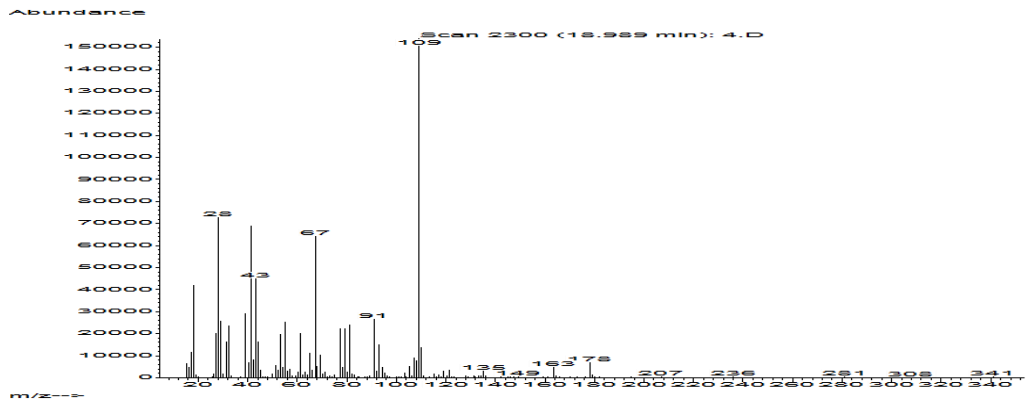
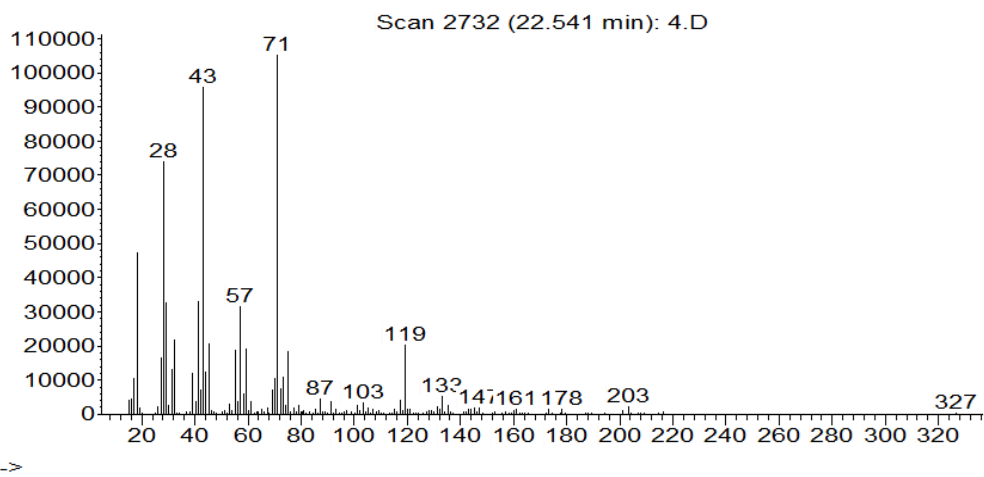


Figure 57: (continued)

Abundance



Abundance

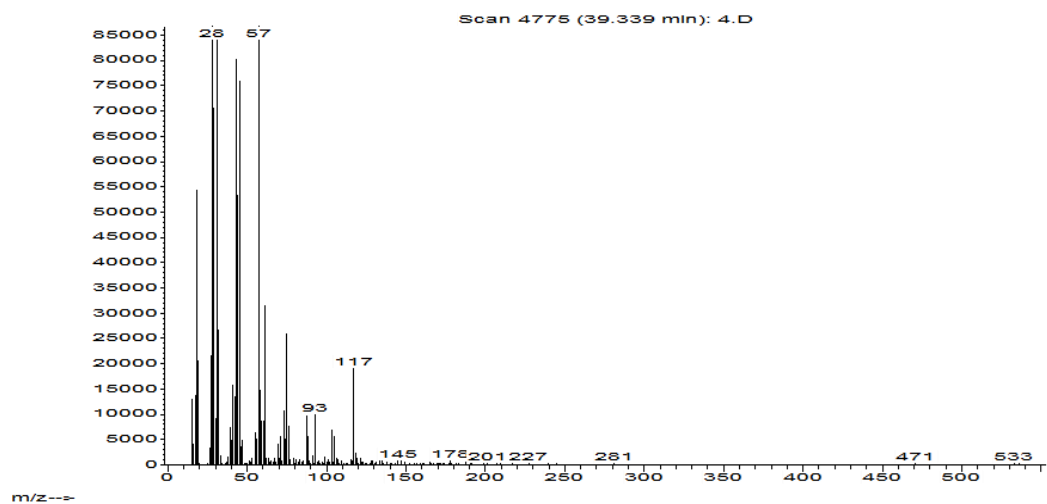


Figure 57: (continued)

## APPENDIX E

### CONVERSION AND SELECTIVITY CALCULATIONS OF ETHERIFICATION OF GLYCEROL WITH 2M2B

Sample calculations for conversion and selectivity of etherification of glycerol with 2M2B are presented in this section.

#### Glycerol Conversion :

$$X_G = \frac{X_{\text{Monoether}} + X_{\text{Diether}} + X_{\text{Triether}}}{X_{\text{Glycerol}} + X_{\text{Monoether}} + X_{\text{Diether}} + X_{\text{Triether}}} \quad [8.1]$$

If Equation 8.1 is written in terms of area and calibration factors;

$$X_G = \frac{A_{\text{Monoether}} \beta_{\text{Monoether}} + A_{\text{Diether}} \beta_{\text{Diether}} + A_{\text{Triether}} \beta_{\text{triether}}}{A_{\text{Glycerol}} \beta_{\text{Glycerol}} + A_{\text{Monoether}} \beta_{\text{Monoether}} + A_{\text{Diether}} \beta_{\text{Diether}} + A_{\text{Triether}} \beta_{\text{triether}}} \quad [E1]$$

$$S_{\text{Monoether}} = \frac{X_{\text{Monoether}}}{X_{\text{Monoether}} + X_{\text{Diether}} + X_{\text{Triether}}} \quad [8.2]$$

If Equation 8.2 is written in terms of area and calibration factors;

$$S_{\text{Monoether/G}} = \frac{A_{\text{Monoether}} \beta_{\text{Monoether}}}{A_{\text{Monoether}} \beta_{\text{Monoether}} + A_{\text{Diether}} \beta_{\text{Diether}} + A_{\text{Triether}} \beta_{\text{triether}}} \quad [\text{E2}]$$

$$S_{\text{Diether/G}} = \frac{X_{\text{Diether}}}{X_{\text{Monoether}} + X_{\text{Diether}} + X_{\text{Triether}}} \quad [\text{8.3}]$$

If Equation 8.3 is written in terms of area and calibration factors;

$$S_{\text{Diether/G}} = \frac{A_{\text{Diether}} \beta_{\text{Diether}}}{A_{\text{Monoether}} \beta_{\text{Monoether}} + A_{\text{Diether}} \beta_{\text{Diether}} + A_{\text{Triether}} \beta_{\text{triether}}} \quad [\text{E3}]$$

$$S_{\text{Triether/G}} = \frac{X_{\text{Triether}}}{X_{\text{Monoether}} + X_{\text{Diether}} + X_{\text{Triether}}} \quad [\text{8.4}]$$

If Equation 8.4 is written in terms of area and calibration factors;

$$S_{\text{Triether/G}} = \frac{A_{\text{Triether}} \beta_{\text{triether}}}{A_{\text{Monoether}} \beta_{\text{Monoether}} + A_{\text{Diether}} \beta_{\text{Diether}} + A_{\text{Triether}} \beta_{\text{triether}}} \quad [\text{E4}]$$

Where;

$A_i$  = Area of component, i

$X_i$  = Molar ratio of component, i

$\beta_i$  = calibration factor of component, i

**Sample Calculation;**

**Conversion of glycerol over A-36 at T=120 °C, Reaction time=1 hour, m<sub>cat</sub>=0.3 g**

$$X_G = \frac{444*0.67+13*0.56+0*0.46}{2960*1.4+444*0.67+13*0.56+0*0.46} = 0.07$$

**Monoether selectivity over A-36 at T=120 °C, Reaction time=1 hour, m<sub>cat</sub>=0.3 g**

$$S_{\text{Monoether/G}} = \frac{444*0.67}{444*0.67+13*0.56+0*0.46} = 0.98$$

**Diether selectivity over A-36 at T=120 °C, Reaction time=1 hour, m<sub>cat</sub>=0.3 g**

$$S_{\text{Diether/G}} = \frac{13*0.56}{444*0.67+13*0.56+0*0.46} = 0.02$$

**Diether selectivity over A-36 at T=120 °C, Reaction time=1 hour, m<sub>cat</sub>=0.3 g**

$$S_{\text{Triether/G}} = \frac{0*0.46}{444*0.67+13*0.56+0*0.46} = 0$$

In Table 24, 25, 25, 26, 27, 28, and 29 average peak areas of each component in etherification of glycerol with 2M2B over Amberlyst-36, Dowex DR-2030 catalysts are given (obtained from GC analysis) respectively. Besides calculated glycerol conversion and product selectivity values are represented.

**Table 24:** Calculated glycerol conversion and product selectivity values at different reaction times over A-36, at T=120°C, m<sub>cat</sub>=0.3 g

A-36, T=120 °C, m <sub>cat</sub> =0.3 g								
time (h)	A <sub>G</sub>	A <sub>Monoether</sub>	A <sub>Diether</sub>	A <sub>Triether</sub>	X <sub>G</sub>	S <sub>Monoether/G</sub>	S <sub>Diether/G</sub>	S <sub>Triether/G</sub>
1	2960	444	13	0	0.07	0.98	0.02	0.00
3	3106	477.5	22	0	0.07	0.96	0.04	0.00
6	1229.5	619	313	14.5	0.26	0.70	0.29	0.01
12	987	524.5	294	13	0.27	0.67	0.32	0.01
24	66.5	463	509.5	59.5	0.87	0.50	0.46	0.04

**Table 25:** Calculated glycerol conversion and product selectivity values at different reaction times over A-36, at T=120 °C, m<sub>cat</sub>=1 g

A-36, T=120 °C, m <sub>cat</sub> =1 g								
time (h)	A <sub>G</sub>	A <sub>Monoether</sub>	A <sub>Diether</sub>	A <sub>Triether</sub>	X <sub>G</sub>	S <sub>Monoether/G</sub>	S <sub>Diether/G</sub>	S <sub>Triether/G</sub>
1	2346	454.7	20	0	0.09	0.96	0.04	0.00
3	2007	805	152	49	0.19	0.83	0.13	0.03
6	380	1590	1230	120	0.77	0.59	0.38	0.03
12	190	385	1236	163	0.79	0.25	0.68	0.07
24	150.5	746	2214	350	0.90	0.27	0.65	0.08

**Table 26:** Calculated glycerol conversion and product selectivity values at different reaction times over A-36, at T=140°C,  $m_{\text{cat}}=0.3$  g

A-36, T=140 °C, $m_{\text{cat}}=1$ g								
time (h)	$A_G$	A Monoether	A Diether	A Triether	$X_G$	S Monoether/G	S Diether/G	S Triether/G
1	1839	344.5	15	0	0.09	0.96	0.04	0.00
3	1363	577	870	80.5	0.32	0.42	0.53	0.04
6	250	950	1800	190	0.84	0.37	0.58	0.04
12	135.5	735	2778	370.5	0.92	0.22	0.70	0.08
24	14.5	1401.5	3361.5	465.5	0.99	0.31	0.62	0.07

**Table 27:** Calculated glycerol conversion and product selectivity values at different reaction times over A-36, at T=140°C,  $m_{\text{cat}}=1$  g

A-36, T=140 °C, $m_{\text{cat}}=1$ g								
time (h)	$A_G$	A Monoether	A Diether	A Triether	$X_G$	S Monoether/G	S Diether/G	S Triether/G
1	105	272	280	22	0.70	0.52	0.45	0.03
3	46.6	576.2	1121.4	84.2	0.94	0.37	0.60	0.04
6	17	500	1125	87	0.98	0.34	0.61	0.04
12	9	1905.5	3179.8	371.8	1.00	0.40	0.55	0.05
24	1	2227.5	2799.3	237.3	1.00	0.47	0.49	0.03

**Table 28:** Calculated glycerol conversion and product selectivity values over Dowex DR-2030, at T=120 °C,  $m_{\text{cat}}=0.3$  and 1 g

<b>Dowex DR-2030, T=120 °C, <math>m_{\text{cat}}=0.3</math> g</b>								
<b>time (h)</b>	<b>A<sub>G</sub></b>	<b>A<sub>Monoether</sub></b>	<b>A<sub>Diether</sub></b>	<b>A<sub>Triether</sub></b>	<b>X<sub>G</sub></b>	<b>S<sub>Monoether/G</sub></b>	<b>S<sub>Diether/G</sub></b>	<b>S<sub>Triether/G</sub></b>
6	1743.5	1070	291.5	15.5	0.27	0.81	0.18	0.01
<b>Dowex DR-2030, T=120 °C, <math>m_{\text{cat}}=1</math> g</b>								
6	145	595.8	766.4	44.2	0.81	0.47	0.51	0.02

**Table 29:** Calculated glycerol conversion and product selectivity values at over A-36, at T=120 °C,  $m_{\text{cat}}=0.3$  and 1 g

<b>A-36, T=120 °C, <math>m_{\text{cat}}=0.3</math> g</b>								
<b>time (h)</b>	<b>A<sub>G</sub></b>	<b>A<sub>Monoether</sub></b>	<b>A<sub>Diether</sub></b>	<b>A<sub>Triether</sub></b>	<b>X<sub>G</sub></b>	<b>S<sub>Monoether/G</sub></b>	<b>S<sub>Diether/G</sub></b>	<b>S<sub>Triether/G</sub></b>
6	1229.5	619	313	14.5	0.26	0.70	0.29	0.01
<b>A-36, T=120 °C, <math>m_{\text{cat}}=1</math> g</b>								
6	380	1590	1230	120	0.77	0.59	0.38	0.03

